UNIVERSITY OF OKLAHOMA

GRADUATE COLLEGE

CHEMICAL REMAGNETIZATION CAUSED BY BURIAL DIAGENESIS: TESTING THE HYPOTHESIS IN THE PENNSYLVANIAN BELDEN FORMATION, COLORADO.

A Dissertation

SUBMITTED TO THE GRADUATE FACULTY

in partial fulfillment of the requirements for the

degree of

Doctor of Philosophy

By

SANJAY BANERJEE
Norman, Oklahoma
1997

UMI Number: 9726711

UMI
300 North Zeeb Road
Ann Arbor, MI 48103

CHEMICAL REMAGNETIZATION CAUSED BY BURIAL DIAGENESIS: TESTING THE HYPOTHESIS IN THE PENNSYLVANIAN BELDEN FORMATION, COLORADO.

A Dissertation APPROVED FOR THE
SCHOOL OF GEOLOGY AND GEOPHYSICS

BY

ACKNOWLEDGEMENTS

My doctoral research has been a rewarding experience thanks to the faculty and facilities of the School of Geology and Geophysics at the University of Oklahoma. My advisor Dr. R. Douglas Elmore has my very special thanks for directing this research and for providing support and encouragement throughout this and other projects on which we have worked together. I wish to thank my committee member Dr. Michael. H. Engel for his generous help and suggestions during this research and Dr. Barry Weaver for reviewing the manuscript and providing thoughtful comments. Sue Halgedahl is thanked for serving on my committee and for her help and advice during my visit to the Rock Magnetic Laboratory at University of Utah, Salt Lake City. I would also like to thank Dr. T. H. Lee Williams for serving on my committee.

I would also like to express my gratitude to all the people who assisted me in the field and laboratory work, especially K.R. Srinivas, Partho Biswas and Jamie Egger. Bodo Katz is thanked for helping with processing rock magnetic samples and also for his helpful comments and advice. I also wish to thank the staff at the School of Geology and Geophysics office, including Donna, Marjorie and Patti for their help during my graduate study at the School. Numerous friends and colleagues including Aditya, Monica, Sankar and Satavisa, among others, helped to make my stay within the School of Geology and Geophysics an enjoyable and memorable experience.

I thank my parents, to whom this work is dedicated, for making it all possible through their efforts and many sacrifices.

Financial support for this research was provided by DOE grant # DEFGO2-93ER14397 and by student research grants from GSA and AAPG.

TABLE OF CONTENTS

CHAPTER 2 MAGNETIC CHARACTERIZATION OF A CRM AND A TVRM, BELDEN FORMATION, NORTHWESTERN COLORADO.

LIST OF TABLES

CHAPTER 1

LIST OF ILLUSTRATIONS

CHAPTER 1

CHAPTER 2

FOREWORD

Remagnetization is a common phenomenon recognized in many rocks [e.g., *Elmore and McCabe*, 1991] and can occur through several mechanisms such as chemical alteration and cooling from elevated burial temperatures. Pervasive, basin-wide, secondary magnetizations have been recognized from many Paleozoic carbonate units within the North American craton [e.g., *Elmore and McCabe*, 1991]. Abundant petrologic and geochemical evidence shows that many of these magnetizations are chemical in origin and reside in authigenic magnetite that formed by alteration of pre-existing pyrite [e.g., *Suk et al.*, 1990b; *Jackson et al.*, 1993]. Many such chemical remanent magnetizations (CRMs) in carbonate have been linked to the action of orogenic fluids [e.g., *Elmore and McCabe*, 1991], first proposed by *Oliver* [1986]. Evidence for this model includes a spatial and temporal association of the CRMs with orogenic belts and events. The orogenic fluids are believed to be responsible for causing widespread mineralization [e.g., *Drobek*, 1989; *Pan et al.*, 1990] and other diagenetic changes in rocks including magnetite authigenesis [e.g., *Oliver*, 1992]. Studies have shown that fluid alteration can explain some of the chemical magnetizations in Paleozoic carbonate [e.g., *Bachtadse et al.*, 1987; *Lu et al.*, 1991; *Symons and Sangster*, 1992; *Elmore et al.*, 1994]. However, a number of pervasive CRMs cannot be satisfactorily explained by the orogenic fluid model [e.g., *Elmore et al.*, 1993b; *Fruit et al.*, 1995], even when there seems to be an apparent spatial and temporal relationship between an orogenic event and remagnetization.

Chapter 1 addresses the issue of the origin of a widespread CRM in magnetite present in the Belden Formation of Central and Nortwestern Colorado. Paleomagnetic and geochemical study of the Early Pennsylvanian Belden Formation at Sweetwater Anticline in Central Colorado by *Fruit et al.* [1995] has shown that the unit contains a Late Cretaceous CRM residing in magnetite. The origin of this CRM was tentatively interpreted to be related to burial diagenesis of organic matter. In this chapter the origin of this CRM is tested by conducting a regional investigation of the Belden Formation. The Belden Formation had a variable thermal and maturation history over different parts of the Paleozoic Central Colorado Trough [*Nuccio et al.*, 1989]. Comparision of the paleomagnetic data with the modeled thermal history of the Belden Formation on a basinwide scale provides a test of the hypothesis that the CRM is related to burial diagenesis.

Chapter 2 focuses on rock magnetic results from remagnetized carbonate in the Pennsylvanian Belden and Morgan formations in Colorado in an effort to characterize the carriers of the magnetizations present in the Belden Formation. In recent years considerable effort has been focused on determining whether there is a rock magnetic fingerprint for different types of magnetizations, particularly those interpreted to be chemical in origin [e.g., *Hart and Fuller*, 1988; *Jackson*, 1990; *Jackson et al.*, 1993, *McCabe and Channell*, 1994]. Chemical remagnetization processes are interpreted to modify the magnetic properties and these modifications are believed to cause a rock magnetic fingerprint which is advocated as an identifier for remagnetized carbonate [e.g., *McCabe and Channell*, 1994]. Recognition of such a rock magnetic fingerprint could potentially provide a faster method of identifying remagnetized sites prior to detailed paleomagnetic (directional) studies. In addition, such a fingerprint could help to identify the composition, grain size, and domain structure of the magnetic phases associated with a particular remagnetization mechanism. The Belden carbonate contain two ancient natural remanent magnetization (NRM) components, of which one is pervasive whereas the other is widespread but found only at certain sites. This distribution provides the opportunity to characterize the two components with rock magnetic parameters and to compare these characteristics to those recently reported for other remagnetized carbonate rocks [*e.g., Jackson et al.*, 1993; *Channell and McCabe*, 1994]. Furthermore, the distribution and rock magnetic properties associated with these two components provide information about the magnetic phases associated with the remagnetization mechanisms.

CHAPTER 1

CHEMICAL REMAGNETIZATION CAUSED BY BURIAL DIAGENESIS: TESTING THE HYPOTHESIS IN THE PENNSYLVANIAN BELDEN FORMATION, COLORADO

ABSTRACT

Lower Pennsylvanian Belden Formation carbonate from Central Colorado were subjected to paleomagnetic, rock magnetic, and geochemical studies to test for a connection between a widespread chemical remanent magnetization (CRM) in authigenic magnetite and diagenesis of organic matter. Thermal demagnetization results show that the Belden Formation carbonate carry up to three components of natural remanent magnetization (NRM), all of which reside in magnetite. A low unblocking temperature (NRM-250°C), northerly and steep down component (#1) is interpreted to be a modern, viscous magnetization. An intermediate unblocking temperature (250-400°C) component (#2) with normal and reversed Tertiary directions is interpreted to be a thermoviscous remanent magnetization. Many Belden Formation limestone also contain a high unblocking temperature (400-570°C) component (#3) interpreted as a CRM. The directions shown by this CRM vary across the basin and the ages range from Late Paleozoic to Cretaceous. Fold tests from different parts of the basin show synfolding to prefolding results and help to define the age of the magnetization relative to the Cretaceous-Tertiary Laramide Orogeny. This CRM is interpreted to reside in authigenic magnetite that formed by partial or complete replacement of pyrite. Hysteresis curves for Belden Formation carbonate samples show the typical "wasp-waisted" loops and are attributed to the mixing of contrasting coercivity fractions. Hysteresis ratios of the Belden Formation carbonate are consistent with those reported for other remagnetized carbonate. Rock magnetic studies indicate that both components 2 and 3 are carried by magnetite of single domain/pseudo-single domain grain size. Although elevated strontium ($^{87}Sr/^{86}Sr$) isotope values relative to Pennsylvanian co-

eval seawater indicate passage of radiogenic fluids through Belden Formation carbonate, contact vein test results indicate that these fluids were not responsible for the CRM. The time of the CRM acquisition, which varies from Late Paleozoic to Cretaceous, coincides with the modeled time of organic matter maturation in the different parts of the basin. This suggests that diagenetic reactions triggered by low to moderate burial temperatures brought about the replacement of pyrite by magnetite and caused acquisition of the CRM.

INTRODUCTION

Pervasive, basin-wide, secondary magnetization have been recognized from many Paleozoic carbonate units within the North American craton [e.g., *Van der Voo*, 1989; *Elmore and McCabe*, 1991; *Lu et al.*, 1991; *Elmore et al.*, 1993b; *Symons*, 1995]. Abundant evidence is present to show that many of these magnetization are chemical in origin and reside in authigenic magnetite that formed by alteration of pre-existing pyrite [e.g., *Suk et al.*, 1990b; *Jackson et al.*, 1993]. A popular mechanism invoked to explain such chemical remanent magnetizations (CRMs) in carbonate is based upon large-scale migration of orogenic fluids [*Oliver*, 1992]. Evidence for this model includes a spatial and temporal association of the CRMs with orogenic belts and events. The orogenic fluids are believed to be responsible for causing widespread mineralization [e.g., *Drobek*, 1989; *Pan et al.*, 1990] and other diagenetic changes in rocks including magnetite authigenesis [e.g., *Oliver*, 1992]. Paleomagnetic and geochemical studies of carbonate units have shown that this model can explain some of the chemical magnetizations in Paleozoic carbonate [e.g., *Bachtadse et al.*, 1987; *Lu et al.*, 1991;

Symons and Sangster, 1992; *Elmore et al.*, 1994]. However, a number of pervasive CRMs cannot be satisfactorily explained by the orogenic fluid model [e.g., *Elmore et al.*, 1993b; *Fruit et al.*, 1995], even when there seems to be an apparent spatial and temporal relationship between an orogenic event and remagnetization. In some cases, burial diagenesis of organic matter has been invoked to explain such CRMs [e.g., *Fruit et al.*, 1995; *Plaster-Kirk et al.*, 1995].

The objective of this study is to test burial diagenesis as a remagnetization mechanism. *Fruit et al.* [1995] have shown that the Pennsylvanian Belden Formation at Sweetwater Anticline in Central Colorado contains a Late Cretaceous CRM residing in magnetite which they interpreted to be related to diagenesis of organic matter. The Belden Formation had a variable thermal and maturation history over different parts of the Paleozoic Central Colorado Trough [*Nuccio et al.*, 1989]. Comparison of the paleomagnetic data with the modeled thermal history of the Belden Formation on a basin-wide scale will provide a test of the hypothesis that the CRM is related to burial diagenesis.

GEOLOGIC SETTING OF THE STUDY AREA

The Lower Pennsylvanian (Morrowan-Atokan) Belden Formation in central Colorado and the Morgan Formation in northwestern Colorado were sampled in this study (Figure 1-1). The lower-middle portion of the Morgan Formation is considered to be equivalent to the Belden Formation [e.g., *Upton*, 1958].

During the early Pennsylvanian, tectonism following the continent-continent collision of North America with South America-Africa resulted in block faulting and

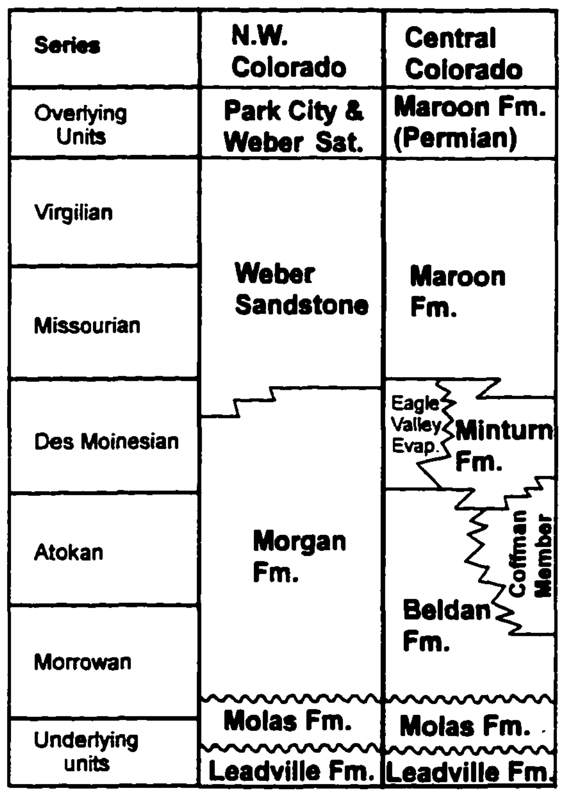

Figure. 1-1 Stratigraphic column of Pennsylvanian rocks in the study area in Colorado (from *Barrs et al.*, 1988).

subsidence in Central Colorado and the development of the NW-SE trending Central Colorado Trough [*Kluth*, 1986]. The subsidence allowed a marine transgression from the northwest over the prevailing Mississippian karst surface which covered much of Colorado [*Barrs et al.*, 1988]. The Belden Formation lithologies were deposited in this developing basin (Figure 1-2). The Belden Formation consists mainly of interbedded black marine shale, carbonate rocks, minor arkose and siltstone resting unconformably on the Mississippian Madison Formation. Within the individual carbonate units, a shallowing up sequence from mudstone to packstone is observed at many localities (Figure 1-3).

Deposition of the Belden Formation sediments continued uninterrupted until the end of the Atokan when carbonate production in the basin was overwhelmed by coarse arkosic detritus of the Minturn Formation shed from the rapidly rising Ancestral Rocky Mountains [*Barrs et al.*, 1988]. The Belden Formation has a gradational contact with the overlying Minturn Formation at most places in the basin and the boundary between the two formations is arbitrarily placed at the base of the first major sand unit [*Brill*, 1958].

The Belden Formation sediment were buried to maximum depths of about 5500 - 8000 meters (in different parts of the basin) and are considered to be overmature in terms of its oil generation potential [*Nuccio et al.*, 1989; *Whalen et al.* 1990]. Due to variations in subsidence and heat flow, the Belden Formation lithologies were buried to depths necessary to generate hydrocarbons at different times in different parts of the basin [*Nuccio et al.*, 1989].

During initial stages of the Laramide Orogeny in the Cretaceous - Early Tertiary,

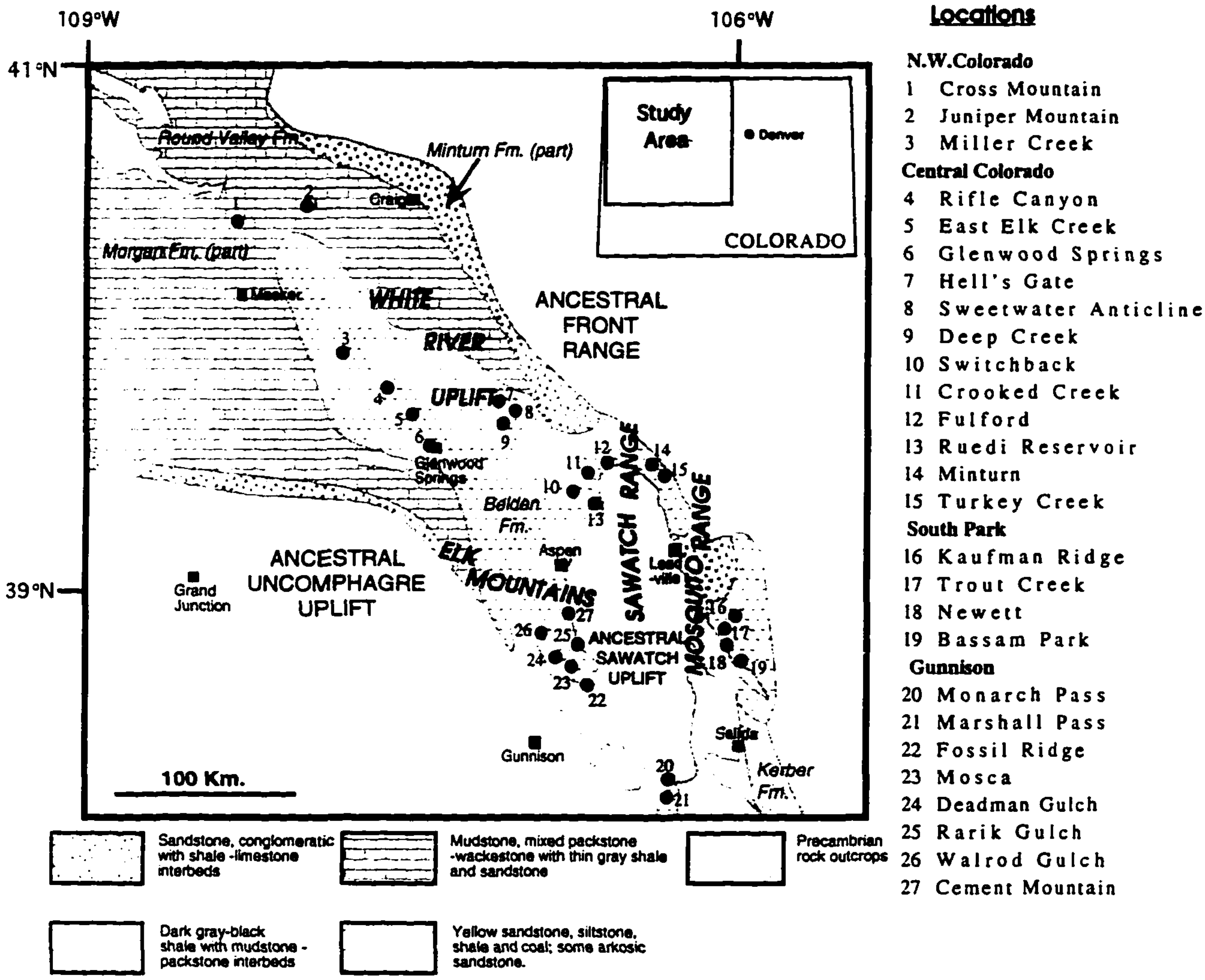

Figure 1-2 Study area in central and northwestern Colorado showing lithofacies in the Belden and Morgan Formations and the sampling locations. Also shown are some of the Late Paleozoic and Tertiary uplifts and mountain ranges. Tertiary features shown with bold lettering. Inset: map of Colorado showing the location of the study area. (lithofacies map modified from *Barrs et al.* [1988]).

Figure. 1-3 Belden Formation outcrop at Hell's Gate, showing mudstone-packstone shallowing-up carbonate cycles. Trees (about 0.5 m high) for scale.

the Sawatch Uplift was reactivated which formed a huge north-south trending anticline with a core of intrusive rocks in central Colorado [*Tweto*, 1977]. This was closely followed by the rise of the Mosquito Range to the east and the Elk Mountains to the west of the Sawatch Range. There was an extended period of volcanic and intrusive igneous activity during this time. The White River Uplift and the Grand Hogback Monocline began to rise at about 67 Ma and were the last major Laramide uplifts in this area [*Nuccio et al.*, 1989].

SAMPLING AND PROCESSING

Representative samples of carbonate lithologies were collected from various Belden Formation and Morgan Formation outcrops from locations throughout the study area (Figure 1-2). Oriented slabs with bedding information were collected in the field from each site. In addition, large oriented slabs with veins of calcite were also collected for vein tests. The slabs were drilled to obtain oriented cores of 2.5 cm. diameter. The ends of the cores were trimmed to remove any surficial weathering products and the longer cores were cut to obtain standard paleomagnetic specimens of 2.2 cm. length. The specimens were then subjected to paleomagnetic and rock magnetic measurements at the Paleomagnetic Laboratories at the University of Oklahoma, Norman, University of Kansas, Lawrence and University of Utah, Salt Lake City. Most magnetic measurements were made with a United Scientific three-axis cryogenic magnetometer or a 2G three-axis cryogenic magnetometer located in a magnetically shielded room at the University of Oklahoma.

The specimens were subjected to standard demagnetization procedures involving both thermal and alternating field (AF) methods. Thermal demagnetization of the natural remanent magnetization (NRM) was carried out by heating the specimens at increasing temperatures to 580°C (in 14-16 steps) in a Schonstedt thermal sample demagnetizer (TSD-1) oven for 30 min followed by cooling in a shielded chamber. The AF demagnetization was done on a 2G three axis AF demagnetizer (model 2G600). The specimens were subjected to successively increasing AF strengths (in 15 steps) from NRM to 170 mT. Demagnetization data so obtained was plotted on orthogonal diagrams [*Zijderveld*, 1967] and components were visually identified. The magnetization directions of the components were calculated using the three-dimensional least squares method [*Kirschvink*, 1980]. A magnetization was taken to be sufficiently resolved if three or more vector end points followed a linear trend with a maximum angle of deviation [*Kirschvink*, 1980] value of 10° or less. Site means and locations were calculated using *Fisher* [1953] statistics.

Selected specimens were subjected to multiple (up to 3) zero-field cycling episodes to investigate the possible effects of viscous overprinting of components [e.g., *Dunlop et al.*, 1995]. The procedure involved keeping the specimens in liquid nitrogen (-196°C) inside a mumetal shield (ambient field 75 nT) for 15 min during each cycle. The specimens were then taken out of liquid nitrogen and allowed to warm up to room temperature inside the shield before being subjected to thermal demagnetization of NRM. Selected specimens were also subjected to low field AF demagnetization (10 mT) before being subjected to regular thermal demagnetization to investigate the possible effects of a modern viscous overprint on the higher temperature components.

Hysteresis measurements were performed at the University of Utah, Salt Lake

City. Rock chips, 2mm by 3mm, were prepared from core ends for measurements. Hysteresis loops were obtained on a Princeton Instruments Model 2900 Alternating Gradient Force Magnetometer (micromag) using an average dwell time of 100 milliseconds and field increments of 2 mT. Values of coercive force (Hc), saturation magnetization (Ms) and saturation remanent magnetization (Mrs) were determined for each hysteresis run after the data was suitably corrected for high field paramagnetic or diamagnetic slope. Values of coercivity of remanence (Hcr) were obtained from backfield measurements.

Isothermal remanent magnetization (IRM) acquisition of selected sample chips was done on the micromag. In addition, IRM acquisition of selected specimens were carried out by successively exposing the cores to increasing magnetization fields of up to 1.3 mT with an impulse magnetizer. The specimens were then given a final magnetization of 0.12, 0.4 and 1.3 T along +X, +Y and +Z sample directions, respectively, following the method of *Lowrie* [1990]. The specimens were then subjected to stepwise thermal demagnetization up to 700°C. The intensity of magnetization along the three directions were analyzed separately for each sample to investigate the presence of possible "hard" and "soft" components.

Petrographic analysis of the sampled carbonate lithologies was done using polished thin sections under transmitted and reflected light. Selected samples were also examined on a Cameca SX-50 electron microprobe equipped with a Kevex energy dispersive analysis system.

Some Belden Formation samples were subjected to Total Organic Carbon (TOC) analysis by Humble Instruments and Services Inc., Humble, Texas. This involved heating a small amount (~100 mg) of finely pulverized rock sample in a Helium atmosphere within a Rock Eval apparatus. During the heating process, the sample was initially heated at 300°C for three minutes, and then the temperature was increased by 25°C/min, up to 550°C. The generated vapors were analysed by a flame ionization detector (FID). The S_1 peak (for free hydrocarbon, oil and gas contained in organic matter) and the S_2 peak (kerogen cracking or pyrolyzate peak, between 350°C and 550°C) were recorded. The CO_2 produced by decomposition of carboxyl compounds between 300-390°C was trapped and analysed later during the cooling cycle, using a thermal conductivity detector and was recorded as the S_3 peak. The organic carbon remaining after the recording of S_2 peak was measured by oxidation in air at 600°C and the resulting CO_2 peak was recorded as the S_4 peak. The T_{max} (temperature of maximum liberation of hydrocarbon) value was obtained from the S_2 peak, while the TOC value was computed from S_1, S_2 and S_4 peaks. The FID was calibrated against a standard (Humble standard # 99986, TOC = 3.11 wt%) which was also run in sequence as an unknown, every 10th sample, to check on the instrument drift.

Strontium ($^{87}Sr/^{86}Sr$) isotope values for representative carbonate samples from different locations in the study area were determined at the University of Texas, Austin. Rock samples were crushed in a ceramic pestle and mortar and then micro-sampled for the carbonate cement. The powdered samples were then washed three times in 0.2N reagent grade ammonium acetate and rinsed three times in ultrapure water (D_3). The cleaned samples were dissolved in 1.4 N acetic acid for about 5 minutes. Sr was isolated and concentrated through cation exchange columns by using 2N HCl. Analysis was performed on MAT 261 mass spectrometer, and fractionation in the mass spectrometer was corrected using $^{86}Sr/^{88}Sr = 0.1194$. Standard NBS 987 was routinely analyzed and yielded 0.710232 ± 0.000012 (1σ, n = 10). The $^{87}Sr/^{86}Sr$ ratios of samples reported in this study were normalized to NBS 987 = 0.71014.

RESULTS AND INTERPRETATIONS

1. Paleomagnetic Results:

Thermal demagnetization of the Belden Formation lithologies indicate that three components of the NRM can be identified on the basis of unblocking temperature ranges (Figure 1-4, a-e): Component 1 (NRM to 250°C), Component 2 (250 to 400°C) and Component 3 (400 to 580°C). Alternating field demagnetization of specimens only resolved component 1 and a vector sum of components 2 and 3. This indicates an overlap in the coercivity spectra of the components 2 and 3. Hence, most of the specimens were thermally demagnetized.

Component 1, with a low unblocking temperature range (NRM to 250°C) is present in all of the samples (Figure 1-4). This component has northerly declinations and steep down inclinations, similar to the present geomagnetic field. On the basis of its direction and the low unblocking temperatures, this component is interpreted to be a modern viscous remanent magnetization (VRM) acquired in the present Earth field.

Component 2, with an unblocking temperature range of 250 to 400°C, is present in almost all of the demagnetized samples (Figure 1-4; Table 1). This component occurs with both normal and reversed directions (Figure 1-5). Fold tests on this component from Central Colorado (Fulford-Minturn) and South Park (Trout Creek-Bassam Park)

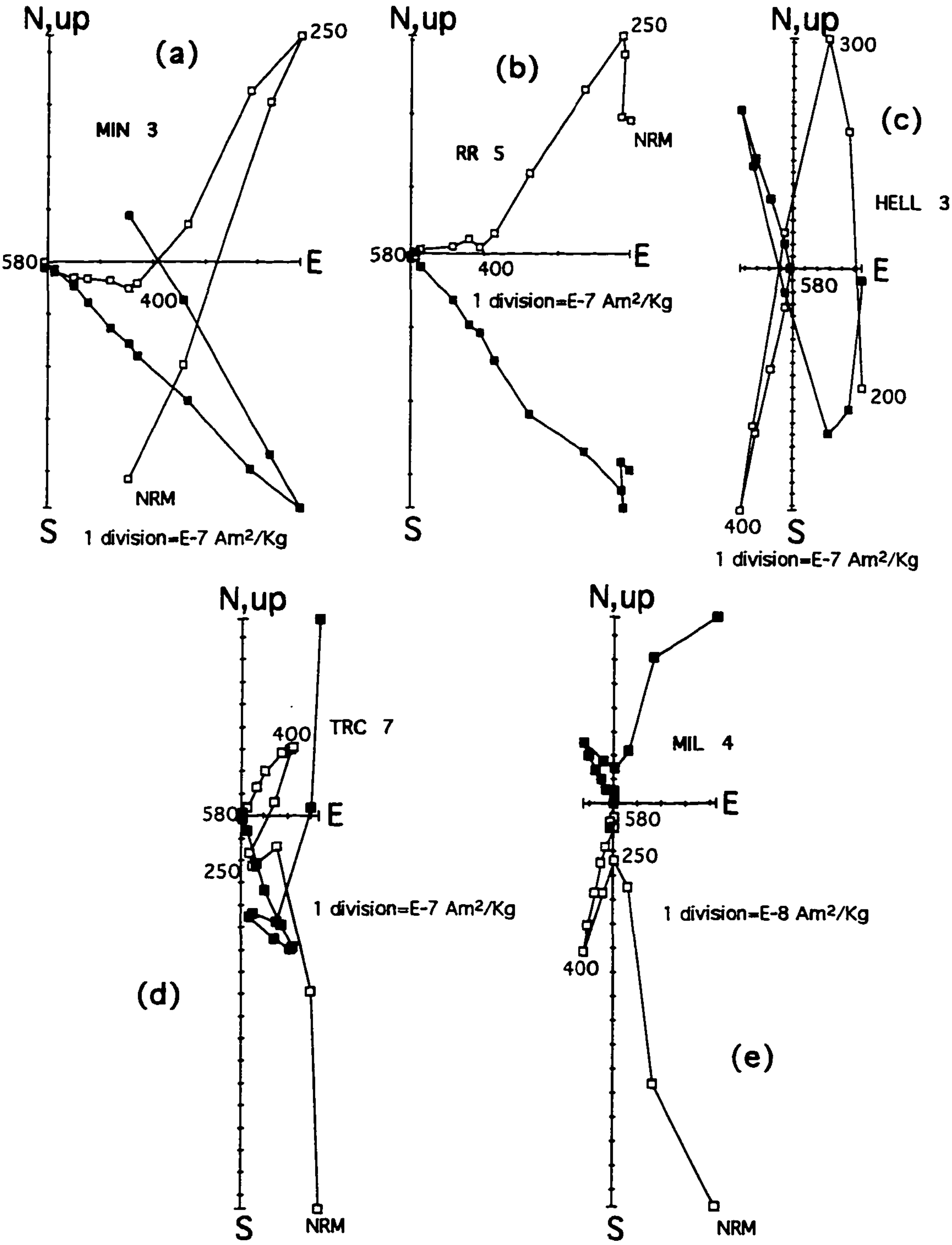

Figure. 1-4 Representative orthogonal (Zijderveld) projections of the thermal demagnetization of Belden Formation specimens from different locations (before structural correction): **a.** Fulford-Minturn **b.** Ruedi Reservoir **c.** Hell's Gate **d.** Trout Creek-Bassam Park **e.** Miller Creek. Open symbols - horizontal components; closed symbols - vertical components.

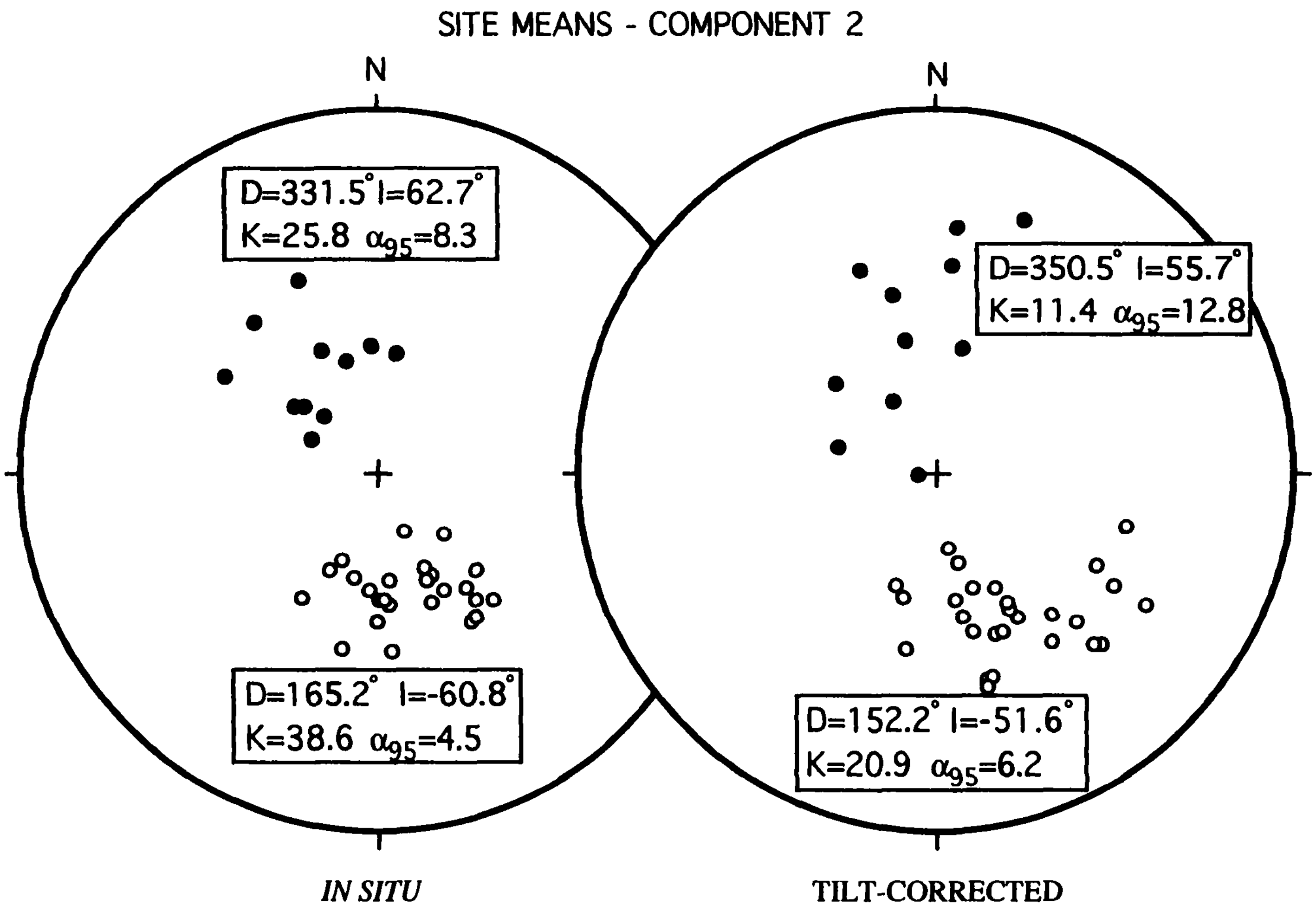

Figure. 1-5 Equal area projection of *in situ* and tilt-corrected mean site directions for the thermoviscous component (component 2) for all locations. Solid symbols - lower hemisphere projection; open symbols - upper hemisphere projections.

Table 1. Location Mean Directions and Statistics for Component 2

Location	N	k	α_{95}	*In situ*				*Tilt-corrected*	
				D/I	lat./long.	dp	dm	D/I	lat./long.
Miller Creek	3	142.6	8.4	147.6/-66.2	65.4N/166.3W*	11.3	13.8	168.1/-59.4	80.9N/178E*
Fulford	8	60.8	6.7	188.7/-61.8	82.6N/47.7W*	8.0	10.4	134.4/-41.4	48.7N/155E*
Minturn-Gilman	4	172.6	6.1	143.1/-52.1	59.6N/162.2E*	5.7	8.4	162.2/-47.7	71.8N/132.9E*
Turkey Creek	1	50.9	11.2	151.0/-50.4	65N/153.1E*	10.1	15.0	152.3/-37.0	59.7N/133.2E*
Ruedi Reservoir	3	23.2	2.1	142.9/-60.5	61.9N/180.5E*	2.5	3.2	150.2/-57.2	66.8N/168.7E*
Hell's Gate	3	106.6	9.8	170.8/-61.4	82.5N/172.1W*	11.6	15.1	188.6/-64.3	81.1N/65.2W*
Crooked Creek	3	453.7	4.7	154.4/-59.4	70.4N/174E*	5.3	7.1	151.9/-56.4	67.9N/166E*
East Elk Canyon	1	33.4	8.0	165.5/8.2	44.2N/92.9E*	4.1	8.1	166.4/-38.0	68.3N/108.8E*
Switchback	1	50.7	8.7	180.1/-55.3	86.3N/72E*	8.8	12.4	122.5/-31.0	35.5N/155.9E*
Rifle Canyon	1	25.4	9.9	202.6/-28.7	58.6N/27.1E*	6.0	10.9	174.7/-44.7	75.8N/92.1E*
Deep Creek	2	-	-	167.0/-61.5	79.8N/176.1W*	-	-	182.5/-64.9	82.6N/93.2W*
Glenwood Springs	1	54.6	12.5	247.8/38.0	2.2N/166.7E	8.7	14.8	253.1/-25.7	21.5N/17W*
Trout Creek	3	167.8	7.8	307.4/71.1	51.7N/152.4E	11.9	13.6	351.9/65.2	79.8N/138.5W
Kaufman Ridge	1	128.4	4.3	311.4/68.0	54.3N/160.8W	6.1	7.2	4.9/42.3	75N/55.6E
Newett	1	132.0	3.4	320.3/46.0	55.1N/156.9E	2.8	4.4	339.7/40.5	66.5N/127.4E
Bassam Park	4	26.2	10.0	356.1/59.8	86.5N/162.3W	11.4	15.1	337.1/67.3	70.2N/153.6W
Mosca	2	-	-	8.5/62.2	82.1N/55.6W	-	-	0.8/29.3	66.8N/71W
Deadman Gulch	1	349.6	5.4	301.8/48.5	41.8N/170.6E	4.7	7.1	316.9/25.4	44.3N/141.5E
Rarik Gulch	1	277.6	6.0	357.9/61.4	86N/129.2W	7.1	9.2	346.5/48.6	75.5N/127.8E
Cement Mtn.	1	44.7	13.9	170.9/-54.5	81.7N/137.6E*	13.8	19.6	179.0/0.9	50.6N/74.8E
Marshall Pass	1	-	-	123.4/9.4	22.1N/137.5E	-	-	135.2/-23.2	24.5N/122.5E*
Walrod Gulch	1	58.4	23.3	191.2/-48.6	76.9N/24.8E*	-	-	189.1/-48.0	77.6N/32.8E*

N = number of sites in a location used to calculate mean (for locations with only 1 site, sample directions were used to calculate means and statistics); **D** = declination; **I** = inclination; **k** = precision parameter [*Fisher*, 1953]; α_{95} = radius of 95% probability cone for the site mean; **lat./long.**= paleopole latitude and longitude; **dp/dm** = semi-axes of 95% cone of uncertainty around the paleopole.
*Values denote antipodal pole.
Note: At Fossil Ridge and Monarch Pass, only the modern VRM and unstable components were identified.

show that the best grouping of specimen directions is neither in an *in-situ* nor in a tilt-corrected position but rather at some intermediate position. This indicates a possible synfolding time of remanence acquisition. The calculated paleo-pole for the best grouping of directions is close to the Tertiary portion of *Van der Voo's* [1989] Apparent Polar Wander Path (APWP) for the North American continent. Based on the component's maximum unblocking temperature, the burial/thermal history of Belden Formation, and the theoretical blocking temperature-relaxation time curves for magnetite [*Pullaiah et al.*, 1975; *Middleton & Schmidt*, 1982], this component is interpreted to be a thermoviscous remanent magnetization (TVRM). This component was acquired while cooling from maximum burial and heating of the Belden Formation during the Laramide Orogeny. This interpretation is consistent with that of *Fruit et al.* [1995] for Sweetwater and of reported occurrences of a similar component in other formations in Colorado [e.g., *Horton et al.*, 1984].

Component 3, with an unblocking temperature range of 400 to 580°C, is present in specimens from some locations in the study area (Figure 1-4; Table 2). Within a particular location, this component is clearly resolved only in specimens from some sites. At other sites and locations, the component is either not present or cannot be resolved. Of particular interest is the fact that this component has different directions at different locations. Maximum unblocking temperatures near 580°C suggest that this component resides in magnetite. The results for this component are presented below, organized by locality.

<u>Fulford-Minturn</u>:

Thermal demagnetization of specimens from Fulford, Minturn and Turkey Creek

Table 2: Summary Statistics of Paleomagnetic Directions for Component 3

Location & site	n/n_0	*In situ*						*Tilt-corrected*	
		D/I	k	α_{95}	lat./long.	dp	dm	D/I	lat./long.
Miller Creek									
Miller 4	9/10	336.0/66.8	123.1	4.1	70.6N/160.6W	7.4	9.0	355.3/56	85.1N/110W
Deep Creek									
NL	5/12	357.3/45.1	30.8	14.0	76.8N/83.4W	11.2	17.7	354.5/70.1	75.2N/119.8W
Fulford									
Ful 1	10/10	131.6/-20.0	35.7	8.2	38.2N/142.7E*	4.5	8.6	126.8/2.2	26.7N/137.1E*
Ful 3	12/12	155.2/-42.7	112.7	3.9	64.5N/135.5E*	3.0	4.8	133/-11.5	36N/137.4E*
Ful 5	2/2	148.8/-44.7	-	-	60.9N/145.9E*	-	-	136.6/-6.1	36.4N/131.8E*
Mean		144.0/-36.3	60.8	13.0	53.6N/141.9E*	8.9	15.1	132.1/-5.1	33N/135.5E*
Minturn-Gilman									
Min 2	11/12	132.9/-10.0	48.2	6.3	35.4N/137.1E*	3.2	6.4	135.3/-11.8	37.7N/135.8E*
Min 3	6/6	145.1/-16.8	268.7	3.7	45.9N/127.8E*	2.0	3.9	149.5/-10.5	45.9/120E*
Min 5	6/6	138.9/-26.9	352.7	4.4	46.1N/140.3E*	2.6	4.9	146.2/-19.9	48.1N/128.6E*
Gil 2	3/3	145.7/-15.6	57.6	16.4	46.0N/126.8E*	9.0	17.2	151.4/-20.7	51.6N/122.6E*
Mean		140.6/-17.4	59.4	10.4	43.4N/133.3E*	5.6	10.8	145.5/-15.8	45.9N/127.4E*
Turkey Creek									
TC1	4/4	132.5/-20.2	102.6	7.9	38.9N/142.3E*	4.3	8.3	134/-8.2	35.5N/135.4E*
Ruedi Reservoir									
RR	9/9	141.1/-2.2	29.8	9.1	37.8N/125.9E*	4.6	9.1	141/-0.3	37N/125.3E*
Hell's Gate									
Hell 3	3/3	358.0/59.8	72.7	11.9	88.2N/163.9W	13.5	17.9	17.4/62.1	76.5N/175.8E
Hell 4	6/6	3.3/61.5	1146.7	1.8	86.2N/167.7W	2.1	2.8	21.2/60.3	73.9N/129.3W
Mean		0.6/60.7	-	-	88N/87.7W	-	-	19.4/61.2	75.2N/146.7W
Glenwood Springs									
WGS	4/4	269.7/12.0	176.2	6.9	3.7N/168.6E	3.6	7.0	255.6/-58.2	33.4N/42.5E
Trout Creek									
TRC 1	9/9	143.8/-34.6	69.2	5.9	53N/142.1E*	4.0	6.8	155.4/-27.8	57.6N/122.7E*
TRC 6	8/8	150.5/-26.8	61.7	6.6	54.2N/128.6E*	4.0	7.2	161.0/-20.0	56.7N/109.7E*
TRC 7	16/16	157.2/-30.5	217.7	2.5	60N/122E*	1.6	2.9	168.4/-20.7	60N/97.3E*
Mean		150.6/-30.7	91.8	10.5	56N/131.3E*	6.5	11.7	161.7/-22.6	58.5N/110.1E*
Kaufman Ridge									
KAUF 2	9/9	120.8/-19.9	115.3	4.5	30.3N/152.1E*	2.5	4.7	135.5/-17.6	40.3N/139.2E*
Newett									
Newett 2	3/3	143.3/-17.0	720.1	2.4	45.4N/131.3E*	1.3	2.5	148.9/-12.9	47.2N/123.1E*
Bassam Park									
BAS 1	13/14	169.6/-15.8	58.7	5.2	57.9N/93.7E*	2.6	5.4	160.8/-42.9	68.7N/129.2E*
BAS 2	7/7	156.3/-7.6	44.2	8.5	49N/111.7E*	4.3	8.7	150.8/-23.3	52.9N/126.2E*
BAS 3	6/6	173.7/-7.6	411.9	3.0	54.6N/85E*	1.5	3.0	163.7/-23.4	59.8N/107E*
BAS 5	11/11	167.3/-4.9	98.9	4.4	51.9N/94.9E*	2.2	4.4	162.9/-32.2	64N/113.8E*
Mean		166.7/-9.0	64.6	10.0	53.8N/96.9E*	5.1	10.1	159.4/-30.6	61.3N/118.7E*
Mosca									
MOS 3	7/7	224.0/-65.0	41.0	6.3	57.2N/45.7W*	8.2	10.2	202.7/-39.4	64.6N/17.1E*
MOS 5	2/3	222.0/-56.0	-	-	57N/26.2W*	-	-	199.1/-42.5	68.5N/19E*
Mean		222.9/-60.5	-	-	57.4N/35.4W*	-	-	200.9/-41	66.6N/17.9E*
Rarik Gulch									
RARIK 1	2/3	94.4/-0.1	-	-	3.5N/160.6E*	-	-	95.8/19.5	1.8N/28.1W
Cement Mountain									
CMNT 1	4/4	220.1/-58.6	108.7	8.9	59.2N/30.4W*	9.8	13.2	205.3/-4.9	46.8N/34.6E*
Marshall Pass									
IND 1	2/3	86.0/46.7	-	-	19.8N/36.8W	-	-	151.5/71.2	7.1N/-90.7W
Walrod Gulch									
WAL 1	2/2	221.1/-48.3	-	-	55N/13.9W*	-	-	217.1/-45.0	56.7N/6.5W*

Fold Test Means	D/I	k	α_{95}	lat./long.	dp	dm
Fulford-Minturn (N=7)						
In situ	143.5/-25.5	17.9	6.5	48.7N/134.8E*	3.7	7.0
Full tilt correction	137.0/-11.5	61.9	3.4	38.7N/134.1E*	1.8	3.5
92% unfolding	137.2/-12.8	63.2	3.4	39.4N/134.4E*	1.7	3.5
Trout Creek-Bassam Park (N=7)						
In situ	162.5/-20.4	24.6	4.0	57.7N/107.5E*	2.2	4.1
Full tilt correction	162.5/-29.8	46.3	2.8	62.5N/112.7E*	1.7	3.2
68% unfolding	163.1/-27.1	62.0	2.4	61.3N/109.8E*	1.4	2.6

n/n_0 = number of samples used to calculate mean/number of samples demagnetized; N = number of sites from which sample directions were used in the fold test; other definitions are the same as for Table 1.

(Figure 1-2) show that some sites contain all three components (Figure 1-4a). Component 2 has a southeasterly and steep negative direction (Table 1), whereas component 3 has a southeasterly and shallow direction (Table 2). A regional fold test was carried out on component 3, between Minturn and Fulford (Figure 1-6) which are on the two flanks of the Sawatch Uplift. The test indicates that whereas the grouping of directions from both limbs is much better in the tilt-corrected position, the directions cross each other during unfolding. An incremental fold test using the program UNFOLD (Appendix 1) indicates that the best grouping of the directions from the two limbs occurs at about 92% unfolding but, based on *McElhinny's* [1964] fold test, the grouping is not significantly different than the 100% unfolding direction (Figure 1-7a). The results of the *McFadden and Jones* [1981] test (Figure 1-7a) indicate that the hypothesis of a common mean for the two limbs can be accepted at the 95% confidence limit between 88% and 100% unfolding and must be rejected for other unfolding values. The results of the fold test indicate that this magnetization was acquired either prior to deformation or at a very early stage of folding. The mean at 100% unfolding has a declination of 137.2°, an inclination of -12.8° with k of 63.2 and α_{95} of 3.4. The calculated paleopole position (135.4°E, 39.7°N) plots near the Late Paleozoic part of *Van der Voo's* [1989] APWP for the North American continent (Figure 1-8).

Ruedi Reservoir:

Most specimens from Ruedi Reservoir (Figure 1-2) show the presence of all three components (Figure 1-4b). Component 2 has southeasterly declinations and steep negative inclinations (Table 1). Component 3 has southeasterly declinations and shallow inclinations (Figure 1-9, Table 2). For the sub-horizontal beds from Ruedi (dips

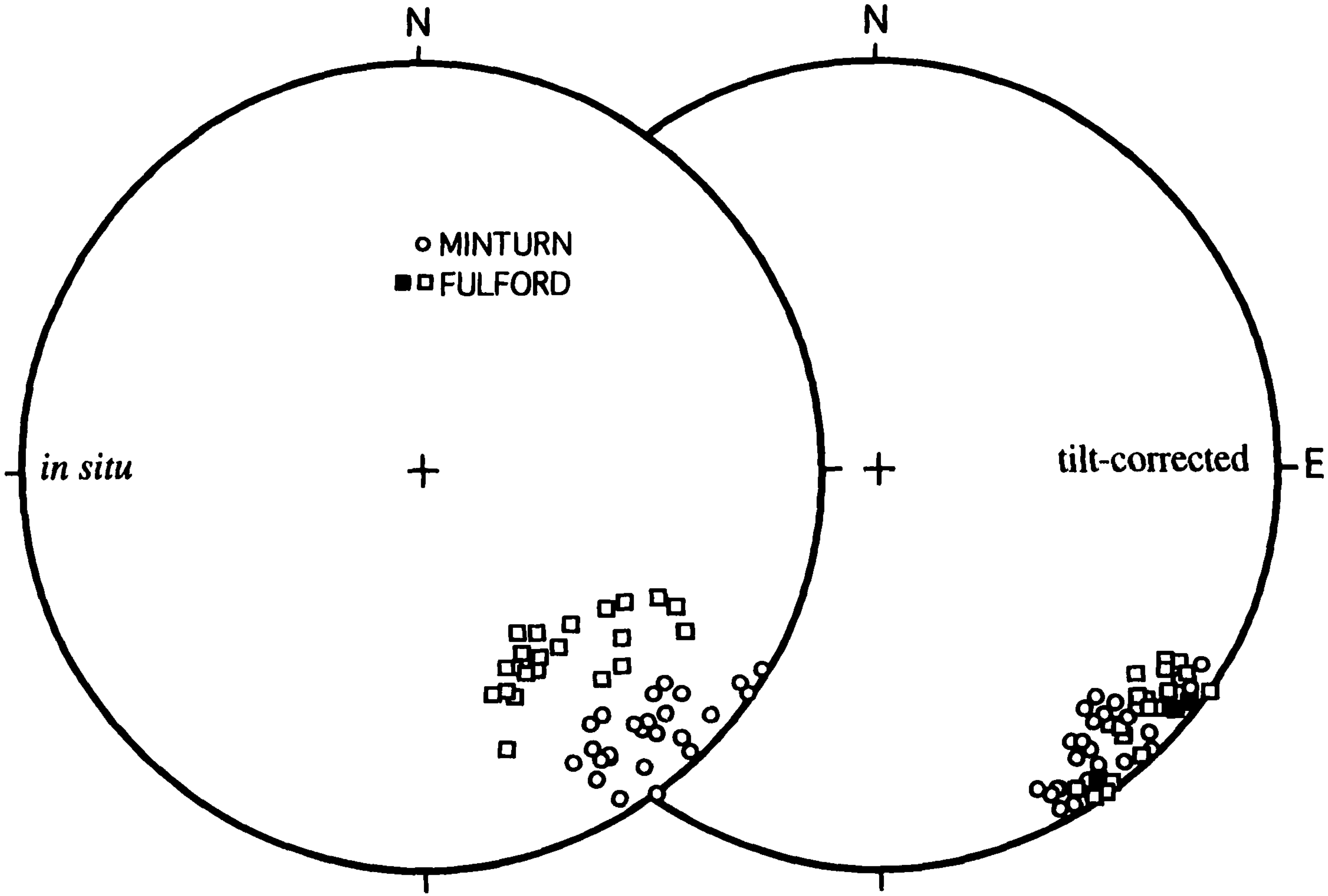

Figure. 1-6 Equal area projection of *in situ* and tilt-corrected specimen directions for component 3 from Fulford (open squares) and Minturn (open circles) . Solid symbols - lower hemisphere projection; open symbols - upper hemisphere projections.

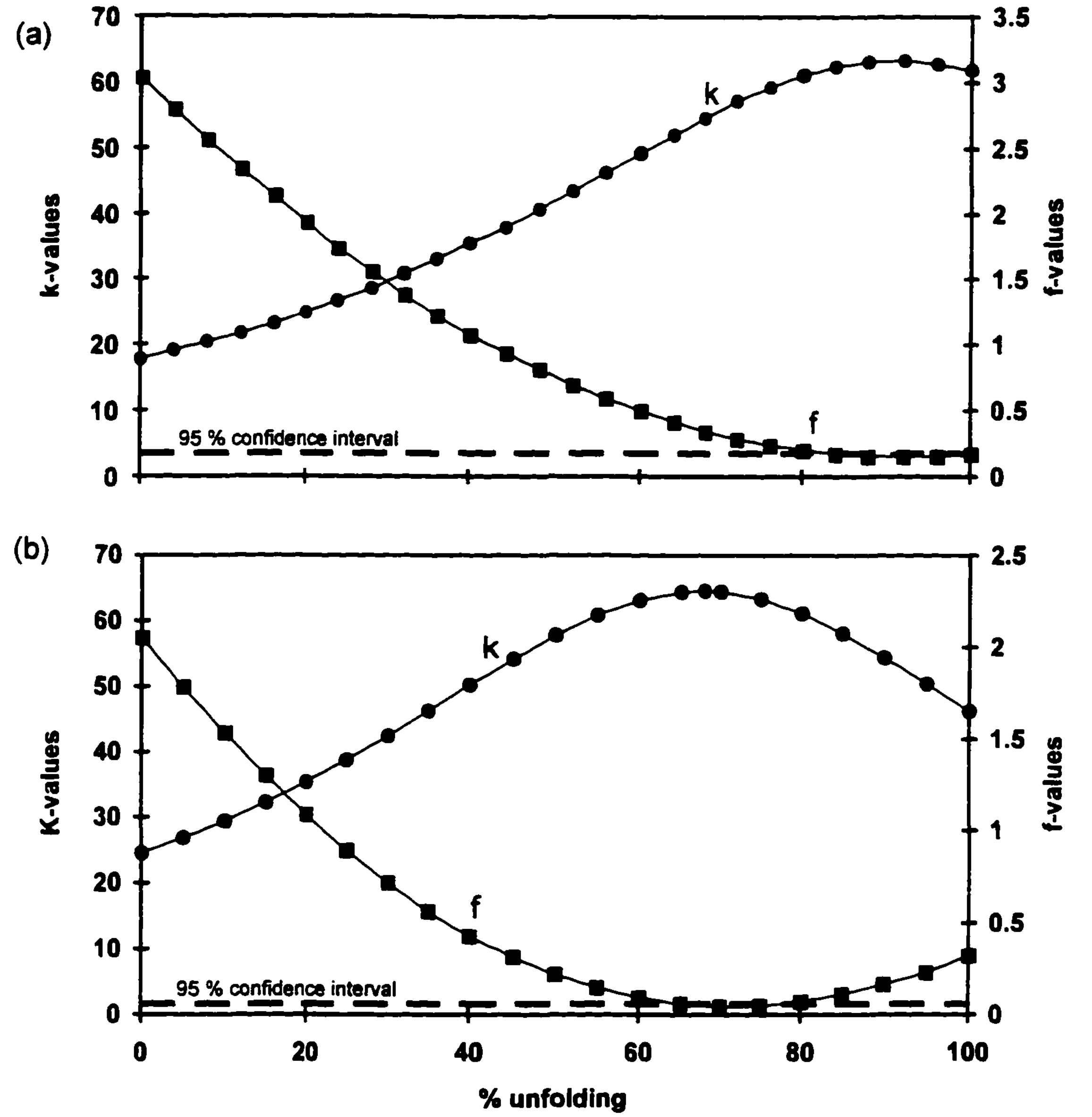

Figure. 1-7 Incremental fold test on component 3: **a.** Fulford-Minturn **b.** Trout Creek-Bassam Park. Values of the *f* [*Mcfadden & Jones*, 1981] fold test statistic and precision parameter *k* [*McElhinny*, 1964] are plotted against percentage unfolding. The 95% confidence interval [*McFadden & Jones*, 1981] for this test is also shown.

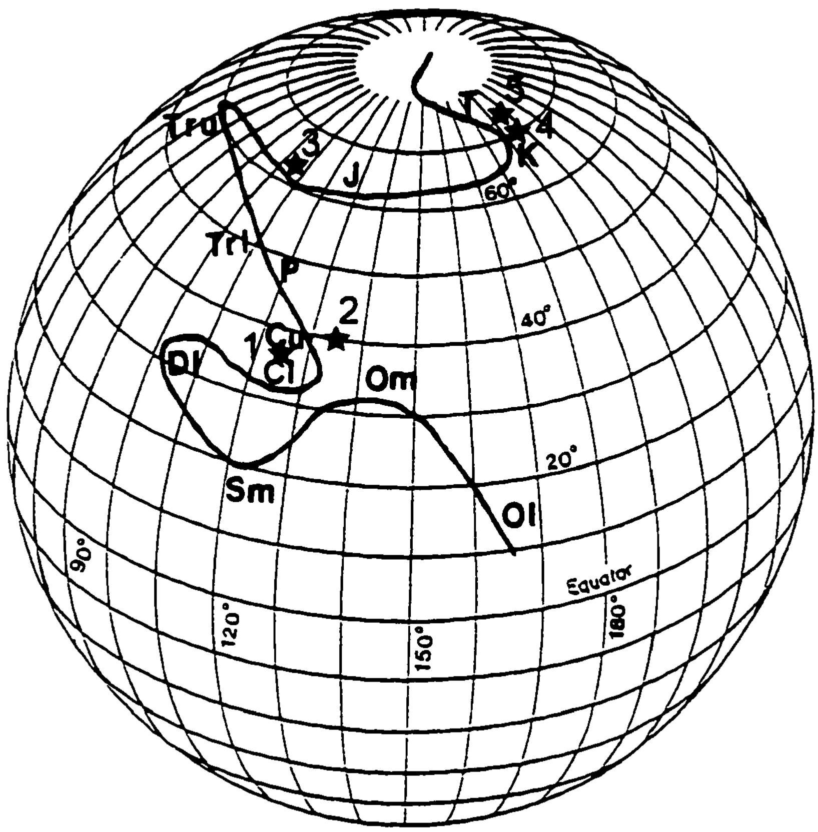

1 - Ruedi Reservoir (*in situ*)
2 - Fulford - Minturn (100% unfolding)
3 - Trout Creek - Bassam Park (68% unfolding)
4 - Miller Creek (*in situ*)
5 - Hell's Gate - Sweetwater [from *Fruit et al.*,1995]

Figure. 1-8 North American APWP for Lower Ordovician through Tertiary [*Van der Voo*, 1989]. Stars show the position of calculated paleopole positions for component 3 from various locations reported in the text.

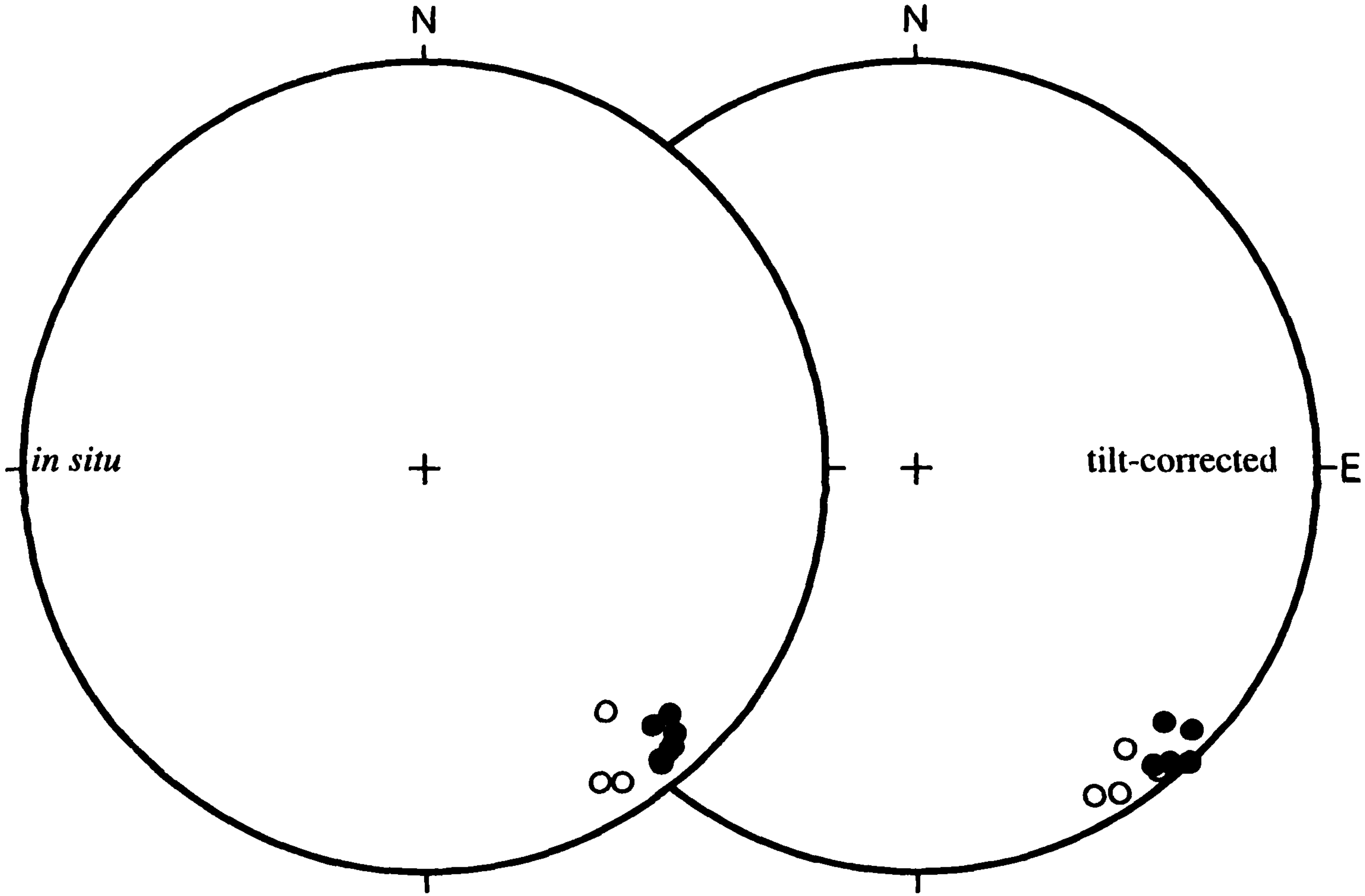

Figure. 1-9 Equal area projections of *in situ* and tilt-corrected specimen directions for component 3 from Ruedi Reservoir. Solid symbols - lower hemisphere projection; open symbols - upper hemisphere projections

of 4°-12°), the grouping of directions in the *in situ* position has a mean declination of 141.1°, mean inclination of -2.2° with the paleopole at 125.8°E, 37.8°N. In the tilt-corrected position, the mean declination is 141.0° and the mean inclination is -0.3° (k = 29.8 and α_{95} = 9.1) with the paleopole at 125.3°E, 37.0°N. The calculated paleopole for both positions plots close to the Late Paleozoic portion of the APWP (Figure 1-8).

Hell's Gate-Sweetwater:

Thermal demagnetization of Belden Formation specimens from Hell's Gate (Figure 1-2) also contain all three components (Figure 1-4c). Component 2 has southerly declinations and steep up inclinations. Component 3 has northerly declinations and down inclination (Figure 1-10, Table 2). The age of the Component 3 magnetization could not be defined at this location due to the lack of results from a fold test. However, the directions are similar to those reported for the shallow flank at the nearby Sweetwater Anticline by *Fruit et al.* [1995] which has the same bedding attitude as at Hell's Gate. *Fruit et al.* [1995] found this component to be synfolding, with the best grouping of directions at about 65% unfolding. Their calculated paleopole (175.6°W, 73.6°N) for this position plots near the Cretaceous-Early Tertiary part of the APWP (Figure 1-8).

Trout Creek-Bassam Park:

Thermal demagnetization of specimens from some Belden Formation limestone sites at Trout Creek, Bassam Park, Chubb Park, Newett and Kaufman Ridge (Figure 1-2) show well defined components 1, 2 and 3 (Figure 1-4d). In other sites, component 1 and 2 are present but component 3 is not resolvable. In those sites where components 2 and 3 are resolvable, component 2 has north-northwesterly declinations and down

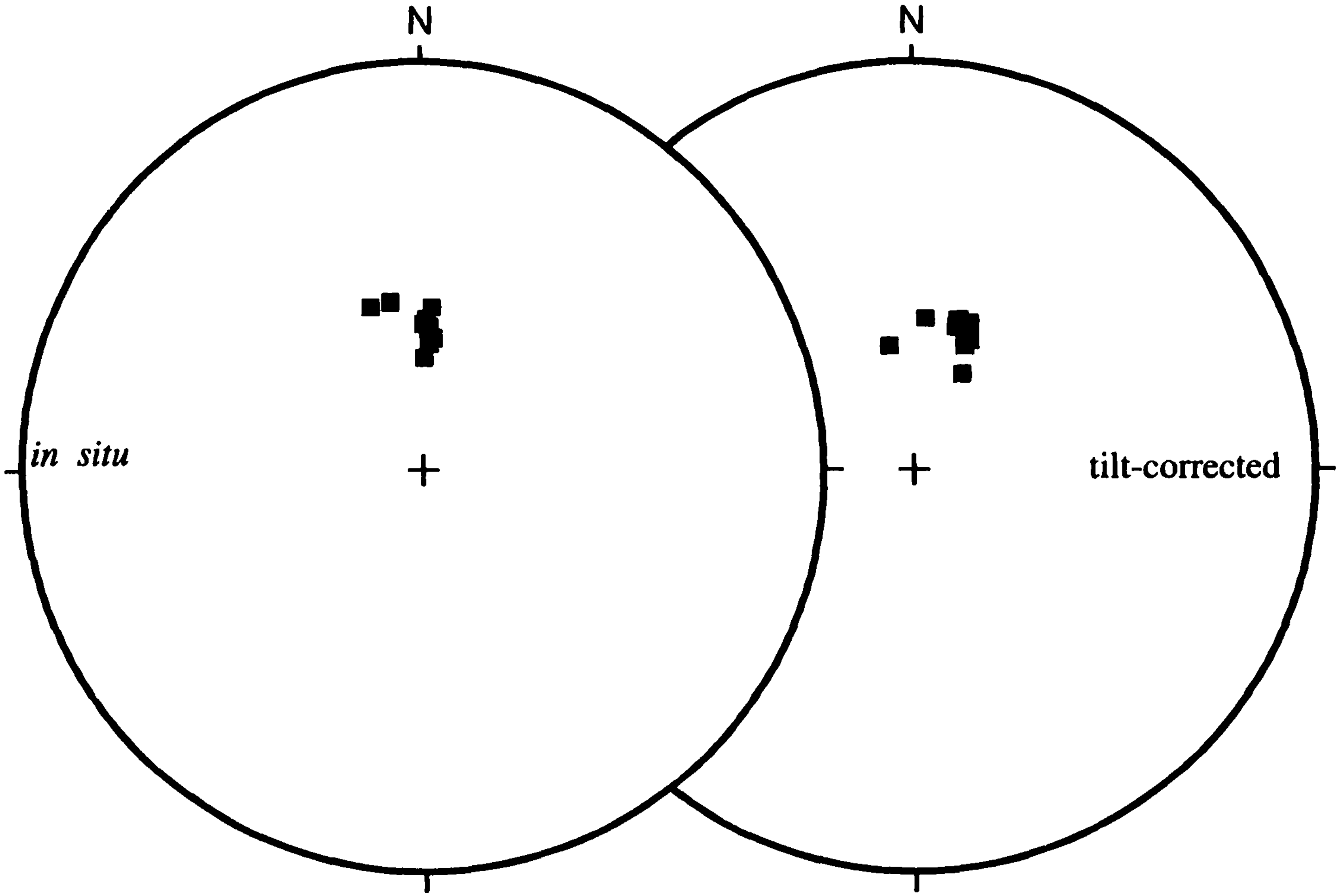

Figure. 1-10 Equal area (lower hemisphere) projection of *in situ* and tilt-corrected specimen directions for component 3 from Hell's Gate

inclination (Table 1) whereas component 3 has a southeasterly declination and up inclination (Table 2).

Component 3 directions in specimens from Trout Creek and Bassam Park were used in a regional fold test (Figure 1-11). The fold test indicates that the best grouping of the directions is neither in the *in situ* nor in the tilt-corrected position but in some intermediate position. An incremental fold test using the program UNFOLD (Appendix 1) shows that the best grouping of directions occurs at 68% unfolding (Figure 1-7b). Testing the results of the incremental fold test following *McElhinny's* [1964] method showed that the results were significant at the 95% confidence level when compared to the prefolding direction. The *McFadden and Jones* [1981] method showed that the assumption of a common mean for both limbs was valid between 65% and 76% unfolding conditions at the 95% confidence level (Figure 1-7b). At 68% unfolding, the mean declination is 163.1°, the mean inclination is -27.1°, the k is 64.6 and the α_{95} is 2.4. The calculated paleopole (109.8°E, 61.3°N) for the position of best grouping plots near the Lower Jurassic part of the APWP (Figure 1-8).

Miller Creek:

Thermal demagnetization results from Miller Creek (Figure 1-2) show that one out of the four Belden Formation (Lower Morgan) sites sampled has clearly resolved components 1, 2 and 3 (Figure 1-4e). Two of the sites have components 1 and 2 and a very weakly developed and not clearly resolved component 3. One site did not show any stable directions apart from component 1.

Component 2 has a southeasterly and up direction (Table 1) while component 3 has a north-northwesterly and down direction (Figure 1-12, Table 2). For the sub-

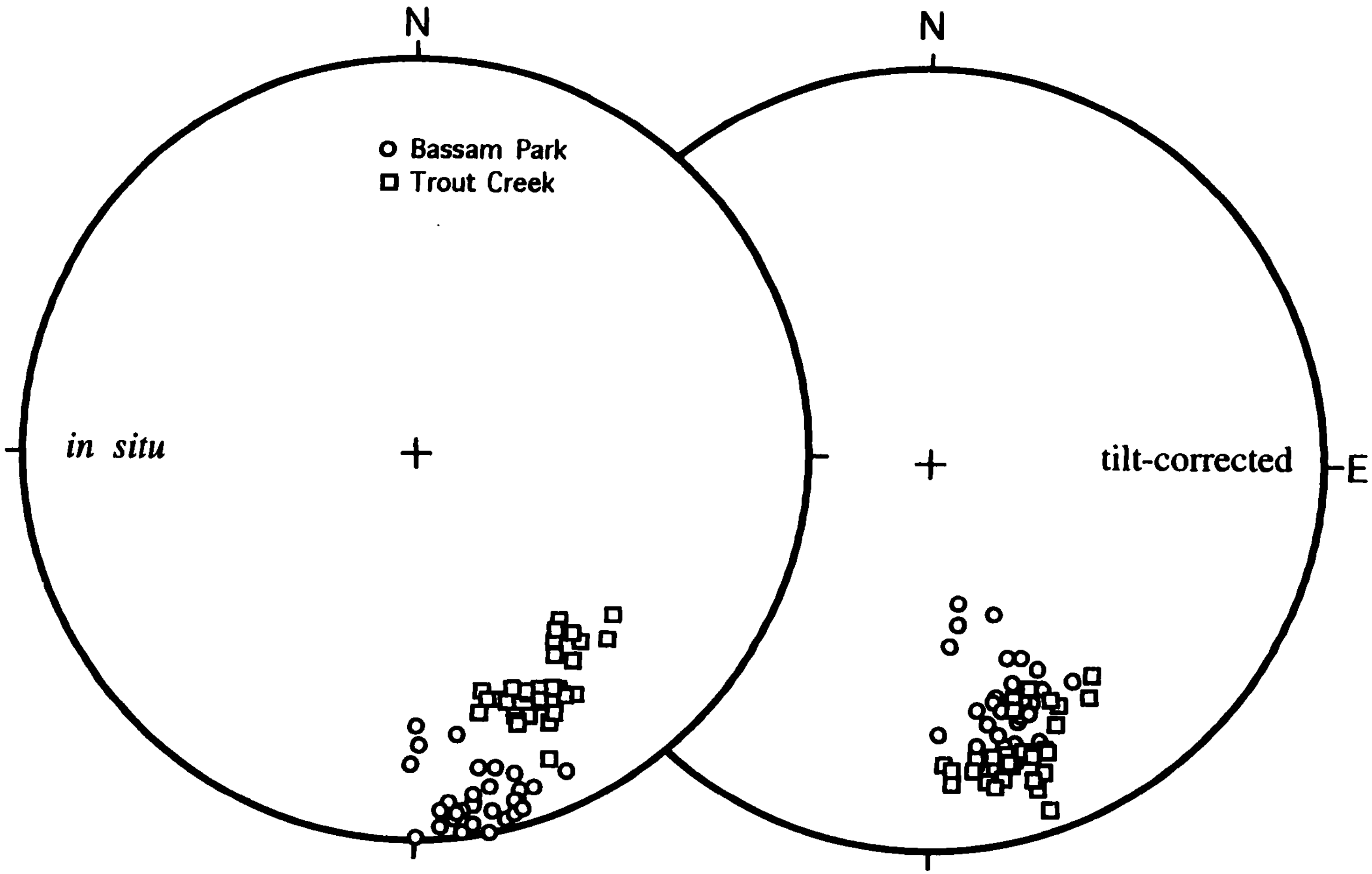

Figure. 1-11 Equal area (upper hemisphere) projection of *in situ* and tilt-corrected specimen directions for component 3 from Bassam Park (circles) and Trout Creek(squares). Directions cross during unfolding.

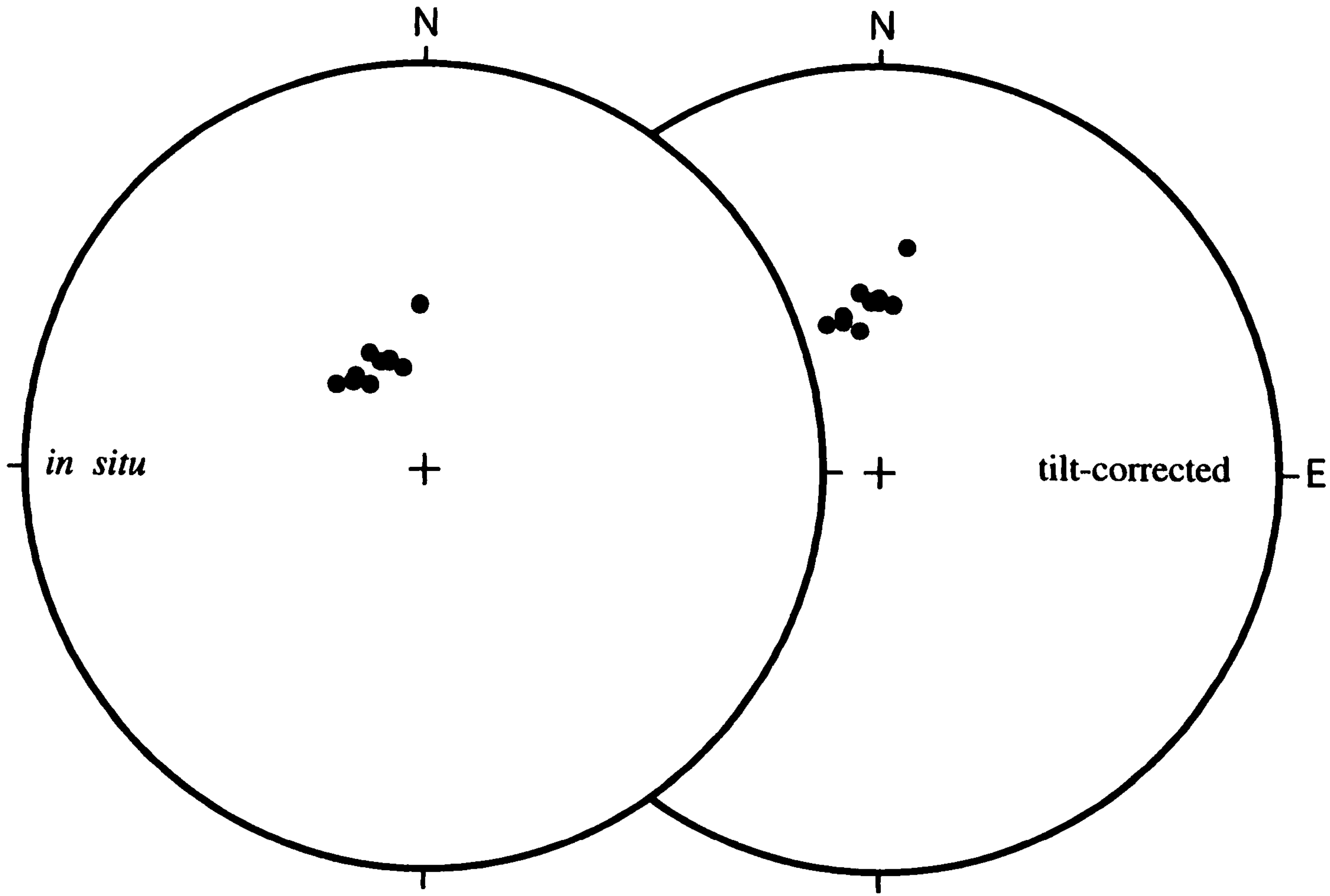

Figure. 1-12 Equal area (lower hemisphere) projection of *in situ* and tilt-corrected specimen directions for component 3 from Miller Creek .

horizontal beds from Miller Creek (dips of 12-15°), the grouping of directions in the in-situ position has a mean declination of 336.0°, a mean inclination of 66.8°, and a paleopole at 160.6°W, 70.6°N. The calculated paleopole for *in situ* position plots near the Cretaceous part of the APWP (Figure 1-8), while the pole for the tilt-corrected position falls far off the path.

Other areas

Most of the Belden Formation specimens from other locations within Central Colorado and the South Park area (Figure 1-2) have components 1 and 2, although they either do not have the high temperature component 3 (e.g. East Elk Creek, Crooked Creek Reservoir, Rifle Canyon) or, if present, the component is very weak and noisy (e.g., Deep Creek; Table 2).

For Glenwood Springs samples (Figure 1-2), demagnetization results show the presence of three components based on unblocking temperature ranges. While component 1 shows its usual direction, the other two components have unusual directions (Tables 1 & 2) and the calculated paleo-poles do not plot in the vicinity of the APWP. It is reasonable to assume that such unusual directions are the result of a complicated history of structural deformation in this area during the Laramide Orogeny [e.g. *Bass & Northrop*, 1963], presumably after the magnetization was acquired.

Thermal demagnetization of the specimens from most sites in the Gunnison Basin (Figure 1-2) contain a clearly resolved component 3 in addition to components and 2. For most sites, Component 2 has a southerly and steep negative or northerly and steep positive direction (Table 1). Component 3 has a consistent southwesterly and steep negative (in-situ) direction at four sites (Table 2). The paleopoles for this component do not plot anywhere close to the APWP. The paleolatitudes are consistent with a Late Cretaceous/ Early Tertiary age and the offset from the path could be due to Laramide deformation This may have been aided by deformation during emplacement of intrusions in the area [e.g., *McFarlan*, 1961; *Bartleson et al.*, 1968].

At Switchback (Figure 1-2), thermal demagnetization shows the presence of all three components. Component 2 has a southerly and steep up direction. However, Component 3 has no consistent direction between sites, possibly due to structural complications related to the presence of a Laramide fault very close to this site.

At Juniper Mountain and Cross Mountain in northwestern Colorado (Figure 3) the carbonate are light gray or pale colored in comparison to the dark gray color at other areas. Thermal demagnetization of Lower Morgan (Belden Formation) samples from Juniper Mountain and Cross Mountain showed that specimens from most sites have very low NRM intensities and do not carry a stable direction other than Component 1.

2. Rock Magnetic Results

IRM Acquisition and thermal decay of IRM

The IRM acquisition of Belden Formation specimens from different sites indicate that most samples achieve near saturation magnetization by about 200 mT (Figure 1-13a) suggesting that a low coercivity mineral is the dominant magnetic mineral present in these rocks. Some IRM curves show a slight increase above 200 mT, indicating that a high coercivity mineral, most likely hematite, is present in some samples.

Thermal demagnetization of three-component saturation IRM [*Lowrie*, 1990] shows that in most specimens the magnetization of all three components decays by

580°C. This indicates magnetite as the major magnetic mineral present in these specimens (Figure 1-3b). In specimens containing an additional high coercivity mineral as shown by IRM acquisition, a portion of the hard component persists up to 680°C, indicating the presence of hematite.

Hysteresis

Hysteresis loops generated from Belden Formation samples from different sites, after they have been suitably corrected for high field diamagnetism or paramagnetism, all have a "wasp-waisted" nature (Figure 1-14), indicating a bimodal distribution of coercivity [*Jackson*, 1990]. Values of coercivity (Hcr/Hc) and remanence (Mrs/Ms) plot outside the experimental boundaries of *Day et al.* [1977] for single domain (SD), pseudo-single domain (PSD) and multidomain (MD) grains from synthetic samples (Figure 1-15), indicating once again a bimodal distribution in coercivity. The anomalous pattern of Hcr/Hc and Mrs/Ms values are consistent with the reported trends for other remagnetized carbonate rocks [*Jackson*, 1990; *Channell & McCabe*, 1994].

The "wasp-waisted" nature of the hysteresis loops has been attributed to mixing of "hard" and "soft" magnetic fractions [e.g., *Roberts et al.*, 1995; *Tauxe et al.*, 1996]. In the case of Belden Formation samples, these can be either two minerals with contrasting coercivities (e.g. hematite and magnetite) or different grain sizes of the same mineral (e.g. SD+MD, SD+superparamagnetic). Although some hematite is present, as indicated by IRM analysis, based on comparision with other studies [e.g., *Roberts et al.*, 1995], its amount is not deemed sufficient to affect the hysteresis properties, especially in the presence of magnetite with its high magnetic moment. Hence, the wasp-

(a)

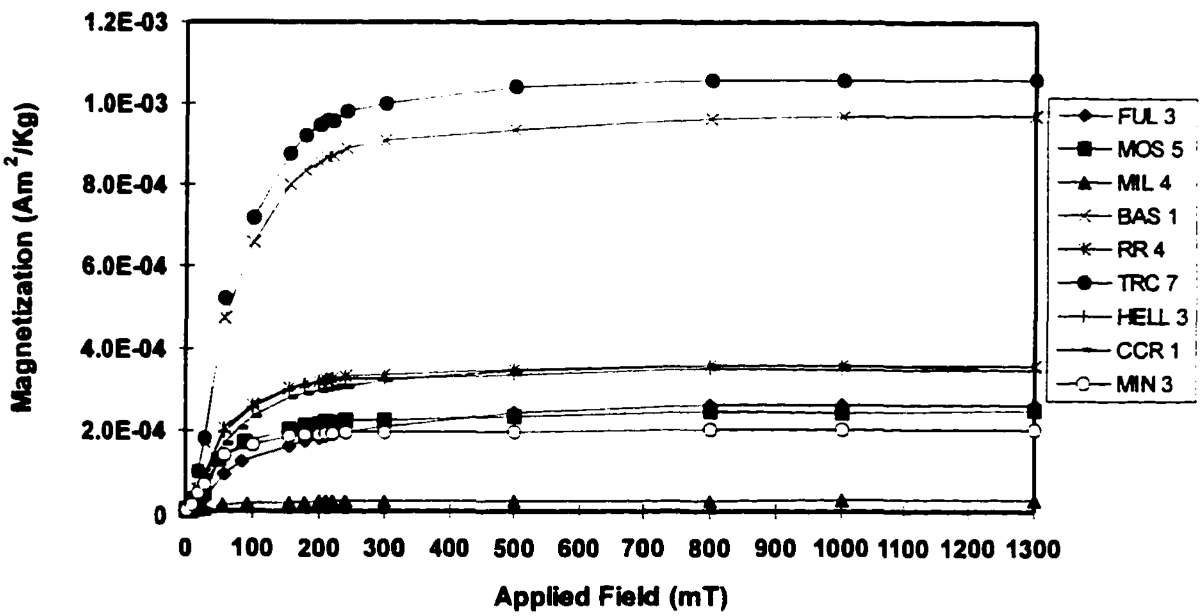

Figure. 1-13 (a) IRM acquisition curves for representative Belden Formation specimens from the study area.

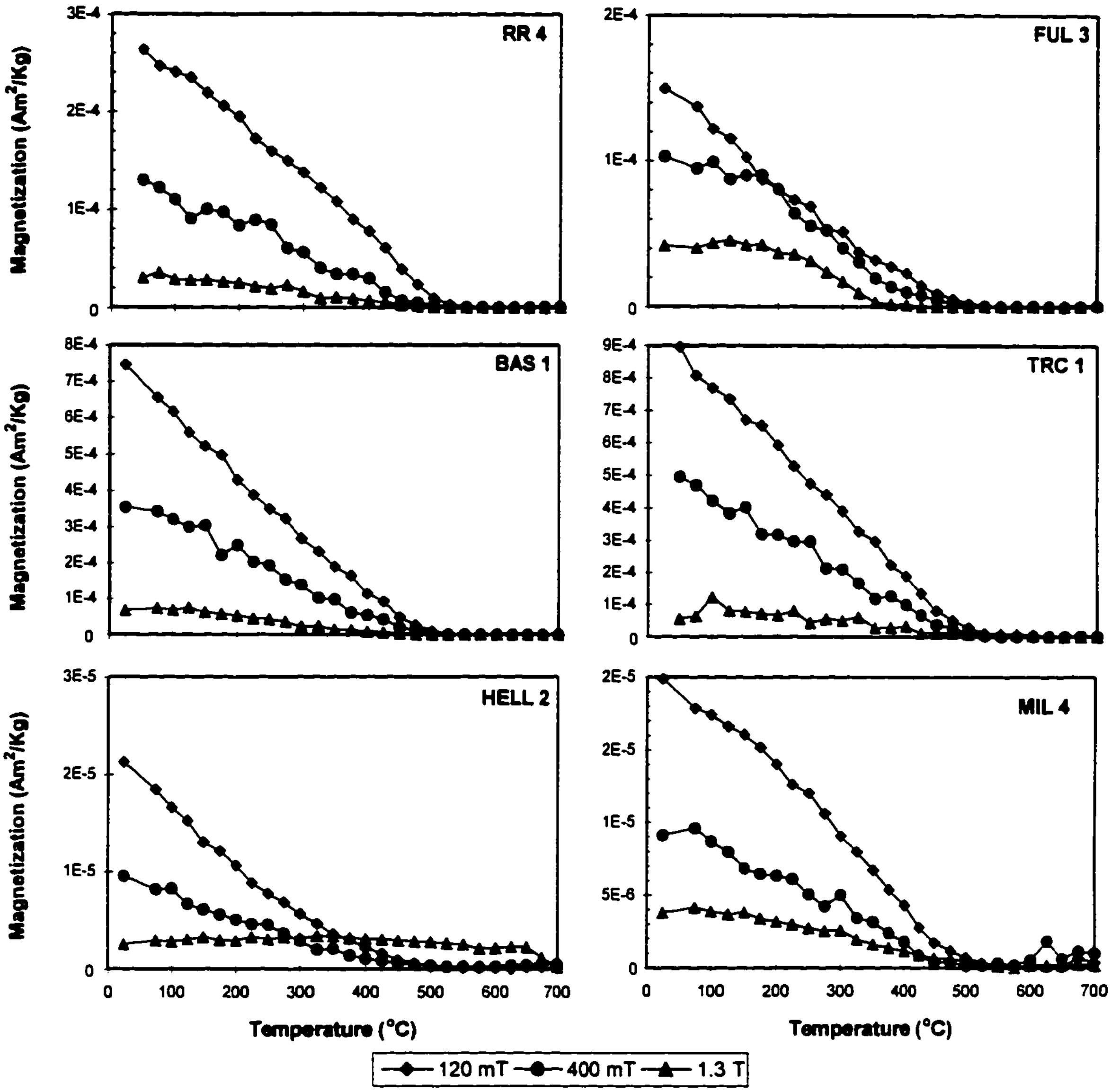

Figure. 1-13 (b) Thermal demagnetization of a three-component IRM for representative Belden Formation specimens.

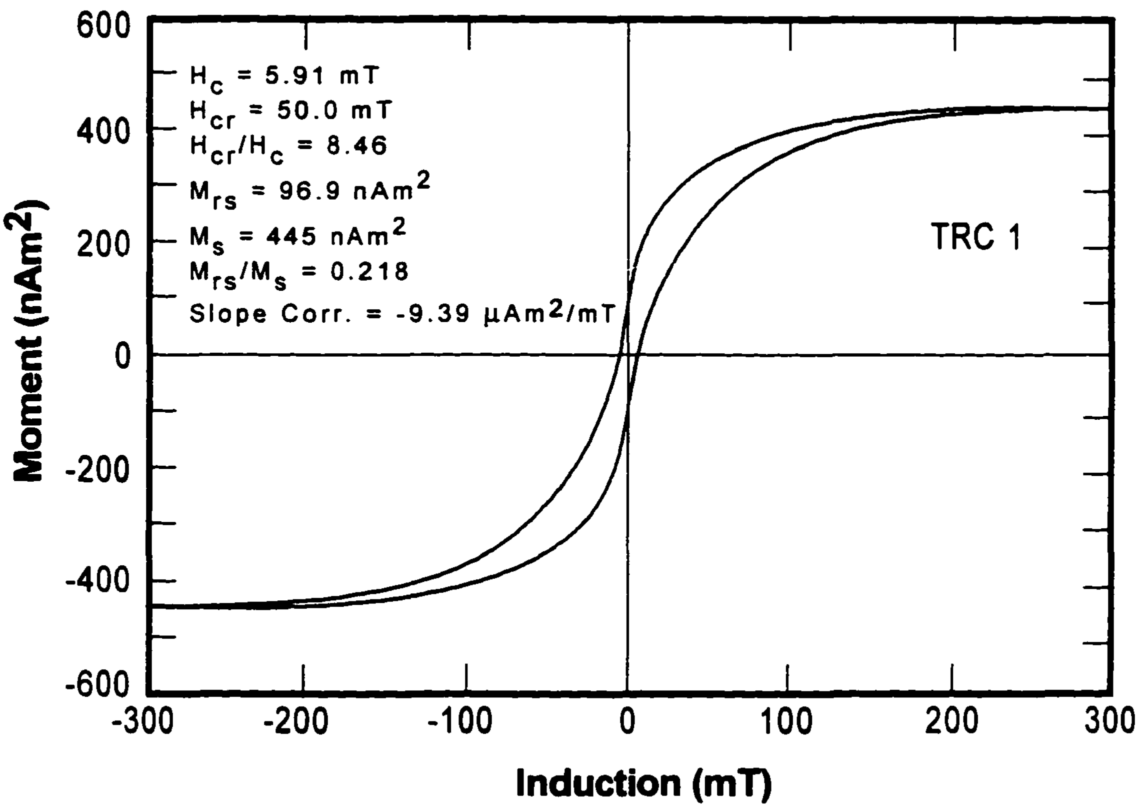

Figure. 1-14 Typical 'wasp-waisted' hysteresis loop for a representative Belden Formation sample.

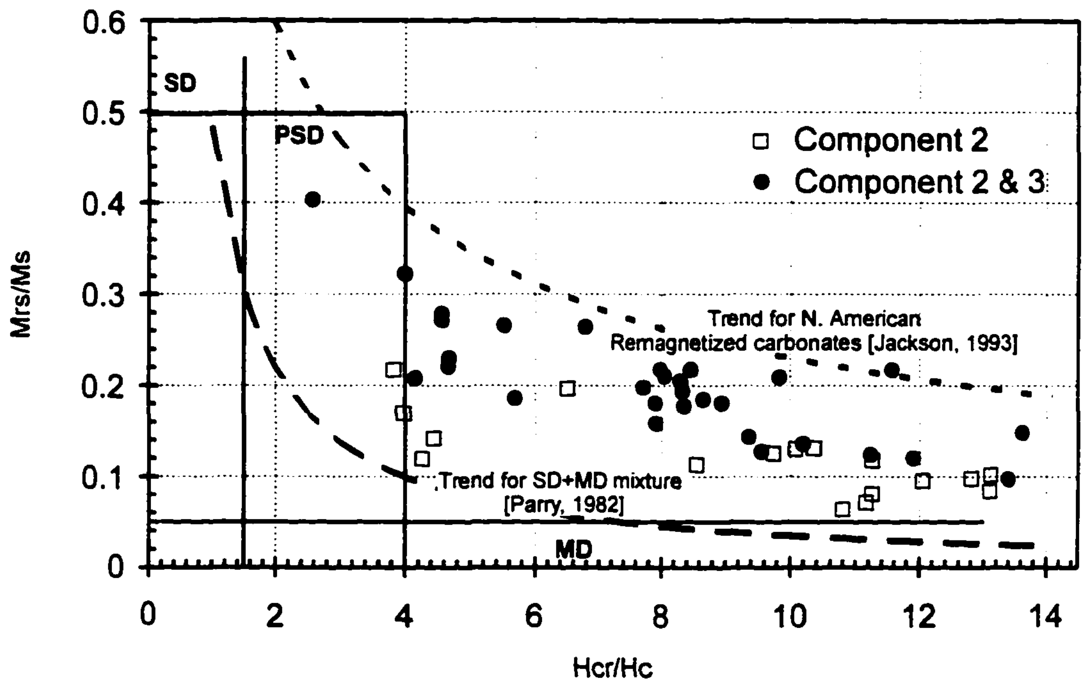

Figure. 1-15 Hysteresis parameters for Belden Formation samples. Mrs - saturation remanence; Ms - saturation magnetization; Hcr - remanent coercivity; Hc - coercive force. Single domain (SD), pseudo-single domain (PSD) and multidomain (MD) fields after Day et al. [1977]. Data for SD+MD mixture [*Parry*, 1982] and remagnetized carbonates [*Jackson et al.*, 1993] is also shown.

waistedness of the Belden Formation samples must be due to the presence of different grain size fractions of magnetite in the rocks.

Analysis of the hysteresis parameters for the Belden Formation samples show that the specimens from sites carrying components 2 and 3 have higher M_{rs}/M_s values (mean = 0.238, standard deviation = 0.06, n = 15) than the specimens from sites with only component 2 (mean = 0.121, standard deviation = 0.03, n = 24). These values for the rocks with both components 2 and 3 are high when compared to values reported by *Parry* [1982] for a synthetic mixture of the SD plus MD grains but are consistent with results for remagnetized carbonate [e.g., *Jackson*, 1990; *Channell and McCabe*, 1994; *McCabe and Channell*, 1994]. These results suggest that limestone with both Components 2 and 3 contain a mixture of SD and MD or SD and superparamagnetic (SP) magnetite [e.g., *Jackson*, 1990; *Jackson et al.*, 1993; *Chanell and McCabe*, 1994]. Following *Jackson's* [1990] argument, the SD magnetite is interpreted to carry Component 3. The M_{rs}/M_s values for the rocks with only Component 2 are closer to the values reported by *Parry* [1982] for a mixture of SD and MD grains. This suggests that the magnetite grains in these rocks are probably coarser (PSD or MD) than those in the rocks with Components 2 and 3.

Low Temperature Demagnetization and AF cleaning of samples

Selected Belden Formation samples from sites having Component 3 were subjected to magnetic "cleaning" procedures before being thermally demagnetized to test for a modern viscous overprint on the high temperature component. Some workers [e.g., *Xu and Dunlop*, 1994] have reported that synthetic samples showed that remanence carried by MD magnetite grains is not removed at low unblocking temperatures of about 250°C as is commonly assumed, but rather it persists up to temperatures close to the Curie Point of magnetite (580°C). Thus, any remanence carried by MD grains (modern VRM?) in rocks can potentially overlap and contaminate the directions of the higher temperature components.

When magnetite grains are cooled below the Verway transition temperature (110-120°K) and isotropic point (130°K), their crystalline habit changes from cubic to rhombic and causes unpinning of the domain walls in MD grains and loss of any remanence carried by these grains [*Dunlop and Argyle*, 1991; *Halgedahl and Jarrard*, 1995]. If the samples are then allowed to warm up to room temperature in zero-field conditions so that the crystal habit of the magnetite grains changes back to cubic, MD grains are not expected to regain their initial remanence. The AF cleaning, which involves demagnetization at low fields of about 10 mT, generally demagnetizes low coercivity MD grains of magnetite and removes any VRM carried by these grains [e.g. *Schmidt*, 1993]. *McClelland* [1996] reports, however, that LTD and AF cleaning are not effective in removing a remanence in some MD grains.

Thermal demagnetization results from specimens subjected to prior LTD and AF cleaning show that the directions obtained are not statistically different from those obtained by thermal demagnetization without such treatment (Figure 1-16). This may indicate that component 3 is not overprinted by a modern VRM, although, due to questions about the effectiveness of LTD and AF cleaning [e.g. *McClelland*, 1996], this test cannot be considered conclusive. Further, since component 3 is observed not to be affected by LTD cleaning, following *Halgedahl and Jarrard* [1995], it is inferred to be

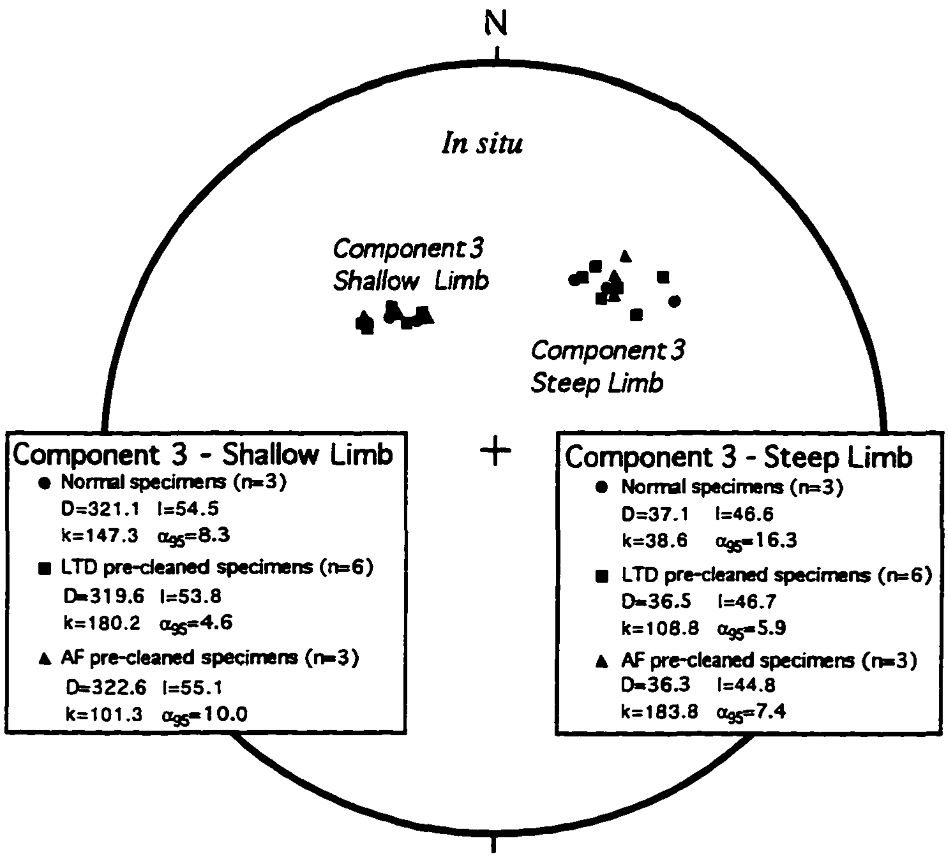

Figure. 1-16 Results of thermal demagnetization of normal, LTD and AF pre-cleaned Belden Formation specimens from the Sweetwater Fold. Equal area (lower hemisphere) projection of component 3 specimen directions from both limbs of the fold are shown.

probably carried by SD grains. This is consistent with the interpretation based on the hysteresis results.

3. Geochemistry and Petrographic Results

Strontium ($^{87}Sr/^{86}Sr$) isotope analysis

Results of strontium isotope ratio analysis of the micro-sampled calcite cement from selected Belden Formation sites carrying component 3 from different locations (Figure 1-17, Appendix 2) indicate elevated, radiogenic values of $^{87}Sr/^{86}Sr$, relative to Pennsylvanian co-eval seawater values of 0.70820-0.70850 [*Burke et al.*, 1982]. This indicates that radiogenic fluids have migrated through and altered the Belden Formation limestone. However, comparison of the intensity of component 3 from these locations with their $^{87}Sr/^{86}Sr$ values (Figure 1-17) do not indicate any systematic variation. The degree of alteration of the rocks is not related to the intensity of the component 3 present in these rocks. These results suggest that the component 3 magnetization is not related to alteration and mineralization by radiogenic (orogenic?) fluids.

Petrographic Study

Thin section study of Belden Formation carbonate samples under transmitted light show the presence of opaque minerals ranging in size between 10-250 μm (Appendix 3). Analysis of these opaque minerals under reflected light indicate the presence of numerous pyrite grains (Figure 1-18). Many of these pyrite grains contain alteration rims of iron-oxide. In many cases, the pyrite grains are completely pseudomorphed by these iron-oxides. Similar iron-oxide grains have been reported from studies of

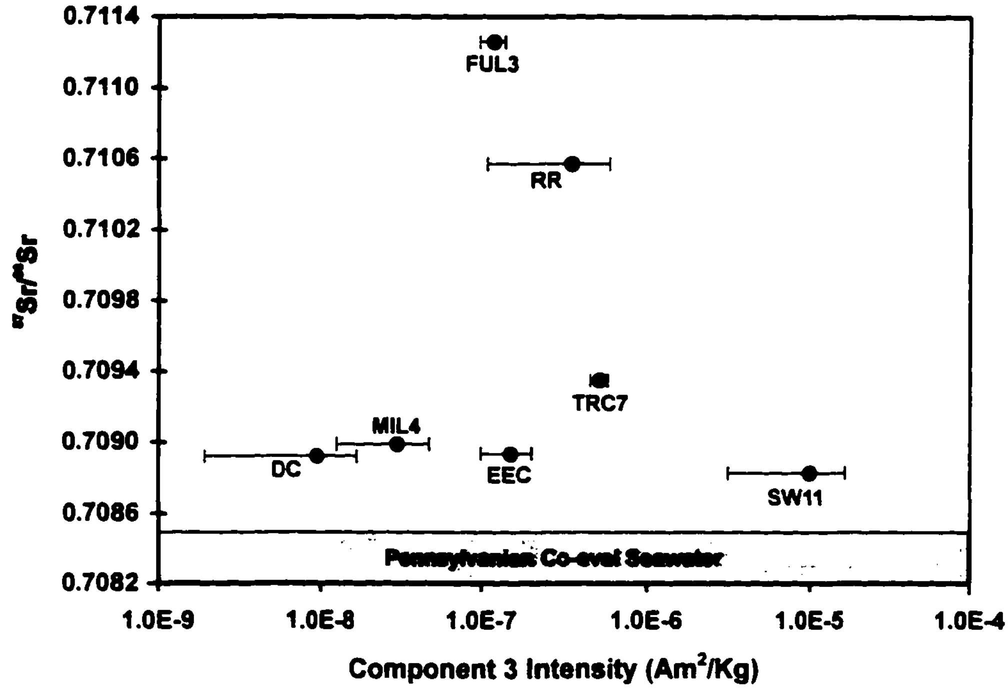

Figure. 1-17 Values of $^{87}Sr/^{86}Sr$ versus component 3 intensity for selected Belden Formation sites from the study area. Horizontal axis is on a log scale. Also shown are the values for Pennsylvanian co-eval seawater are from Burke et al. [1982]. Error bars = ± 1 standard deviation. SW11-Sweetwater (n=24); RR-Ruedi Reservoir (*n*=9); DC-Deep Creek (*n*=5); MIL4-Miller Creek (*n*=8); TRC7-Trout Creek (*n*=13); FUL3-Fulford (*n*=9); EEC-East Elk Creek (*n*=8); *n* is the number of samples used in calculating mean and standard deviation of component 3 intensity from each site. Number of samples and range of $^{87}Sr/^{86}Sr$ values (for sites from which multiple samples were analysed): DC - 4, 0.708822-0.70918; RR - 2, 0.710489-0.710572; SW - 2, 0.708808-0.708828; EEC - 2, 0.708638-0.708942. Data from EEC, which does not have component 3, is plotted versus NRM intensity.

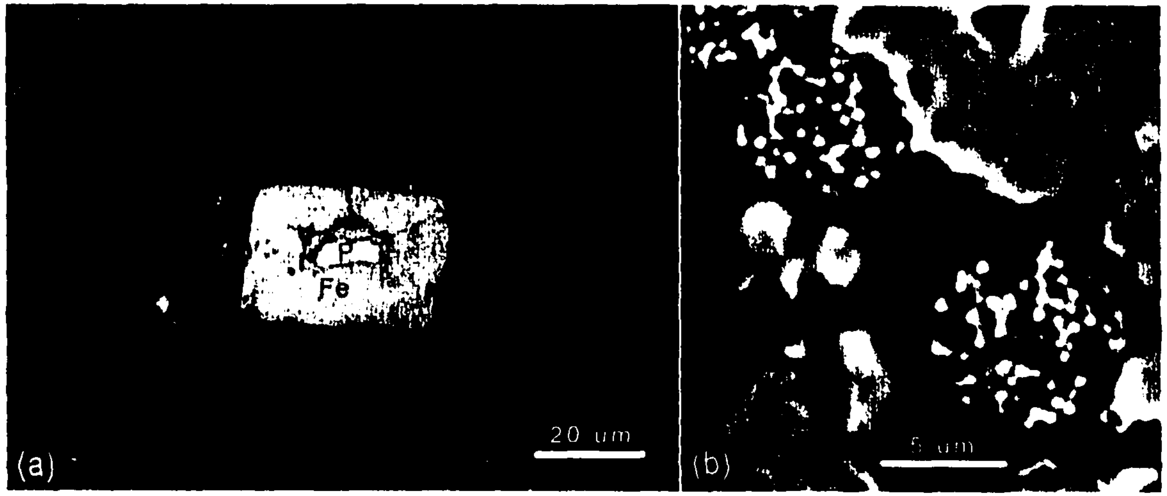

Figure. 1-18 Pyrite replacement features from Belden Formation samples: **(a)** Reflected light photomicrograph showing pyrite (P) replaced by iron-oxides (Fe). Both hematite and magnetite were identified from similar features from Sweetwater Anticline. **(b)** Backscattered electron (BSE) image showing a pseudoframboidal texture. EDAX analysis show only iron to be present in the framboids. Such texture has been associated with magnetite by *Suk et al.* [1993].

Appalachian carbonate and some of them have been identified as mixtures of dominantly magnetite with subordinate amounts of hematite [e.g., *Lu et al.*, 1990; *Suk et al.*, 1993]. Scanning transmission electron microscope (STEM) analysis of similar iron-oxide rims from Belden Formation carbonate samples from Sweetwater by *Fruit et al.* [1995] show these rims to be mixtures of magnetite and hematite. It is interpreted that similar features seen in the Belden carbonate samples from different locations across the basin are also a mixture of magnetite and hematite.

Contact vein tests:

In order to test for the possible influence of fluids on magnetization, contact tests around veins [e.g., *Elmore et al.*, 1993b; *Fruit et al.*, 1995] were carried out on the Belden Formation rocks. Strontium ($^{87}Sr/^{86}Sr$) isotope values indicate that regionally, the Belden Formation was affected by radiogenic fluids (orogenic?) that could have potentially caused a remagnetization. Numerous calcite veins present in the Belden Formation lithologies indicate the conduits for such fluid flow. If these fluids caused magnetite authigenesis, the magnetite might be expected to be more abundant next to the veins. Thus, rocks with a large number of calcite veins would be expected to show a higher NRM intensity.

Using hand specimen analysis and petrographic studies, Belden Formation samples from two localities were divided into five categories based on the presence/absence and abundance of calcite veins in the rocks (Figure 1-19, a & b). The average volume percentage of vein material was estimated from measurements made on several representative samples from each group. If magnetite was created due to fluid

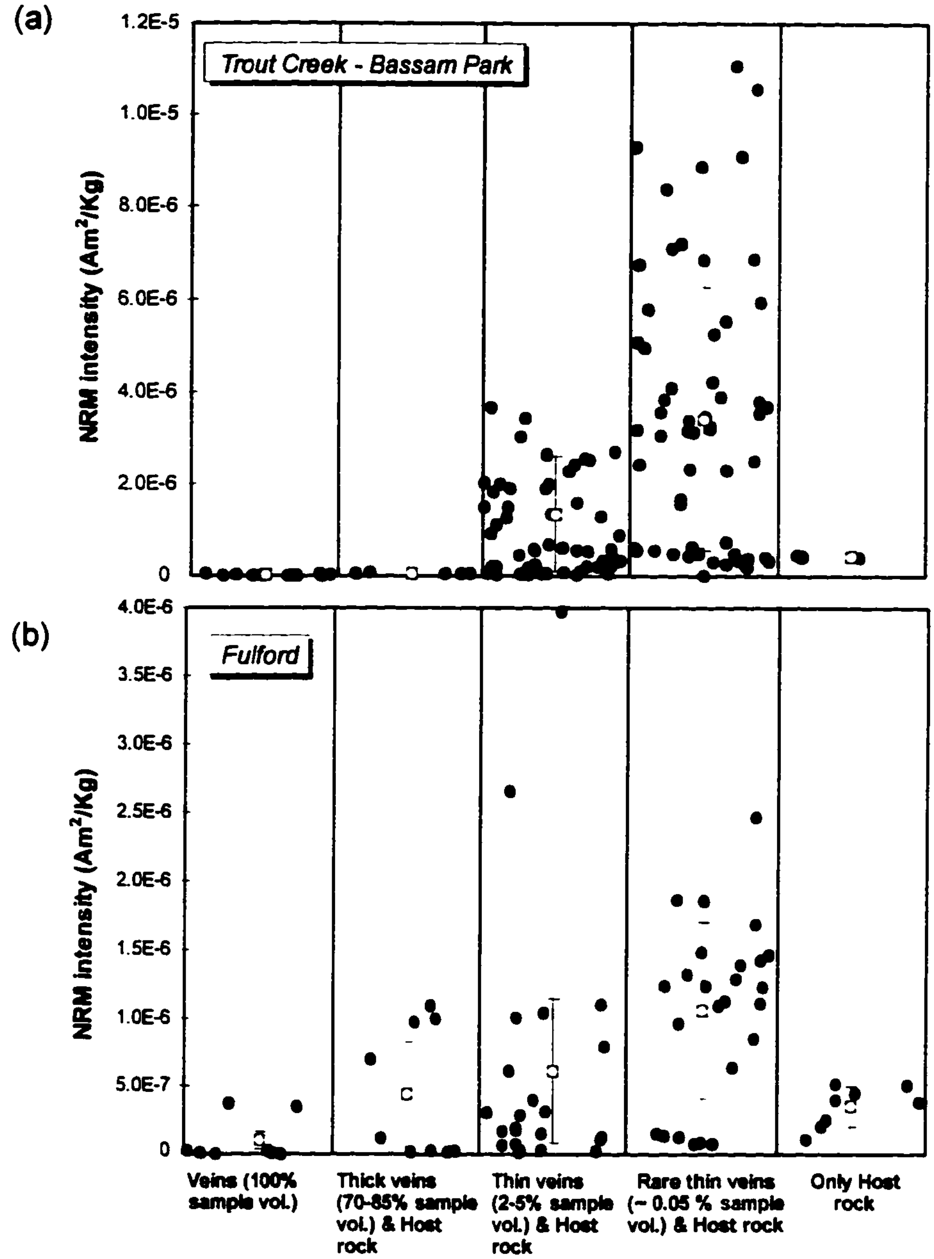

Figure. 1-19 Contact (vein) tests from (a). South Park (Trout Creek and Bassam Park) and (b). Fulford. Samples from these areas are divided into 5 categories based on their calcite vein characteristics. These categories are **veins**, for samples consisting almost 100% of vein materials; **thick veins and host rock**, for carbonate samples with few thick (up to 5mm) calcite veins; **thin veins and host rock**, for samples with multiple thin (1mm. or less) veins; **rare thin veins and host rock**, for samples with isolated very thin calcite veins (requiring microscopic identification)and **only host rock**, for rocks with no identifiable calcite veins. Mean NRM intensities and error bars (error bars ± 1s.d.) for different categories from the two locations are shown. Means without error bars have standard deviations less than the height of the symbols.

rock interaction, it is reasonable to expect higher magnetization intensity in samples from second and third group. Analysis of the NRM intensities from each group indicates that the rocks with calcite veins do not show higher NRM intensities than those which have fewer or no veins. This is contrary to what might be expected if the radiogenic fluids responsible for precipitating the vein calcites were also involved in causing the magnetization. The results of these tests suggest that the mineralizing fluids were not responsible for the CRM in the Belden Formation. This interpretation is consistent with that of *Fruit et al.* [1995].

Test for lithologic controls on magnetization:

As indicated above, Belden Formation outcrops typically consist of repetitive cycles of different carbonate lithologies ranging from mudstone to packstone. *Fruit et al.* [1995], in their study of the Belden Formation at Sweetwater, report a lithologic control on the CRM, with the packstone showing the strongest remanence. In an attempt to test for a possible basinwide lithologic control on magnetization, the samples in the present study were sorted into five categories following *Dunham's* [1962] classification (Appendix 3). After sorting into these groups, the samples were compared with respect to their NRM intensities to see if there was any possible trend or pattern (Figure 1-20). The mean NRM intensities from mudstone (1.13E-6 Am^2/Kg), packstone (1.63E-6 Am^2/Kg), and wackestone (4.42E-6 Am^2/Kg), are about an order of magnitude higher than those from boundstone (2.03E-7 Am^2/kg), and grainstone/crystalline limestone (2.68E-7 Am^2/kg). However, between the first three groups there is not much difference in the mean NRM intensities. All the three groups have a big spread in the NRM

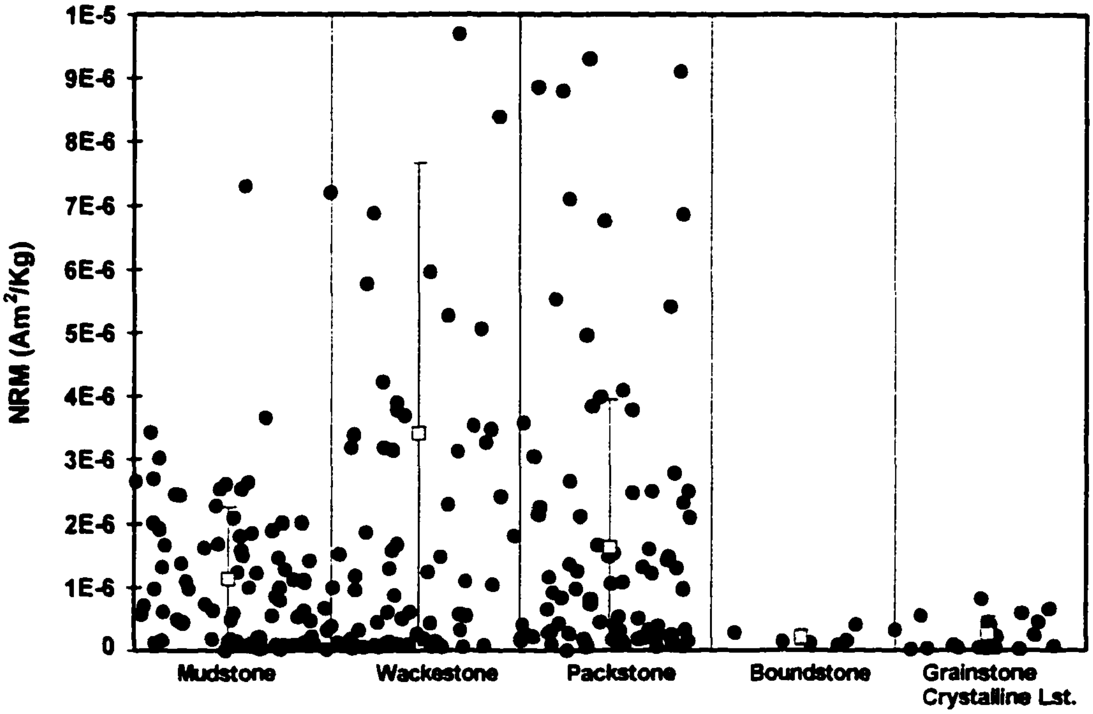

Figure. 1-20 Test for lithologic control on magnetization (NRM intensities plotted versus rock type). Open squares - mean NRM intensity for each rocktype. Error bars ± 1s.d..

intensity values and it is not possible to conclude that there is any clear lithologic control on magnetization.

TOC and T_{max} Analysis:

Results of the TOC analysis of selected dark colored Belden Formation samples show most of the analyzed samples have low TOC values, mostly below 0.5 weight percent organic carbon (Appendix 4). Because the values are so low, they are not reproducible and we cannot make any inference about a relation between TOC and the magnetization intensity. The high T_{max} values of all the analyzed samples indicates that they are mature to overmature rocks. This is consistent with the finding of *Whalen et al.* [1990] from their study of the Belden Formation samples from some locations in Colorado.

DISCUSSION

Component 2 is interpreted as a thermoviscous remanent magnetization (TVRM). Maximum unblocking temperatures (400°C) from some locations are consistent with acquisition of this component during cooling from modeled burial temperatures [*Nuccio et al.*, 1989], based on the theoretical blocking temperature-relaxation time curves for SD magnetite [*Pullaiah et al.*, 1975] and experimental evidence presented by *Smith and Verosub* [1994]. Maximum unblocking temperatures from several locations, however, are more consistent with experimental evidence presented by *Kent* [1985] which assumes the presence of MD magnetite. The TVRM interpretation for this component is consistent with other reported occurrences of a similar component in Colorado [e.g., *Horton et al.*, 1984].

The origin of component 3, which resides in magnetite and has different directions in the study area, is a crucial issue. A thermoviscous remagnetization is not considered likely because burial temperatures were too low, based on the maximum unblocking temperatures (580°C) and a consideration of the theoretical blocking temperature-relaxation time curves for magnetite [e.g., *Pullaiah et al.*, 1975]. A detrital remanent magnetization (DRM) or a postdepositional DRM could apply to the Belden Formation in the Minturn-Fulford and Ruedi Reservoir areas where the component is Late Paleozoic in age. This is not considered likely, however, because the characteristics of the magnetization at these localities are the same as for the areas with a clearly secondary time of remanence acquisition.

Component 3 is, therefore, interpreted to be a CRM. The presence of abundant pyrite grains with replacement rims of iron-oxides (Figure 1-18) is consistent with a chemical origin for the component. The similarity in the unblocking temperature ranges and rock magnetic characteristics at the different locations suggests that this component was caused by the same chemical remagnetization process. In order to explain the widespread origin of this CRM, a diagenetic process which occurs on a basinwide scale is needed.

One possible mechanism for creating such a CRM is mineralization by migrating orogenic fluids [e.g., *Oliver*, 1992]. Previous workers [e.g., *McCabe and Elmore*, 1989] have inferred such a mechanism based on spatial and temporal connection between CRMs and orogenic belts and orogeny. There is a spatial connection with the Belden CRM and the orogenic belts/orogeny in all areas except South Park (Figure 1-2) where the lower Jurassic pole does not coincide with any known orogeny in the region. The presence of extensive calcite mineralization and the radiogenic $^{87}Sr/^{86}Sr$ values suggest that orogenic-type fluids did permeate the Belden Formation lithologies. The results of vein/contact tests and the lack of a relation between the degree of alteration and component 3 intensity (Figure 1-17), however, do not support the hypothesis that the fluids were responsible for the CRM. This is consistent with the results of *Fruit et al.* [1995] who did not find a connection between the degree of mineralization/alteration and the high temperature component in the Belden Formation at Sweetwater.

Burial diagenetic processes can occur basinwide and are likely candidates for the origin of the CRM [e.g., *Fruit et al.*, 1995]. *Nuccio et al.* [1989] reconstructed the burial and thermal history of the Belden Formation in the Central Colorado Trough and modeled the timing of oil generation in different parts of the basin, using the time temperature index (TTI) method of modeling. Their modeling utilized measured vitrinite reflectance data to estimate the maximum temperatures to which Belden rocks have been exposed, Rock Eval pyrolysis data to define the maximum level of thermal maturity and determine the quantity and quality of organic matter in the rocks and stratigraphic thickness data from different sections in Central Colorado for use in contructing the burial history curve for Belden sediments. As previously stated, the Belden Formation is classified as an over mature rock [e.g., *Nuccio and Schenk*, 1987; *Whalen et al.*, 1990] and oil-generation (oil window) occurred in different parts of the basin at different times [*Nuccio et al*, 1989].

A test of the burial diagenesis model is to compare the time of CRM acquisition with the time of burial diagenesis as indicated by the modeled time of organic matter maturation (oil-window) at a location. In the Minturn-Gilman area, according to *Nuccio et al.* [1989], the Belden Formation passed through the oil-window during the Late Paleozoic (between 284 and 263 Ma) and the paleopole position for the CRM from this location also plots near the Late Paleozoic part of the APWP and within the oil window (Figure 1-21a). In the Miller Creek area, the CRM is inferred to be of Late Cretaceous age. Modeling studies by *Nuccio et al.* [1989] from the nearby Buford area show that the Belden Formation passed through the oil window between Late Jurassic and Late Cretaceous (140 and 73 Ma) and the time of the remanence acquisition is within the oil window (Figure 1-21b). At other two locations (Sweetwater and South Park) the paleopoles are also consistent with the oil- window, although the Belden Formation was within the window for a long duration. At the Sweetwater locality, *Nuccio et al.* [1989] calculated that the Belden Formation was within the oil window between 238 and 80 Ma and the Cretaceous paleopole position for the CRM [*Fruit et al.*, 1995] places the age of the remanence acquisition within the limits of the oil window (Figure 1-21c). In the South Park area, according to *Maughn* [1989], the Belden Formation lithologies were within the oil-window between Late Paleozoic and Early Tertiary. The age of the CRM in this area is estimated to be Jurassic, which places the age of remanence acquisition within the oil-window (Figure 1-21d).

Although there is an apparent connection between the CRM and maturation, at a more fundamental level, the connection is with low to moderate burial temperatures (<150°C). Several processes operating during burial diagenesis can cause magnetite authigenesis and CRM. The empirical relations between the age of the CRM and the timing of the oil-window in locations widely dispersed in the basin suggest that burial

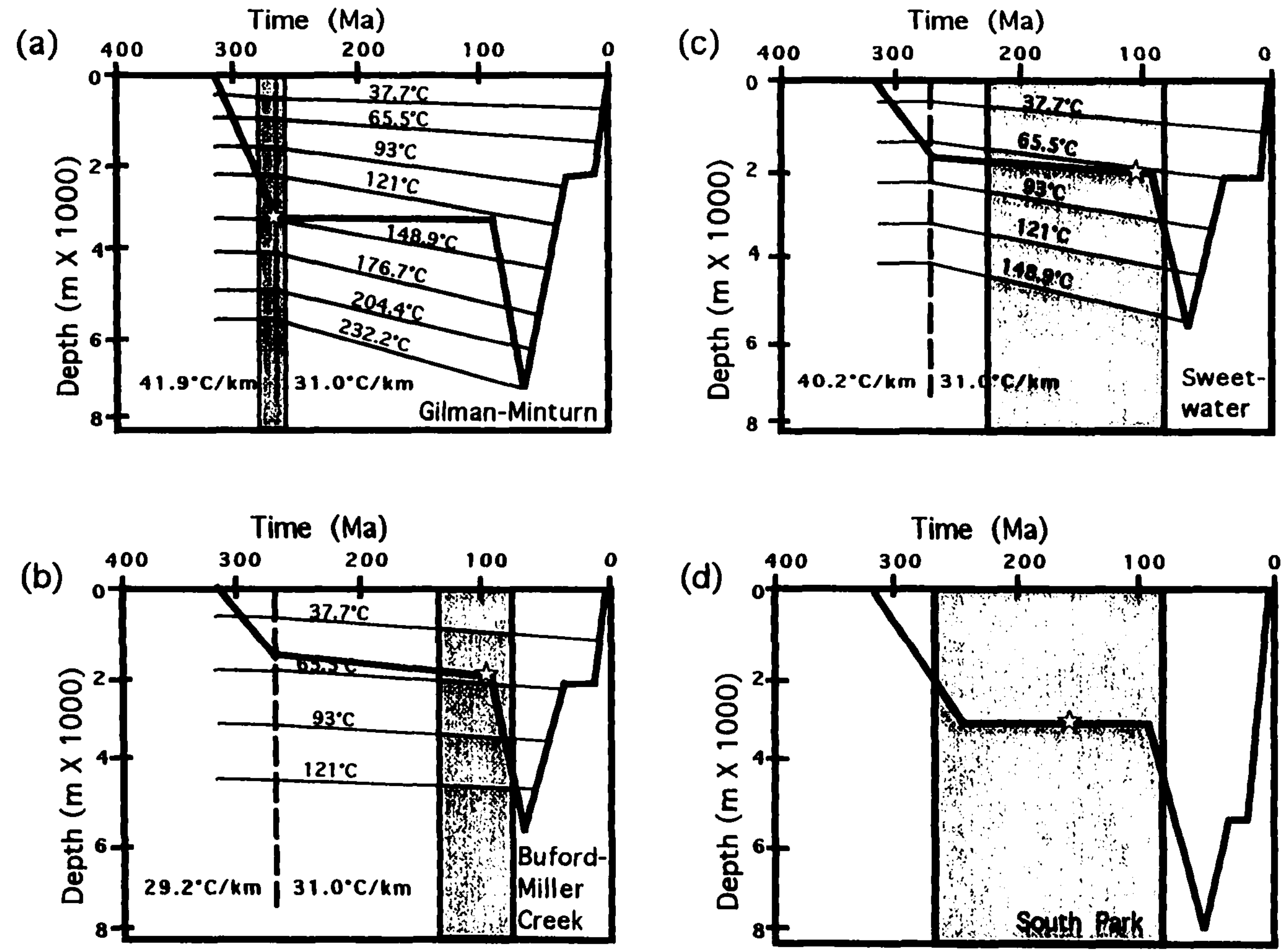

Figure. 1-21 Burial and thermal history for the Belden Formation for different parts of the Central Colorado Trough **(a.)** Gilman-Minturn, **(b.)** Buford-Miller Creek, **(c.)** Sweetwater, **(d.)** South Park. Shaded area - oil window for the location; star - calculated age for CRM from this location. **(a),(b),(c)** are modified from *Nuccio et al.* [1989]; burial curve in **(d)** is extrapolated from burial data from *Maughn*, [1989]; range of oil window is also from *Maughn* [1989].

diagenesis of organic matter could be a possible remagnetization mechanism. The CRM is widely present where the Belden Formation is dominated by dark, organic-rich shale and carbonate. It is not found, however, in the Morgan Formation in the northwestern part of the basin where the carbonate are much lighter colored and perhaps less organic-rich. Other studies have also reported a connection between diagenesis of organic-rich carbonates and pervasive CRMs in magnetite [e.g., *Elmore et al.*, 1993a; *Plaster-Kirk et al.* 1995]. Studies of organic-rich lithologies around dikes also suggest a connection between magnetite authigenesis and maturation of organic matter due to heating [*Bixler et al.*, 1996]. *Brothers et al.* [1996] have modeled magnetite authigenesis from pyrite during the late stages of diagenesis in organic-rich environment. Basing the design of their expriments on the hypothesized geochemical conditions for *in situ* diagenesis in the Belden Formation, *Brothers et al.* [1996] have demonstrated that authigenic magnetite can form by replacing pyrite in the presence of organically complexed ferric iron which can act as an oxidizing agent, at temperatures of about 90°C.

Another burial diagenetic process which may also create a CRM in magnetite is the smectite to illite transformation. Several studies [e.g., *Hower et al.*, 1976] have shown that smectite to illite transformation occurs over the burial depth interval from 2000 to 3700 m and in a temperature interval from 45 to 95°C. Iron ions released during this process could potentially form authigenic magnetite. *Katz et al.*, [1996] have shown a connection between clay diagenesis and a CRM in magnetite in Jurassic limestone/marl alternations in the Vocontian Trough, SE France.

Another possible remagnetization mechanism is oxidation of pyrite due to moderate burial temperatures. Previous studies [*e.g.*, *Tkhoa*, 1985] have demonstrated that pyrite oxidation to magnetite in open air requires heating to 450-500°C. Burial temperatures for Belden rocks at the time of CRM acquisition were less than 150°C which are not considered to be sufficiently high to cause pyrite oxidation given the length of burial. The presence of abundant unaltered pyrite in these rocks is also inconsistent with this model.

The connection between burial and remagnetization has obvious implications for paleomagnetic studies of rocks in basins with unequal subsidence and spatial variability in thermal history. Such CRMs would be expected to show different ages over different parts of the basin, closely paralleling the maturition history of the formation, although the mechanism for the CRM would be the same.

In addition to the origin of the CRM, another important issue is the interpretation of the synfolding test results [e.g., *McCabe et al.*, 1983; *Kodama*, 1988; *Fruit et al.*, 1995]. An explanation of the synfolding test results for both components 2 and 3 requires analysis of the components vis-à-vis their age and sampling locations. For the magnetization to be truly synfolding the age of the magnetization must correspond to that of a known period of deformation in the area. This criterion is partially met for the Belden Formation components. Component 2 (the TVRM) was acquired during the Tertiary, which coincided with the Laramide Orogeny in the region when the folded structures attained their maximum amplitudes. This component could be a true synfolding magnetization.

In the case of component 3 (the CRM), the age of the component is variable over the basin. At Sweetwater, *Fruit et al.* [1995] found this component to have a synfolding behavior with a Late Cretaceous age that coincides with Laramide orogeny. However, they did not interpret this component to be a true synfolding magnetization but rather an artifact of oversteepening of directions, perhaps due to overprinting of a prefolding CRM by a postfolding viscous magnetization residing in MD magnetite. Demagnetization results from specimens from Sweetwater that were pre-cleaned using LTD and AF methods do not appear to indicate any overprinting by viscous components, although recent studies [e.g., *McClelland*, 1996] indicate that such cleaning methods do not necessarily remove a remanence in MD grains. The timing of the CRM at Sweetwater relative to the folding, therefore, is still open to question [e.g. *Fruit et al.*, 1995].

In the Minturn-Fulford area, component 3 has a Late Paleozoic age that coincides with the Ancestral Rocky Mountain Orogeny. The fold test in this region, however, determines the age of the component relative to the Tertiary Laramide Orogeny. Although the fold test shows that the CRM could be very early synfolding, or pre-folding, the latter is the preferred interpretation.

In the South Park area, component 3 shows a synfolding result with a Lower Jurassic age. As mentioned above, there were no known Jurassic deformation events in the area. This component cannot be a true synfolding component. One hypothesis for the origin of this component is that it was acquired after the Belden Formation beds were partially deformed by drape folding associated with Late Paleozoic block faulting in the area. There is independent evidence that structural elements in the South Park area were probably reactivated during the Laramide Orogeny which resulted in the tightening of the folds [e.g., *DeVoto*, 1971]. When the beds are rotated back to the horizontal in the fold test, the directions corresponding to the CRM cross during unfolding, thus producing an apparent synfolding magnetization.

Another issue involving the magnetization in the Belden Formation is the presence of component 3 at some sites and its absence at others. While no definite conclusions can be made as to why this component is not present at all sites, a hypothesis can be offered as an explanation. The hysteresis properties suggest that the presence of the CRM is linked to the presence of finer grained magnetite in these beds. In all the sites, the TVRM is carried by coarser magnetite. One possibility is that magnetite of different grain sizes formed at the same time by the burial diagenesis process. During Tertiary heating and subsequent cooling, larger magnetite grains with lower relaxation periods were reset to carry the Tertiary TVRM (component 2) while the smaller-sized fraction with longer relaxation times, still carried the older CRM. This would make the present distribution of the CRM a function of some factor, presently unknown, that resulted in differential sizes of magnetite growth in different beds.

CONCLUSION

A regional paleomagnetic and geochemical study of the carbnonates from the Lower Pennsylvanian Belden Formation in Central Colorado was undertaken to test for a connection between a CRM residing in magnetite and burial diagenesis. Thermal demagnetization of Belden carbonate samples show the presence of two components, in addition to a low unblocking temperature modern VRM. An intermediate temperature Tertiary component, present at all locations, is interpreted to be a TVRM, acquired by the rocks during cooling from maximum burial and heating. A widespread, locally synfolding, CRM is present at selected locations within the basin. Rock magnetic studies, including IRM analysis, hysteresis studies, and LTD/AF treatment suggest that the CRM is carried by magnetite, probably of SD grain size. Based on petrographic analysis and results from previous studies [e.g. *Fruit et al.*, 1995] this CRM is interpreted to be carried by magnetite that has formed by replacing pyrite.

Based on the results of contact vein tests, orogenic fluids are not considered a likely remagnetization mechanism. The age of the CRM is found to vary across the basin, and its age is consistent with the modeled timing of oil generation. This CRM is interpreted to be related to burial diagenetic processes. Although there is an empirical connection with maturation of organic matter, this is not a unique solution and other processes such as clay diagenesis could also create this CRM. Although, further studies are needed to test this "burial diagenesis" model of CRM acquisition, it could apply to other pervasive CRM's in carbonate. Any CRMs acquired following the "burial diagenetic model" would be expected to show differences in age over different parts of the basin, though the mechanism for the CRM would be the same. This may necessitate the evaluation of magnetic components in such rocks in terms of their unblocking temperature range rather than just their directional properties.

REFERENCES CHAPTER 1

Bachtadse, V., R. Van der Voo, F.M. Haynes, and S.E. Kesler, Late Paleozoic magnetization of mineralized and unmineralized Ordovician carbonate from east Tennessee: evidence for a post-ore chemical event, *J. Geophys. Res., 92*, 14,165-14,176, 1987.

Barrs, D.L., B. Bartleson, C. Chapin, B.Curtis, R. DeVoto, J. Everett, R. Johnson, C.F. Molenarr, F. Peterson, C. Shenk, J. Love, I. Merin, P. Rose, R. Ryder, N. Waechter and L. Woodward, Basins of the Rocky Mtn. region, in, Sedimentary cover of the North American Craton, edited by L.L. Sloss, *The Geology of North America, D-2*, 109-220, 1988.

Bartleson, B.L., B. Bryant and F.E. Mutschler, Permian and Pennsylvanian stratigraphy and nomenclature, Elk Mountains, Colorado, *USGS Professional Paper, 600-C*, 53-60, 1968.

Bass, N.W. and S.A. Northrop, Geology of the Glenwood Springs quadrangle and vicinity, northwestern Colorado, *U.S.G.S. Bulletin, 1142-J*, 74p, 1963.

Bixler, W.G., B. Katz, R.D. Elmore and M.H. Engel, The origin of magnetization in Jurassic organic rich limestone adjacent to a dike, Isle of Skye, Scotland (abstract), *Eos Trans. AGU 77-17*, 86, 1996.

Brill, K. G., Jr, The Belden Formation, in, *Symposium on Pennsylvanian rocks of Colorado and adjacent areas,* edited by B. Curtis, Rocky Mtn. Assoc. Geologists, 103-106, 1958.

Brothers, L., M.H. Engel and R.D. Elmore, The late diagenetic conversion of pyrite to magnetite by organically complexed ferric iron, *Chemical Geology, 130*, 1-14, 1996.

Burke, W. H., R.E. Denison, E.A. Hetherington, R.B. Koepnick, H.F. Nelson and J.E. Otto, Variation of seawater $^{87}Sr/^{86}Sr$ through Phanerozoic time, *Geology, 10*, 516-519, 1982.

Channell J.E.T. and C. McCabe, Comparison of magnetic hysteresis parameters of unremagnetized and remagnetized limestone, *J. Geophys. Res., 99*, 4613-4623, 1994.

Day, R., M. Fuller and V.A. Schmidt, Hysteresis properties of titanomagnetites: grain-size and compositional dependence, *Physics Earth Planet. Inter., 13*, 260-267, 1977.

De Voto, R.H., Geologic history of South Park and geology of the Antero Reservoir quadrangle, Colorado, *Quarterly Colorado School of Mines, 66*, 1-90, 1971.

Dunham, R.J., Classification of carbonate rocks according to depositional texture, in, Classification of carbonate rocks, edited by W.E. Ham, *AAPG Memoir, 1,* 108-121, 1962.

Dunlop, D.J. and K.S. Argyle, Separating multidomain and single-domain-like remanences in pseudo-single-domain magnetites (215-540 nm) by low temperature demagnetization, *J. Geophys. Res., 96*, 2007-2017, 1991.

Dunlop, D.J., Ö. Özdemir and P.W. Schmidt, Thermoviscous remagnetization of multidomain magnetite, IUGG XXI General Assembly, Boulder (abstract), B-136, 1995.

Elmore, R.D., K. Cates, G. Gao and L. Land, Geochemical constraints on the origin of secondary magnetizations in the Cambro-Ordovician Royer Dolomite, Arbuckle Mountains, southern Oklahoma, *Physics Earth Planet. Inter.*, *85*, 3-13, 1994.

Elmore, R.D., S. Imbus, M.H. Engel and D. Fruit, Hydrocarbons and Magnetizations in Magnetite, in, *Applications of paleomagnetism to sedimentary geology*, edited by D. M. Aissaoui et. al., SEPM Special. Pub., 50, 181-191, 1993a.

Elmore, R.D., D. London, D. Bagley, D. Fruit and G. Gao, Remagnetization by basinal fluids: testing the hypothesis in the Viola limestone, southern Oklahoma, *J. Geophys. Res., 98,* 6237-6254, 1993b.

Elmore, R.D. and C.R. McCabe, The occurrence and origin of remagnetization in the sedimentary rocks of North America, in, Contributions in Geomagnetism and Paleomagnetism, U.S. National Report 1987-1990, *Reviews in Geophysics, Supplement, 29*, 377-383, 1991.

Fisher, R. A, Dispersion on a sphere, *Proc. R. Soc London, A*, *217*, 295-305, 1953.

Fruit, D., R.D. Elmore, and S. Halgedahl, Remagnetization of the folded Belden Formation, *J. Geophys. Res., 100*, 15,009-15,023, 1995.

Halgedahl, S.L. and R.D. Jarrard, Low-temperature behavior of single-domain through multidomain magnetite, *Earth Planet Sci. Lett, 130*, 127-139, 1995.

Horton, R.A., J.W. Geissman and R.J. Tschauder, Paleomagnetism and rock magnetism of the Mississippian Leadville (carbonate) formation and implications for the age of sub-regional dolomitization, *Geophys. Res. Lett., 11*, 649-652, 1984.

Hower, J., E.V. Elsinger, M.E. Hower and E.A. Perry, Mechanism of burial metamorphism of argillaceous sediments: 1. Mineralogical and chemical evidence, *Geol. Soc. Amer. Bull., 87,* 725-737.

Jackson, M., Diagenetic sources of stable remanence in remagnetized Paleozoic cratonic carbonate: a rock magnetic study, *J. Geophys. Res., 95*, 2753-2761,1990.

Jackson, M., P. Rochette, G. Fillion, S. Banerjee and J. Marvin, Rock magnetism of remagnetized Paleozoic sedimentary carbonate: low temperature behavior and susceptibility characteristics, *J. Geophys. Res., 98*, 6217-6226, 1993.

Katz, B., R.D. Elmore, M. Cogoini and S. Ferry, Remagnetization and diagenesis of clays (abstract), *Eos Trans. AGU 77-46*, 159, 1996.

Kent, D.V., Thermoviscous remagnetization in some Appalachian limestone, *Geophys. Res. Lett., 12*, 805-808, 1985.

Kirschvink, J. L., The least square line and plane and analysis of paleomagnetic data, *Geophys. J. R. Astron. Soc., 45*, 699-718, 1980.

Kluth, C.F., Plate Tectonics of the Ancestral Rocky Mountains, in, Paleotectonics and sedimentation in the Rocky Mountain region, United States, edited by J. A. Peterson, *AAPG Memoir, 41*, 353-369, 1986.

Kodama, K.P., Remanence rotation due to rock strain during folding and the stepwise application of the fold test, *J. Geophys. Res., 93*, 3357-3371, 1988.

Lowrie, W., Identification of ferromagnetic minerals in a rock by coercivity and unblocking temperature properties, *Geophys. Res. Lett., 17*, 159-162, 1990.

Lu, G., C. McCabe, J. Hanor, and R.E. Ferrell, A genetic link between remagnetization and potassic metasomatism in the Devonian Onodaga Formation, northern Appalachian Basin, *Geophys. Res. Lett., 18*, 2047-2050, 1991.

Lu, G., S. Marshak, and D.V. Kent, Characteristics of magnetic carriers responsible for late Paleozoic remagnetization in carbonate strata of the mid-continent, USA, *Earth Planet. Sci. Lett., 99*, 351-361, 1990.

Maughn, E.K, Hydrocarbon exploration plays in the Colorado Park Basin province, in, *Energy Frontiers in the Rockies*, edited by J.C. Lorenz and S.G. Lucas, Albuquerque Geological Society, 79-83, 1989.

McCabe C. and J.E.T. Channell, Late Paleozoic remagnetization in limestone of the Craven Basin (northern England) and the rock magnetic fingerprint of remagnetized sedimentary carbonate, *J. Geophys. Res., 99*, 4603-4612, 1994.

McCabe, C. and R.D. Elmore, The Occurrence and origin of late paleozoic remagnetization in the sedimentary rocks of North America, *Reviews of Geophysics, 27*, 4, 471-494, 1989.

McCabe, C., R. Van der Voo, D.R. Peacor, C.R. Scotese, and R. Freeman, Diagenetic magnetite carries ancient yet secondary remanence in some Paleozoic sedimentary carbonate, *Geology, 11*, 221-223, 1983.

McClelland, E. , Experimental constraints on models of remanence in multidomain magnetite (abstract), *Eos Trans. AGU 77-46*, 160, 1996.

McElhinny, M. W., Statistical significance of the fold test in paleomagnetism, *Geophys. J. R. Astron. Soc., 8*, 338-340, 1964.

McFadden, P. L. and D.L. Jones, The Fold test in paleomagnetism, *Geophys. J. R. Astron. Soc., 67*, 53-58, 1981.

McFarlan, A.C., Outline of the geology of the Cement Creek area, Gunnison County, Colorado, in, *Lower and Middle Paleozoic rocks of Colorado*, edited by R.R. Berg and J.W. Rold, Rocky Mountain Association of Geologists, 125-132, 1961.

Middleton, M.F. and P.W. Schmidt, Paleothermometry of the Sydney Basin, *J. Geophys. Res., 84*, 5351-5359, 1982.

Nuccio, V. F., S.Y. Johnson and C.J. Schenk, Paleogeothermal gradients and timing of oil generation in the Belden Formation, Eagle Basin, northwestern Colorado, *The Mountain Geologist, 26*, 31-41, 1989.

Nuccio V.F. and C.J. Schenk, Burial reconstruction of the Early and Middle Pennsylvanian Belden Formation, Gilman area, Eagle Basin, Northwestern Colorado, *USGS Bulletin, 1787-C*, 31-36, 1987.

Oliver, R., The spots and stains of plate tectonics. *Earth Sci. Rev., 32*, 77-106, 1992.

Oliver, R., Fluids expelled tectonically from orogenic belts: their role in hydrocarbon migration and other geologic phenomena, *Geology, 14,* 99-1021, 1986.

Parry, L.G., Magnetization of immobilized particle dispersions with two distinct particle sizes, *Phys. Earth Planet. Inter.*, *28*, 230-241, 1982.

Plaster-Kirk, L.E., R.D. Elmore, M.H. Engel and S.W. Imbus, Paleomagnetic investigation of the organic-rich lacustrine deposits, Middle Old Red Sandstone, Scotland, *Scot. Jour. Geol.*, *31*, 97-105, 1995.

Pullaiah, G., E. Irving, K.L. Buchan and D.J. Dunlop, Magnetization changes caused by burial and uplift, *Earth Planet Sci. Lett.*, *28*, 133-143, 1975.

Roberts, A.P., Y. Cui and K.L. Verosub, Wasp-waisted hysteresis loops: mineral magnetic characteristics and discrimination of components in mixed magnetic systems, *J. Geophys. Res.*, *100*, 17,900-17,924, 1995.

Schmidt, P. W., Paleomagnetic cleaning strategies, *Phys. Earth Planet. Inter.*, *76*, 169-178, 1993.

Smith, R.T., and K.L. Verosub, Thermoviscous remanent magnetism of Columbia River Basalt blocks in the Cascade Landslide, *Geophys. Res. Lett.*, *21*, 2661-2664, 1994

Suk, D., R. Van der Voo and D.R. Peacor, Origin of magnetite responsible for remagnetization of Early Paleozoic limestone of New York State, *J. Geophys. Res*, *98*, 419-434, 1993.

Suk, D., R. Van der Voo and D.R. Peacor, Scanning and transmission electron microscope observations of magnetite and other iron phases in Ordovician carbonate from east Tennessee, *J. Geophys. Res.*, *95*, 12,327-12,336, 1990a.

Suk, D., D. R., Pecor and R. Van der Voo, Replacement of pyrite framboids by magnetite in limestone and implications for paleomagnetism, *Nature*, *345*, 611-613, 1990b.

Symons, D.T.A., Coincidence of Host rock remagnetization, Mississippi Valley-type mineralization and orogenic events, IUGG XXI General Assembly, Boulder, (abstract), B-136, 1995.

Symons, D.T.A. and D.F. Sangster, Late Devonian paleomagnetic age for the Polaris Mississippi Valley-type Zn-Pb deposit, Canadian Arctic Archipalago, *Can. Jour. Earth Sci.*, *29*, 15-25, 1992.

Tkhoa, N.T.K., On the stability relationships of the values of crystallization, ideal and thermoremanent magnetization of magnetite formed by alteration of pyrite, *Izvestiya-Earth Physics*, *21*, 561-564, 1985.

Tauxe, L., T.A.T. Mullender and T. Pick, Potbellies, wasp-waists and superparamagnetism in magnetite hysteresis, *J. Geophys. Res.*, *101*, 571-583, 1996.

Tweto, O., Tectonic history of West-Central Colorado, in, *Exploration Frontiers of the Central and Southern Rockies*, edited by H.K. Veal, Rocky Mtn. Assoc. Geologists, 11-22, 1977.

Upton, R.A., Pennsylvanian section at Juniper Mountain, Moffat County, Colorado, in, *Symposium on Pennsylvanian rocks of Colorado and adjacent areas*, edited by B. Curtis, Rocky Mtn. Assoc. Geologists, 99-102, 1958.

Van der Voo, R., Paleomagnetism of North America: The craton, its margins and the Appalachian Belt, *Mem. Geol. Soc. Am.*, *172*, 447-470, 1989.

Whalen, J., R. Carangelo, P.R. Solomon and W.G. Dow ,TG/plus - a new method for following maturation of oil and gas generation zones using T_{max} of methane, *Org. Geochem., 16*, 1187-1201, 1990.

Xu, S., and D. J. Dunlop, Theory of partial thermoremanent magnetization in multidomain grains: 2. Effect of microcoercivity distribution and comparision with experiment, *J. Geophys. Res., 99*, 9025-9033, 1994.

Zijderveld, J.D.A., A.C. Demagnetization of rocks: Analysis of results, in, *Methods in Paleomagnetism*, edited by D.W. Collinson et al., Elsevier, 254-286, 1967.

CHAPTER 2

MAGNETIC CHARACTERIZATION OF A CHEMICAL REMANENT MAGNETIZATION AND A THERMOVISCOUS REMANENT MAGNETIZATION, BELDEN FORMATION, COLORADO.

ABSTRACT

Pennsylvanian Belden Formation carbonate in Central and Northwestern Colorado contain a maximum of three components of the natural remanent magnetization (NRM): a modern viscous remanent magnetization (VRM) removed at low unblocking temperatures, an intermediate unblocking temperature (250 - 400°C) normal and reversed Tertiary thermoviscous remanent magnetization (TVRM) and a high unblocking temperature (400 - 575°C) chemical remanent magnetization (CRM). The TVRM is pervasive whereas the CRM is widespread but site specific. This distribution provides an opportunity to magnetically characterize the CRM and the TVRM. Specimens with the CRM have higher saturation remanence and an anhysteretic magnetization (ARM) is acquired over a broader coercivity range than the TVRM. The CRM has higher coercive force (Hc) and saturation remanence/saturation magnetization (M_{rs}/M_s) values, which indicates it is carried by finer grains of magnetite than the TVRM. Coercivity and saturation magnetization ratios are consistent with other carbonate interpreted to be remagnetized by chemical processes. The TVRM is carried by coarser grains of magnetite than the CRM. These grains could be detrital or authigenic in origin.

INTRODUCTION

Remagnetization is a common phenomenon recognized in many rocks [e.g., *Elmore and McCabe*, 1991] and can occur through several mechanisms such as chemical alteration and cooling from elevated burial temperatures. In recent years considerable effort has been focused on determining whether there is a rock magnetic fingerprint for different types of magnetization, particularly those interpreted to be chemical in origin [e.g., *Hart and Fuller*, 1988; *Jackson*, 1990; *Jackson et al.*, 1993, *McCabe and Channell*, 1994]. Chemical remagnetization processes are interpreted to modify the magnetic properties and these modifications are believed to cause a rock magnetic fingerprint which is advocated as an identifier for remagnetized carbonate [e.g., *McCabe and Channell*, 1994]. Recognition of such a rock magnetic fingerprint could potentially provide a faster method of identifying remagnetized sites prior to detailed paleomagnetic (directional) studies. In addition, such a fingerprint could help to identify the composition, grain size, and domain structure of the magnetic phases associated with a particular remagnetization mechanism.

In this paper we focus on rock magnetic results from remagnetized carbonate in the Pennsylvanian Belden and Morgan formations in Colorado. The carbonate contain two ancient natural remanent magnetization (NRM) components, one of which is pervasive whereas the other is widespread but found only at certain sites. This distribution provides the opportunity to characterize the two components with rock magnetic parameters and to compare these characteristics to those recently reported for other remagnetized carbonate rocks [*e.g., Jackson et al.*, 1993; *Channell and McCabe,* 1994]. Furthermore, the distribution and rock magnetic properties associated with these two components provide information about the magnetic phases associated with the remagnetization mechanisms.

GEOLOGIC SETTING OF THE STUDY AREA

Carbonate in the Lower Pennsylvanian Belden Formation in central Colorado and the laterally equivalent Morgan Formation in northwestern Colorado were sampled in the study. Both formations consist of a series of shale and limestone with occasional interbedded sandstone, which were deposited in the Late Paleozoic Central Colorado Trough. The Belden Formation was buried to a maximum depth of about 7500 m just before the onset of the Laramide Orogeny during the Cretaceous - Early Tertiary [*Nuccio et al.*, 1989]. The burial and maturation history of the Belden Formation varies across the basin, due to variations in subsidence and heat flow [*Nuccio et al.*, 1989].

METHODS

Representative samples (oriented cores and slabs) of carbonate lithologies were collected from various outcrops of Belden and Morgan formations at 27 locations throughout the study area (Figure 2-1). Standard specimens (cores 2.5 cm diameter, 2.2 cm long) were then subjected to paleomagnetic and rock magnetic measurements.

Remanence measurements were made with a United Scientific three-axis cryogenic magnetometer or a 2G three axis cryogenic magnetometer, located in a magnetically shielded room at the University of Oklahoma. Specimens were thermally demagnetized in a Schonstedt TSD-1 oven up to 700°C in 16-18 steps. AF demagnetization was performed using a 2G three axis AF demagnetizer (model 2G600). Directional and intensity data were plotted on orthogonal projections diagrams [*Zijderveld*, 1967] and components were visually identified. Best fit demagnetization trajectories were calculated using principal component analysis [*Kirshhvink*, 1980] and statistics [*Fisher*, 1953] calculated.

Selected specimens were subjected to isothermal remanent magnetization (IRM)

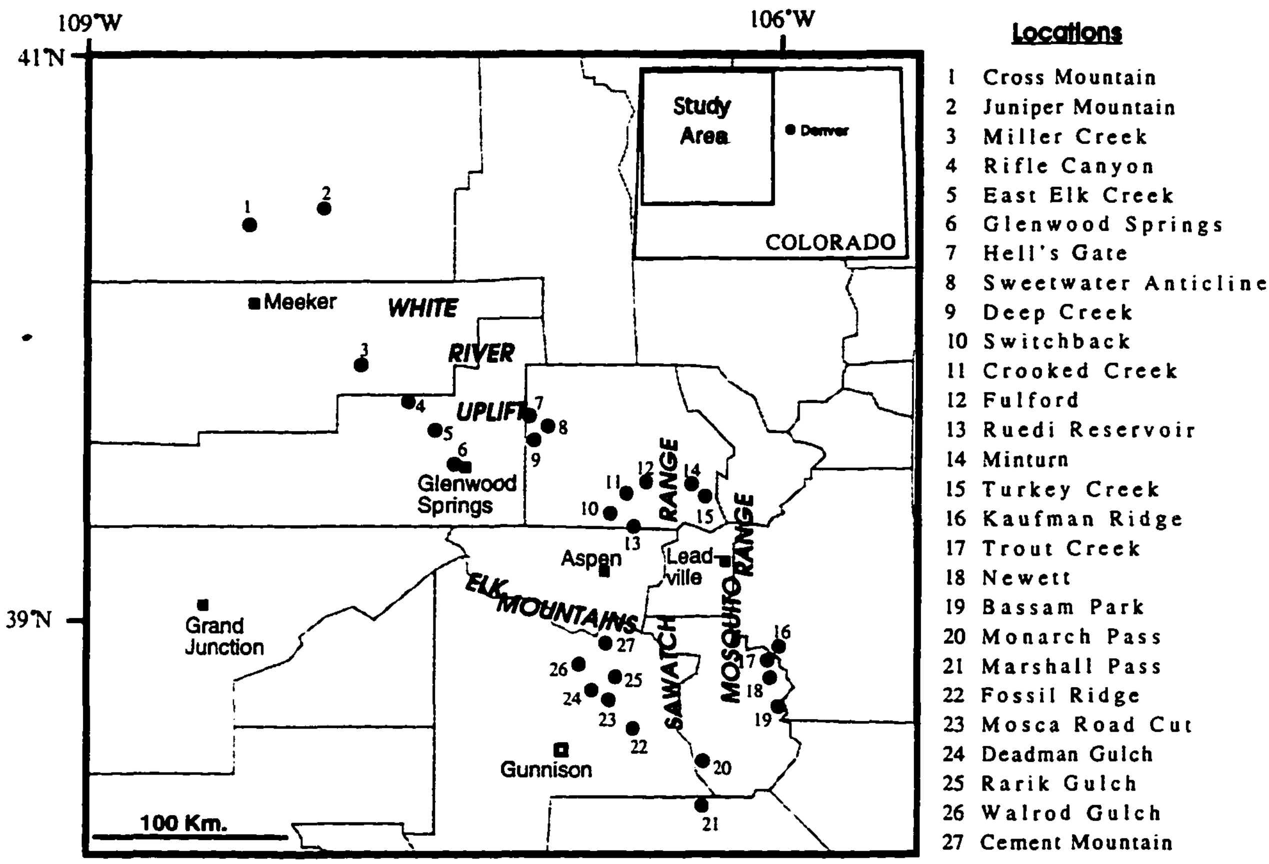

Figure. 2-1 Map of the study area in central and northwestern Colorado showing the sampling locations. Also shown are the Tertiary uplifts and mountain ranges (with bold lettering). Inset: map of Colorado showing the location of the study area.

and anhysteretic remanent magnetization (ARM) acquisition and AF decay measurements. Specimens were exposed to successively increasing direct fields up to 1.3 T using an ASC impulse magnetizer and then AF demagnetized. Selected specimens were given a three component IRM (0.12, 0.4 and 1.3 T) and thermally demagnetized [*Lowrie*, 1990]. Acquisition of ARM was performed on selected specimens with a biasing field of 0.1 mT and a peak field of 100 mT.

To investigate the possible presence of multi-domain (MD) grains and its effects on the magnetic components, specimens from selected sites were subjected to low temperature demagnetization (LTD) and AF 'cleaning' [e.g., *Dunlop & Argyle*, 1991; *Heider et al.*, 1992; *Schmidt*, 1993]. In LTD cleaning, specimens were subjected to multiple (3-5) zero-field cycling episodes [e.g., *Dunlop et al.*, 1995] which involved immersing the specimens in liquid nitrogen (77°K) inside a mumetal shield for 30 minutes during each cycle, [e.g., *Heider et al.*, 1992]. The ambient field inside the mumetal shield (< 75 nT) was comparable to the 50 nT reported by *Heider et. al.* [1992]. The specimens were removed from liquid nitrogen and allowed to warm up to room temperature inside the shield before being subjected to thermal and AF demagnetization of the NRM. In the AF cleaning procedure, specimens were subjected to low field (up to 10 mT, in 3 steps) AF demagnetization [e.g., *Schmidt*, 1993] before being subjected to regular thermal demagnetization. In addition, to obtain an estimate of the relative amounts of MD magnetite grains present in different units, selected specimens were given a room temperature IRM (at 1.3 T) and subjected to 3 cycle LTD as described above. The remanence was measured after each cycle and compared to the initial SIRM [e.g., the method of *Halgedahl and Jarrard*, 1995].

Hysteresis measurements were performed on a Princeton Corporation Micromag Alternating Gradient Force Magnetometer (AGFM) at the University of Utah Paleomagnetic Laboratory, Salt Lake City. Average dwell times were of 100 milliseconds with field increments of 2 mT. Values of coercive force (H_c), saturation magnetization (M_s) and saturation remanent magnetization (M_{rs}) were determined for each hysteresis run after the data was suitably corrected for high field paramagnetic or diamagnetic slope. Values of coercivity of remanence (H_{cr}) were obtained from backfield measurements.

Low temperature measurements on selected Belden carbonate samples were made on a Quantum Design Magnetic Properties Measurement System (MPMS) at the Institute of Rock Magnetism at the University of Minnesota, Minneapolis. Samples were cooled to about 10°K in liquid helium, exposed to a direct field of 2.5 T and warmed to 300°K in approximately zero field, as the remanence was periodically measured. Selected samples were also examined using a reflected light microscope and on a Cameca SX-50 electron microprobe equipped with a Kevex energy dispersive analysis system.

RESULTS and INTERPRETATIONS

Thermal and AF demagnetization

Thermal demagnetization of Belden Formation carbonate show the presence of up to three components of NRM (Figure 2-2a) in each specimen: component 1, with a low unblocking temperature range (NRM to 250°C), component 2, with intermediate unblocking temperature ranges (250 to 400°C) and component 3, with high unblocking

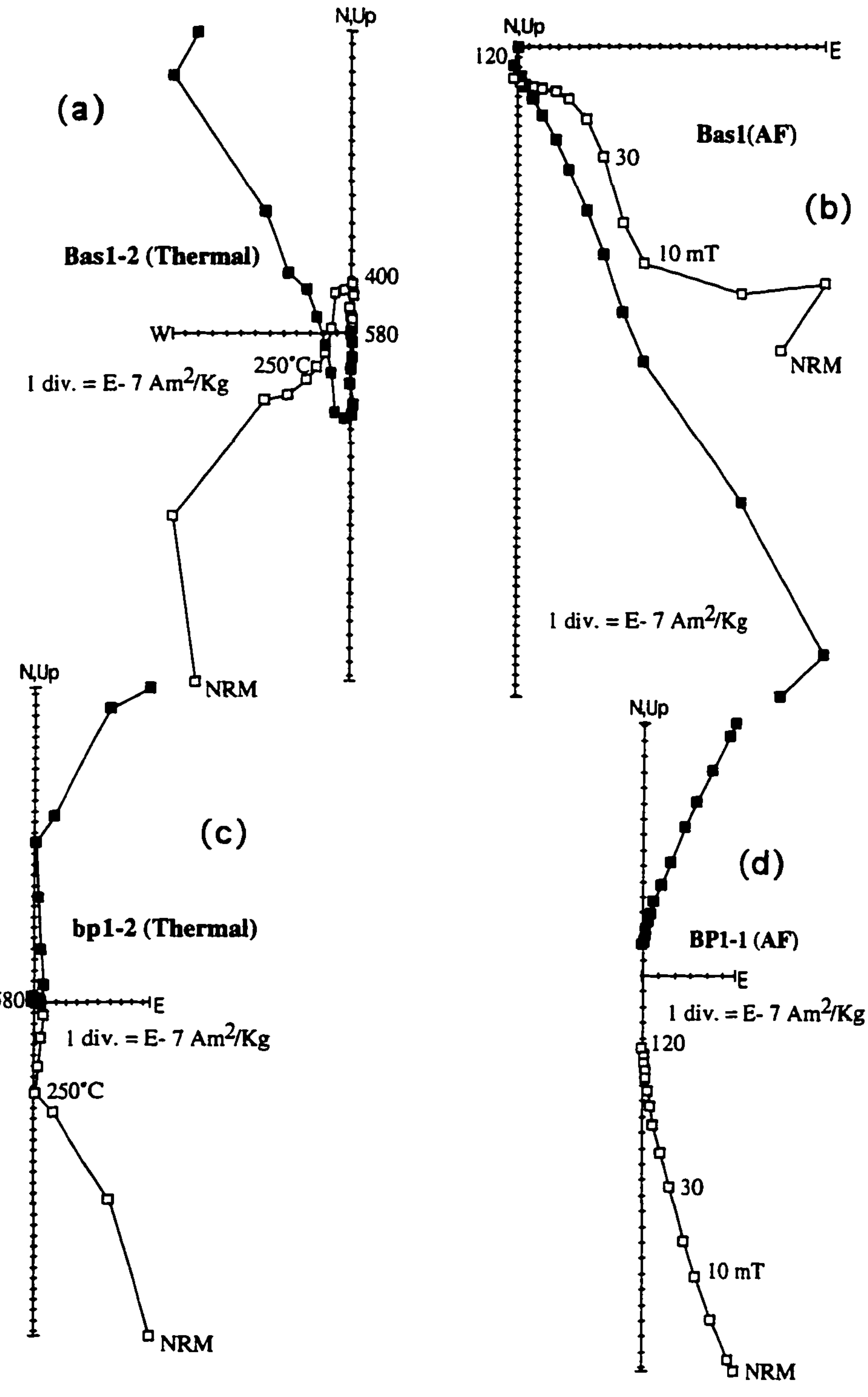

Figure. 2-2 Representative orthogonal (Zijderveld) projections of the thermal and AF demagnetization of Type A (with component 1 and 2) and Type B (with all three components) Belden Formation specimens (before structural correction). Open symbols - horizontal components; closed symbols - vertical components.

temperature ranges (400 to 575°C). Comparison of NRM intensities for specimens that carry only components 1 and 2 (Type A) versus those which carry all three components (Type B) indicate that the mean NRM intensities for both types are about the same with values of approximately 2 x 10^{-6} Am^2/Kg.

Demagnetization by AF treatment does not effectively resolve the true multicomponent nature of the NRM. AF demagnetization of Type B specimens from sites where other specimens contain all three components (based on thermal demagnetization), shows removal of component 1 and a vector sum of components 2 and 3 (Figure 2-2b). This indicates that the latter two components have overlapping coercivity spectra. AF demagnetization up to 120 mT of Type A specimens from sites where only components 1 and 2 are present produces similar directions as shown by thermal demagnetization (Figure 2-2c,d).

Component 1, present in all demagnetized specimens, has a northerly and steep down inclination and is interpreted to be a viscous remanent magnetization (VRM) acquired in the present Earth field.

Component 2 is present in 95% of the specimens (Figure 2-2a,c). Specimens from a single site have either normal (northerly and steep down) or reversed (southerly and steep up) directions (Figure 2-3, Table 1). At many sites this component and the VRM are the only components found. Fold tests were carried out on this component at two different locations to define the age of this magnetization relative to the Laramide deformation which produced the folds. The results of a regional fold test using site-mean directions from Fulford and Minturn, which are on the opposite flanks of the Sawatch Range (Figure 2-1), show that directions cross during unfolding (Figure 2-4a).

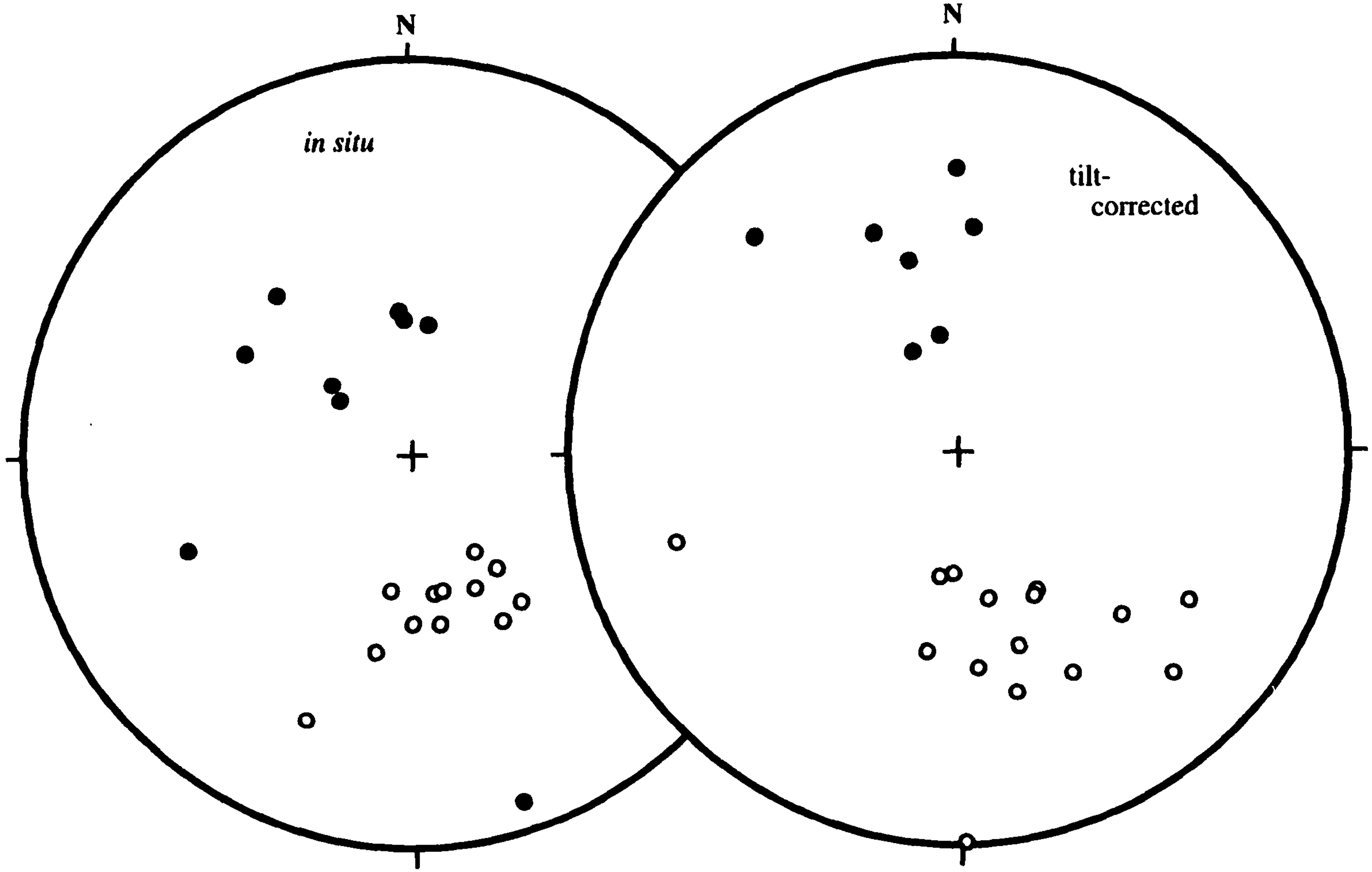

Figure. 2-3 Equal area projection of *in situ* and tilt-corrected site mean directions for component 2 for all locations. Solid symbols - lower hemisphere projections; open symbols - upper hemisphere projections

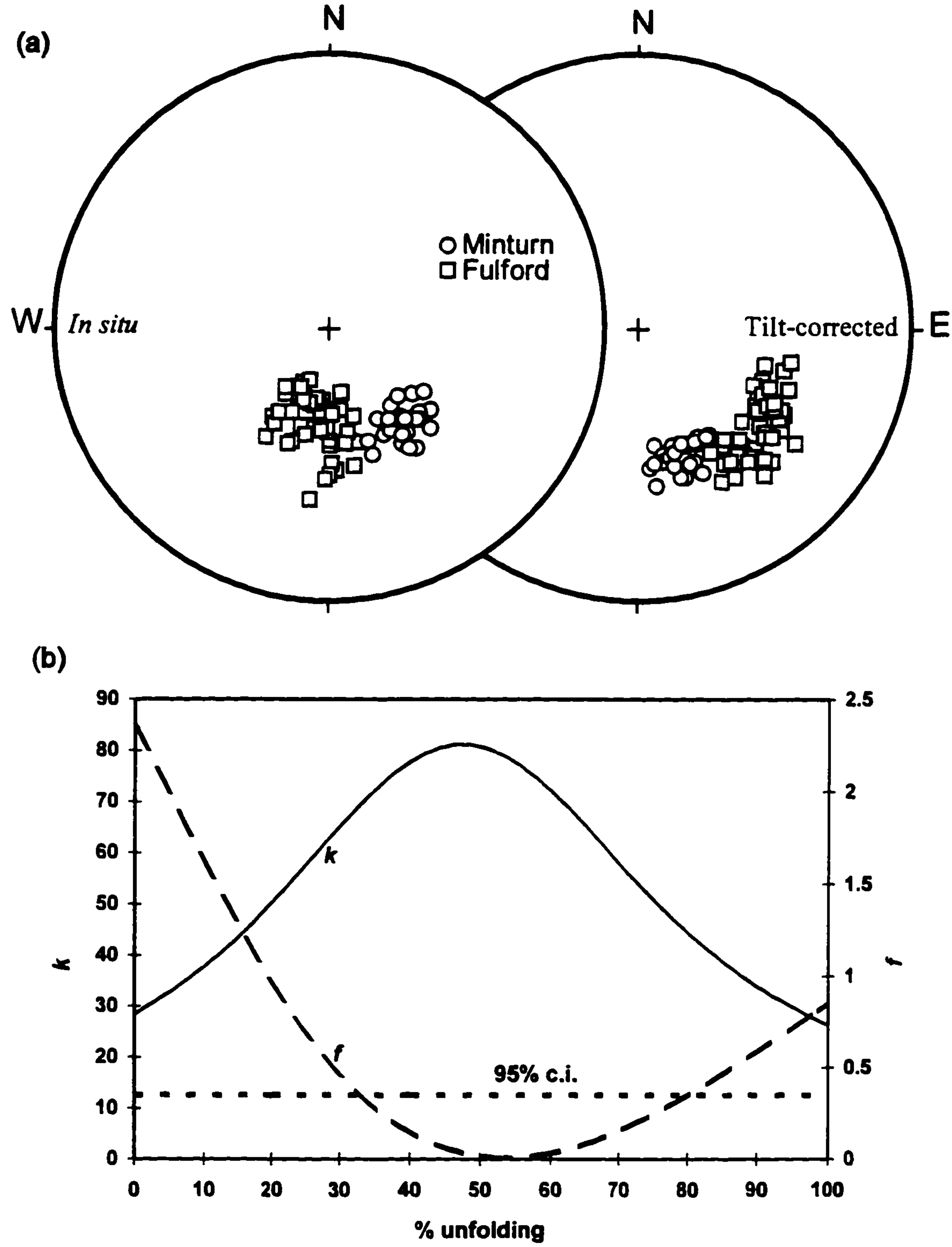

Figure. 2-4 (a) Equal area (upper hemisphere) projection of *in situ* and tilt-corrected specimen directions for component 2 from Fulford (squares) and Minturn (circles) in central Colorado. The directions cross during unfolding. **(b)** Incremental fold test on component 2 from Fulford-Minturn. Values of the *f* [*Mcfadden & Jones*, 1981] fold test statistic and precision parameter *k* [*McElhinny*, 1964] are plotted against percentage unfolding. The 95% confidence interval [*McFadden & Jones*, 1981] for this test is also shown.

Evaluation of the directions using an incremental fold test (Figure 2-4b) indicate that best grouping of directions occurs at 50% unfolding. This fold test result is significant at the 95% confidence interval based on *McElhinny* [1964]. The *McFadden and Jones* [1981] formulation of the fold test shows that the hypothesis of a common mean for the two limbs is valid at 95% confidence limit between 31% and 80% unfolding. The magnetization is apparently synfolding. A fold test from the South Park area also gives a similar synfolding result with probable remanence acquisition at about the 50% unfolding. Based on the synfolding test results and comparison of the paleopole positions to the apparent polar wander path (APWP) for North America [*Van der Voo*, 1989], the age of this magnetization is interpreted to be Tertiary.

Component 3 is widespread but is not present or clearly resolved at all sites or at all locations (see Chapter 1). The directions and inferred age of this magnetization varies between locations. At Fulford, Minturn, and Ruedi Reservoir this component has a southeasterly and shallow direction with the paleopole position near the Late Paleozoic portion of the APWP. At Bassam Park and Trout Creek, this component has a southerly and negative direction suggesting an Early Jurassic age. At Hell's Gate, Miller Creek and Sweetwater [*Fruit et al.*, 1995] this component has a northerly and positive direction with a Cretaceous paleopole.

IRM and ARM acquisition and demagnetization

The IRM acquisition curves (Figure 2-5a) for most specimens show saturation by 300 mT, indicating that a low coercivity mineral is present. Some specimens show a slight increase in slope beyond 300 mT, indicative of a high coercive phase. The saturation remanence is generally higher in Type B specimens than in Type A specimens. AF demagnetization of SIRM shows that more than 80% of the imparted remanence is removed by 100 mT in both Type A and B specimens.

Thermal demagnetization of a multi-component SIRM for most Type A and B specimens show that all three IRM components are almost completely demagnetized by 580°C, indicating magnetite as the primary magnetic carrier in these rocks (Figure 2-5b). In specimens with a high coercivity component, the decay continues up to about 680°C, indicating the presence of hematite.

Analysis of IRM acquisition and AF demagnetization of IRM results indicate that the curves cross at near 50% of the normalized moment (Figure 2-6) for both Type A and B specimens. According to *Cisowski* [1981], this suggests that the remanence is dominated by non-interacting fine particles. A modified Lowrie-Fuller test [*Johnson et. al.*, 1975], however, shows that the ARM in both groups of specimens is less stable than the IRM to AF demagnetization (Figure 2-6). According to *Johnson et. al.* [1975] this indicates the predominance of coarse multidomain (MD) grains of magnetite in the specimens, and thus these results are at odds with the results of *Cisowski's* [1981] test. Similar results have also been reported from studies on other remagnetized carbonate units [e.g., *McCabe & Channell*, 1994].

Partial ARM (PARM) analysis of the Belden Formation Type A and Type B specimens from Sweetwater Anticline by *Fruit* [1994] show that PARM curves for both specimens peak at 10 mT (Figure 2-7), which is interpreted to indicate the presence of low-coercivity material in this range. However, the PARM curves for Type A specimens drop off quickly at higher field strengths, whereas curves for Type B

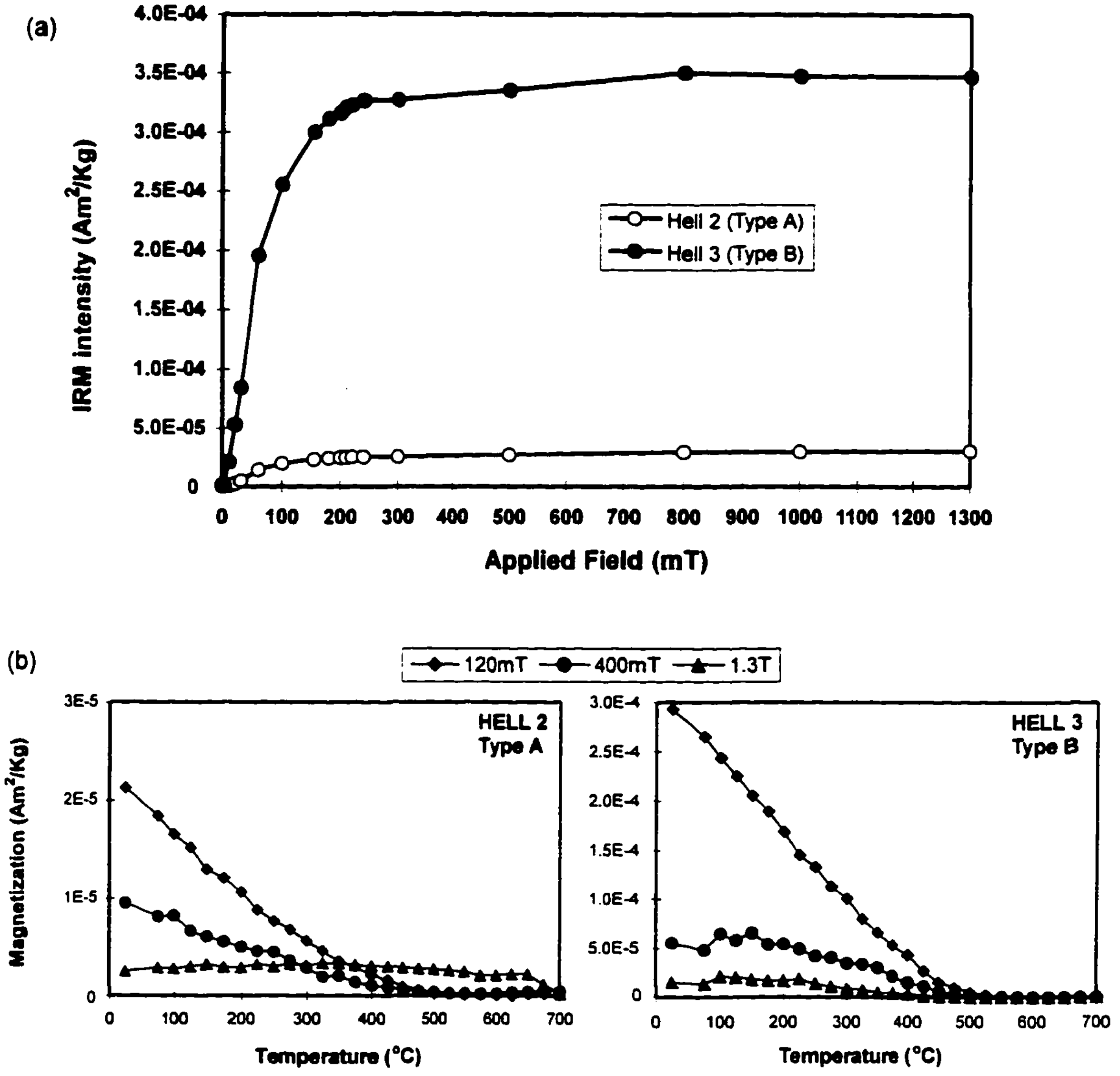

Figure. 2-5 (a) IRM acquisition curves for representative Type A and Type B Belden Formation specimens from the study area. **(b)** thermal demagnetization of three-component IRM for representative Type A and B specimens.

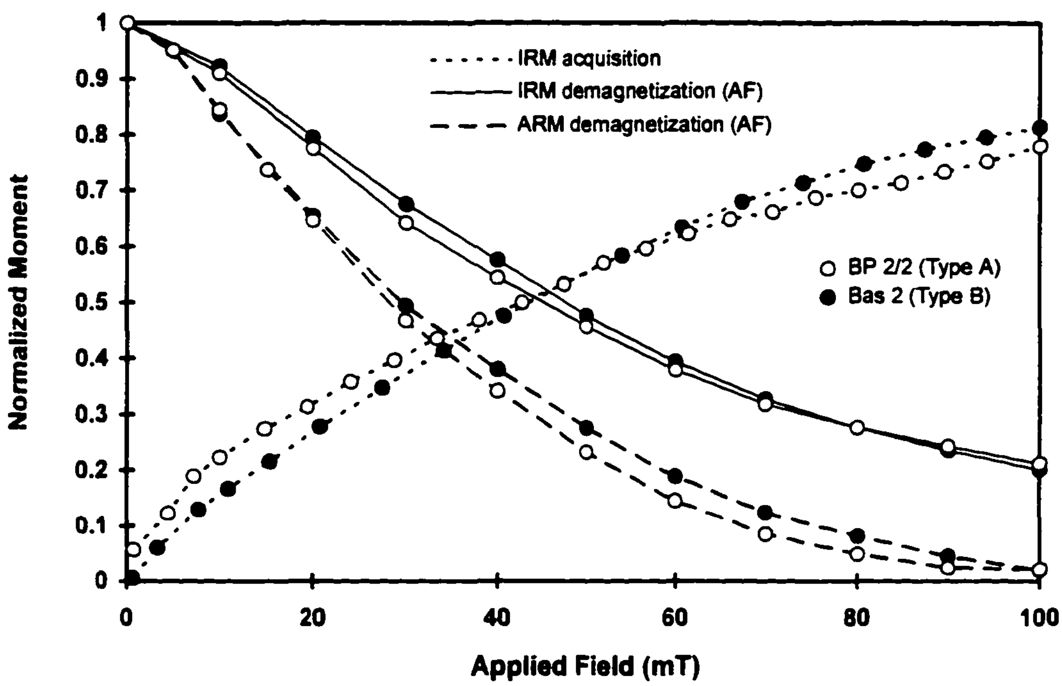

Figure. 2-6 *Cisowski* [1981] and modified Lowrie-Fuller [*Johnson et al*, 1975] tests on representative Type A and B Belden Formation specimens. Acquisition and AF demagnetization of IRM, AF demagnetization of ARM. *Cisowski* [1981] interprets symmetrical curves crossing at normalized moment of around 0.5 as diagnostic of fine grained non-interacting magnetite.

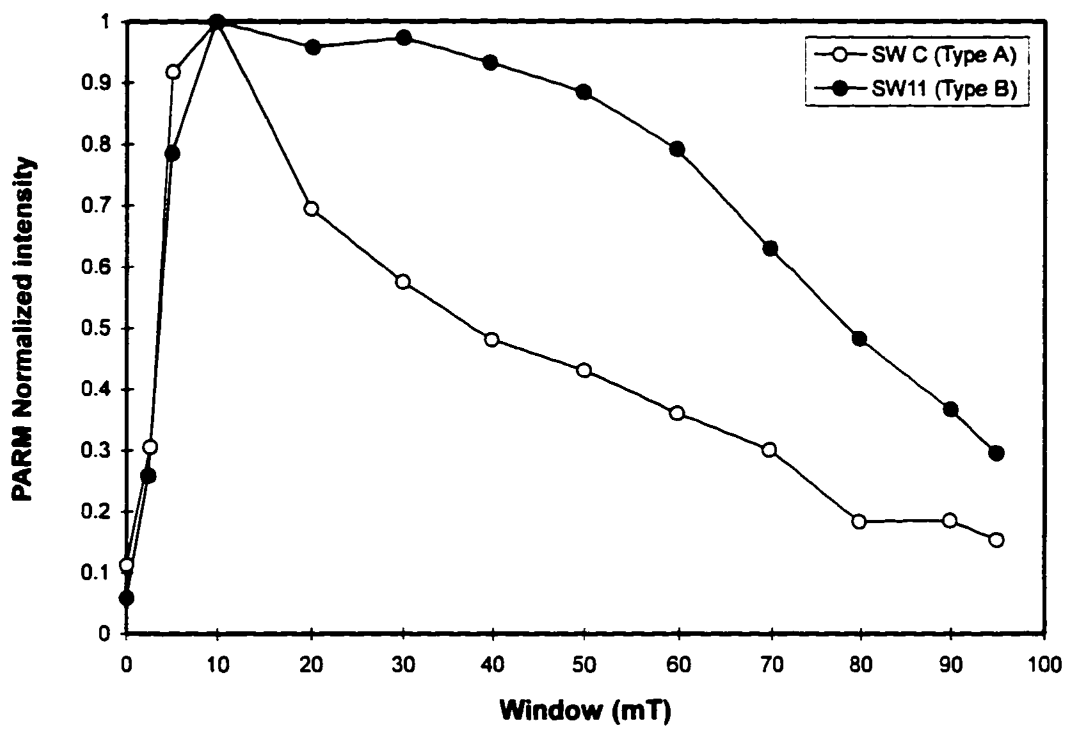

Figure. 2-7. Acquisition of partial anhysteretic magnetization by representative Type A and B Belden Formation specimens from Sweetwater Anticline using a 10 millitesla (mT) window, a 0.1 mT biasing field, and 90 mT alternating field (from *Fruit* [1994]).

specimens maintain relatively high values up to higher coercivities (about 70 mT). The different shapes and the stability values of the PARM curves have been interpreted by *Fruit* [1994] to indicate that Type B sites carry more higher coercivity material and that Type A sites are dominated by more low-coercivity material.

Hysteresis properties

Hysteresis loops of the analyzed Belden samples have a constricted or 'wasp-waisted' shape (Figure 2-8 a-d). The wasp-waistedness of hysteresis loops reported from other remagnetized carbonate units has been attributed to the presence of a bimodal distribution in coercivities [e.g., *Jackson*, 1990; *Channell and McCabe*, 1994; *McCabe and Channell*, 1994; *Roberts et al.*, 1995].

In the case of the Belden samples, some hematite is present, and the contrasting coercivities could theoretically be caused by a mix of magnetite and hematite. All hysteresis loops close by 300 mT (Figure 2-8 a-d), however, which indicates that hematite is not significantly affecting the hysteresis properties and hence is probably not contributing to the wasp-waistedness of the loops [e.g. *Roberts et. al.*, 1995]. Since magnetite is the only other ferrimagnetic mineral identified in these samples, the constriction in the loops must be due to presence of different coercivities of magnetite grains. According to *Roberts et. al.* [1995], wasp-waistedness can occur by mixing of single domain (SD) grains with significant amounts of superparamagnetic (SP) and/or MD grains.

Hysteresis properties differ for Type A and Type B samples. Type A samples have generally lower H_c and M_{rs}/M_s values compared to Type B samples (Figures 2-9

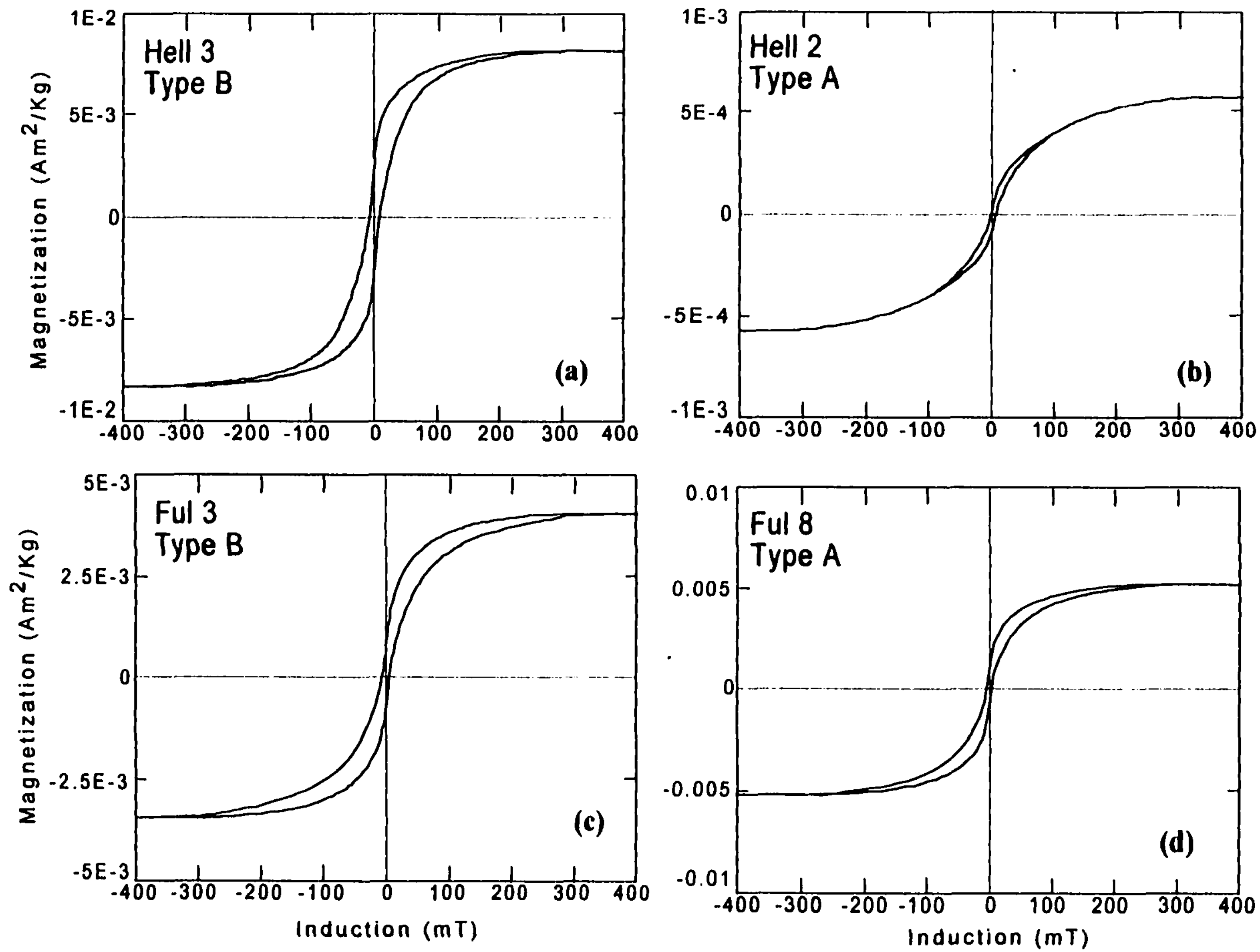

Figure. 2-8 Typical wasp-waisted hysteresis loop for representative Type A and B Belden Formation samples from Hell's Gate (a,b) and Fulford (c,d).

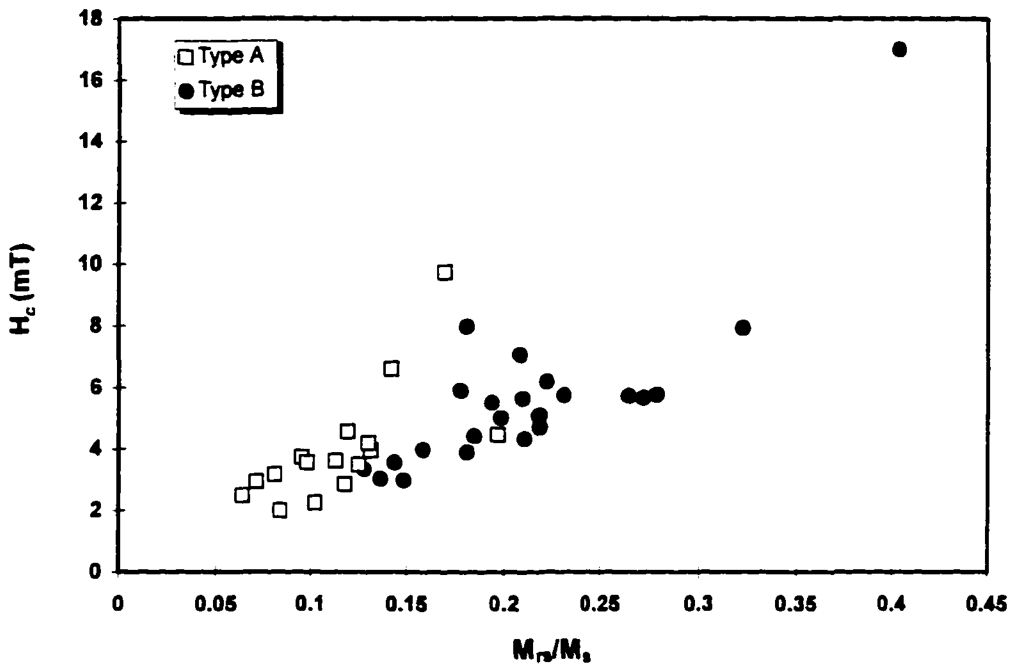

Figure. 2-9 Plot of H_c against M_{rs}/M_s for Type A and B Belden Formation samples.

and 2-10). For assemblages of magnetic minerals, it is known that both M_{rs}/M_s and H_c increase as the particle size decreases [e.g., *Dunlop*, 1986; *Suk and Halgedahl*, 1996]. Hence, Type B samples are interpreted to be dominated by more fine grained magnetic particles than Type A samples.

Previous studies on synthetic samples with mixtures of grain sizes [e.g. *Parry*, 1980; 1982] and from studies of remagnetized carbonate [e.g., *Jackson*, 1990] show that M_{rs}/M_s versus H_{cr}/H_c values are related by a power law. The hysteresis values for the Type B Belden samples also seem to follow a power law trend with $(M_{rs}/M_s) = 0.68(H_{cr}/H_c)^{-0.63}$ and have a regression coefficient of 0.85. The slope of the best fit line (Figure 2-10) is similar to that reported by *Jackson* [1990], but the intercept value (0.68) is lower.

The Type A samples (Figure 2-10) plot away from the remagnetized carbonate trend line of *Jackson* [1990]. Assuming that, like other remagnetized carbonate data, Type A data also follow a power law, the trend line for this data has the relation $(M_{rs}/M_s)=0.56(H_{cr}/H_c)^{-0.84}$ with a regression coefficient of 0.73. The slope and the intercept values for this trend are quite different from those obtained by *Jackson* [1980]. The significance of this is discussed later.

LTD and AF treatment

Stepwise AF and LTD cleaning of Belden specimens removes a component directed along the present earth field (Figure 2-11 a,b) and is interpreted to be carried by MD magnetite. The results of thermal demagnetization of Belden specimens pre-cleaned by the AF and LTD methods show that the component 2 and 3 directions are

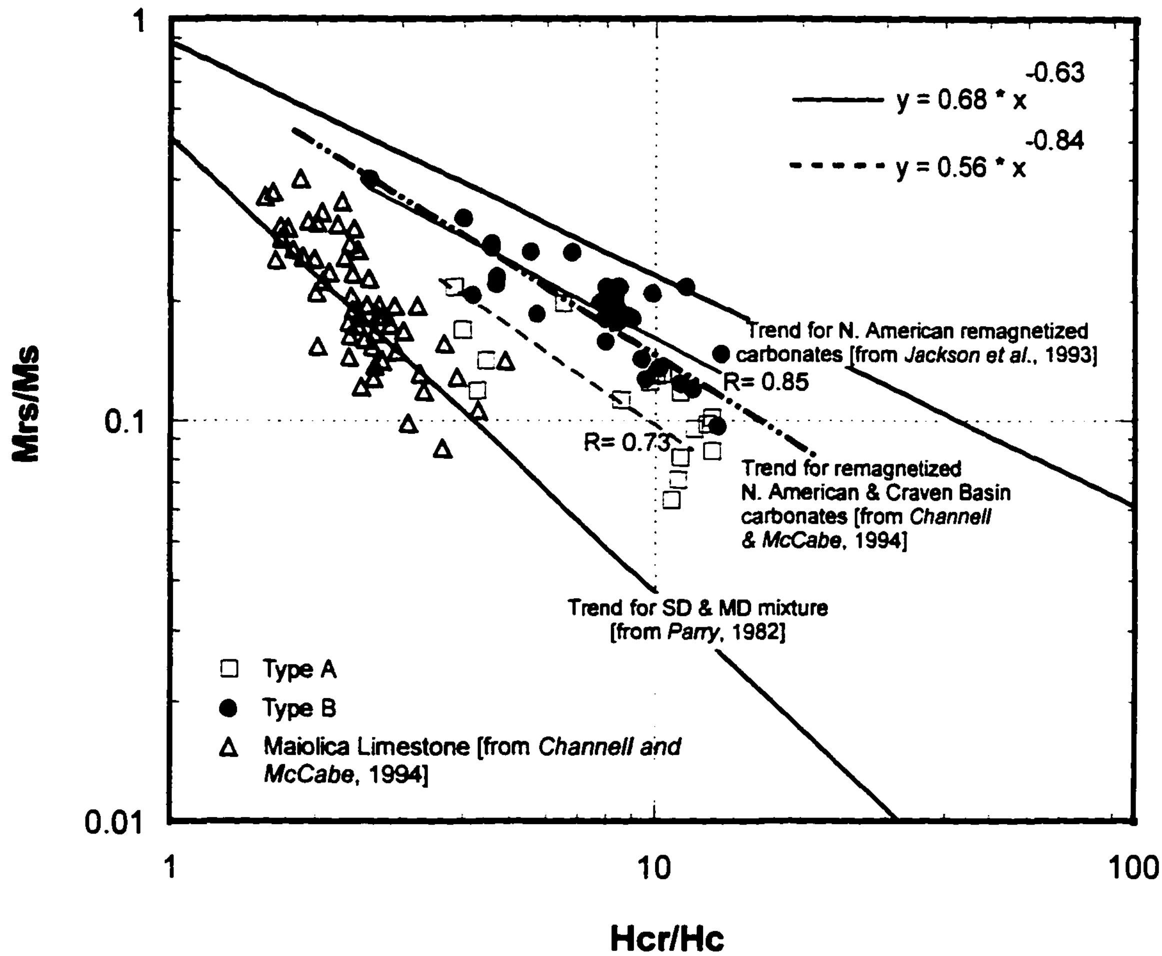

Figure. 2-10 Bilogarithmic plot of hysteresis parameters for Type A and B Belden Formation samples along with the best fit line for each type (dashed line - Type A samples; solid line - Type B samples; R - regression coefficient for ech type). Data for SD+MD mixture [*Parry,* 1982], remagnetized carbonates [*Jackson et al.*, 1993] and unremagnetized Maiolica Limestone, Italy [*Channell and McCabe*, 1994] is also shown. The bold dashed and dotted line is from *Channell and McCabe* [1994] for remagnetized N. American and Craven Basin carbonates.

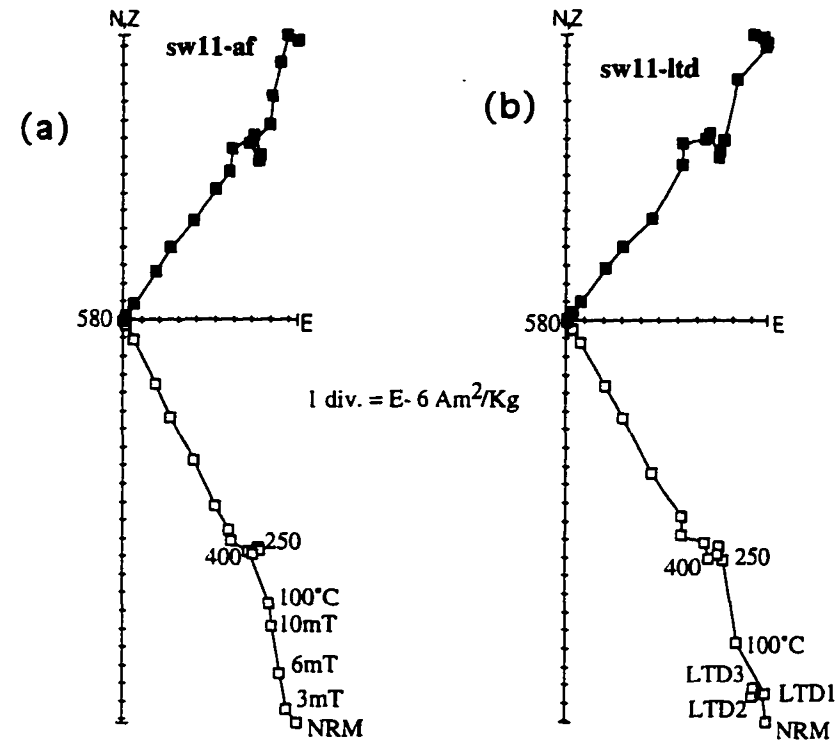

Figure. 2-11a Orthogonal (Zijderveld) projection of thermal demagnetization of **(a)** AF **(b)** LTD precleaned samples from steep limb of Sweetwater Anticline (before structural correction).

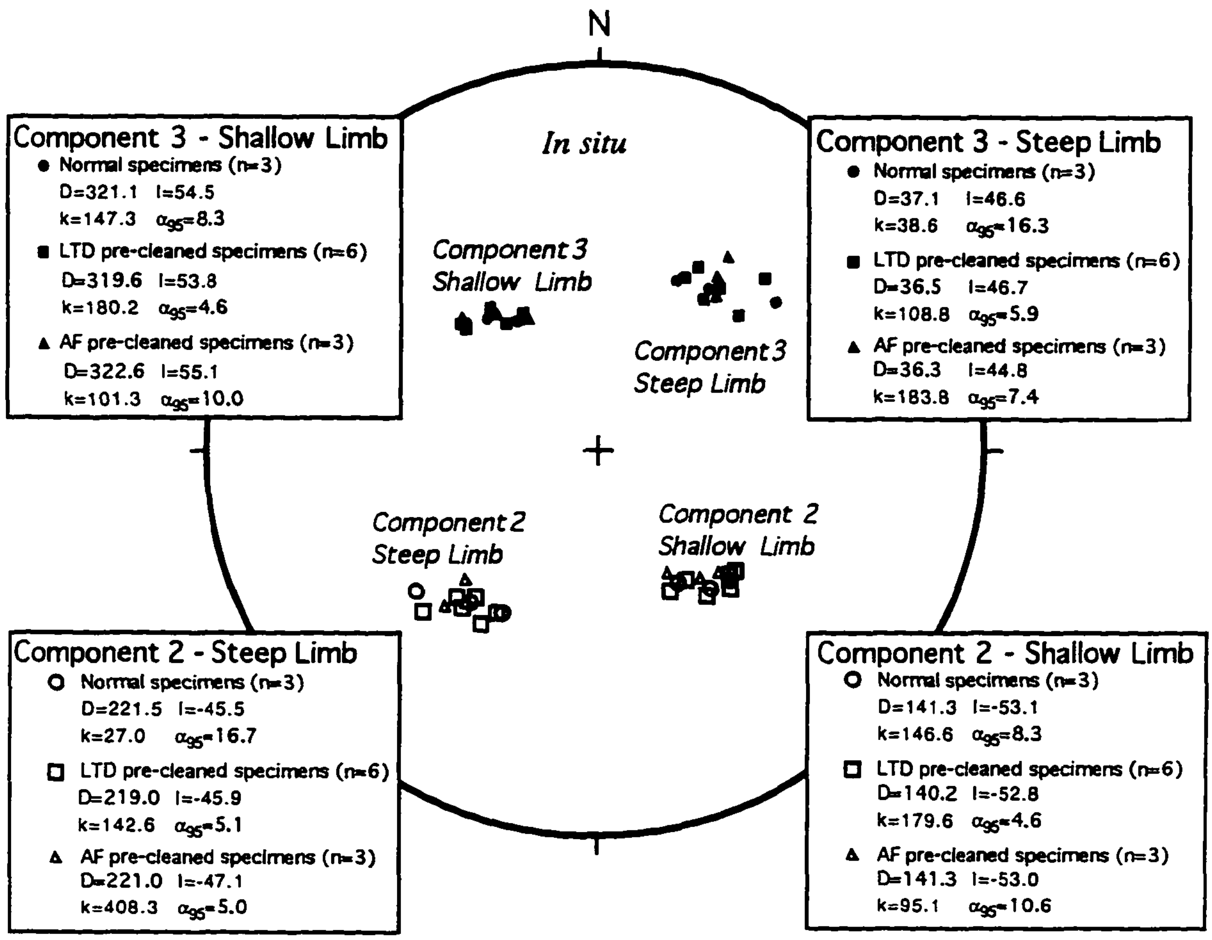

Figure. 2-11(c) Equal area projection of *in situ* component 2 and 3 specimen directions from thermal demagnetization of normal (untreated), AF and LTD precleaned specimens from both limbs of the Sweetwater Anticline. Solid symbols - lower hemisphere projections; open symbols - upper hemisphere projections.

statistically similar to those obtained from untreated samples (Figure 2-11c). Although these results suggest that normal demagnetization removes any magnetization in MD grains, other studies report that LTD and AF cleaning are not effective in removing a remanence from some MD grains [e.g., *McClelland*, 1996]. The results of this test, therefore, are not considered conclusive.

The results of LTD and zero-field cycling on SIRM-imparted specimens show that they retain between 89% and 95% of the SIRM after 3 LTD cycles. Following *Halgedahl and Jarrard* [1995], such high "memory" rates do not appear to be consistent with the presence of abundant MD grains.

Low temperature remanence measurements

The results of low temperature measurements of SIRM (Figure 2-12 a-c) show that the decay curves for all the analyzed samples have an initial steep slope between 10-50°K, which is in part due to the presence of superparamagnetic (SP) grains. None of the samples show the presence of the Verway transition (expected at about 110-120°K). *Özdemir et. al.* [1993] report that the Verway transition can take place in both SD and MD grains and that the transition is suppressed with increasing oxidation of the magnetite grains. Since the presence of magnetite of varying grain sizes in the Belden specimens has already been established by IRM, ARM and low temperature demagnetization studies, the lack of Verway transition in Belden samples suggests that the magnetite grains may have been exposed to oxidizing conditions.

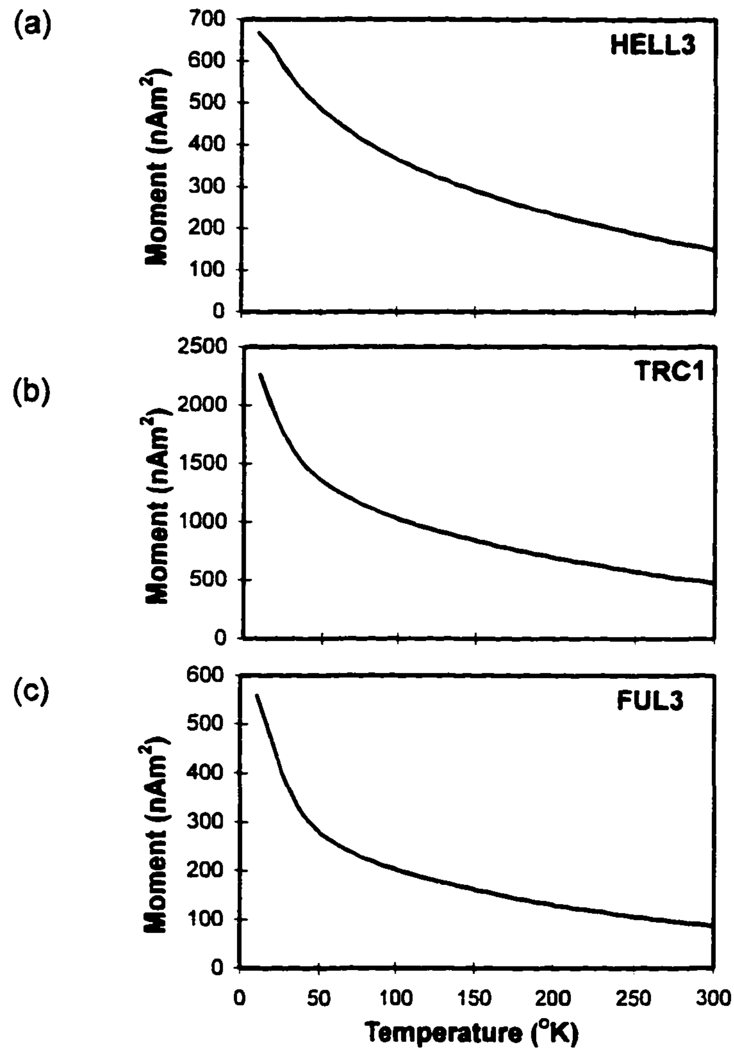

Figure 2-12 Decay of an IRM imparted at 10°K upon warming to room temperature on Type B Belden Formation samples from **(a)** Hell's Gate, **(b)** Fulford, and **(c)** Trout Creek.

Petrographic and microprobe analysis

Petrographic analysis of Type A and B samples indicate abundant authigenic iron-oxides, many pseudomorphed after pyrite. No detrital magnetite grains were observed based on shape or composition (e.g., Ti content).

DISCUSSION

Components 2 and 3 in the Belden Formation are both carried by magnetite but the magnetite that carries each component has different rock magnetic properties. Specimens that carry both components 2 and 3 (Type B) have higher saturation remanence and coercivity than those that that carry only Component 2 (Type A). Hysteresis properties suggest that component 2 magnetite is coarser than component 3 magnetite. Differences in the trends on the log-log plots for hysteresis parameters (M_{rs}/M_s and H_{cr}/H_c) also indicate that the two groups of samples have different magnetic properties.

Component 2 could be interpreted as a TVRM based on the maximum laboratory unblocking temperatures (350-425°C), the age of the component and the burial/thermal history of the Belden Formation. In the Sweetwater and Miller Creek (near Buford) areas, the maximum unblocking temperatures (400°C) are consistent with acquisition of the component during cooling from the modeled burial temperature of approximately 150°C [*Nuccio et al.*, 1989] based on experimental evidence from *Kent* [1985] which assumes the presence of multi-domain magnetite (Figure 2-13). At Minturn (near Gilman) and in the South Park areas (locations 16-19, Figure 2-1), the maximum unblocking temperatures (425°C) are consistent with the modeled burial

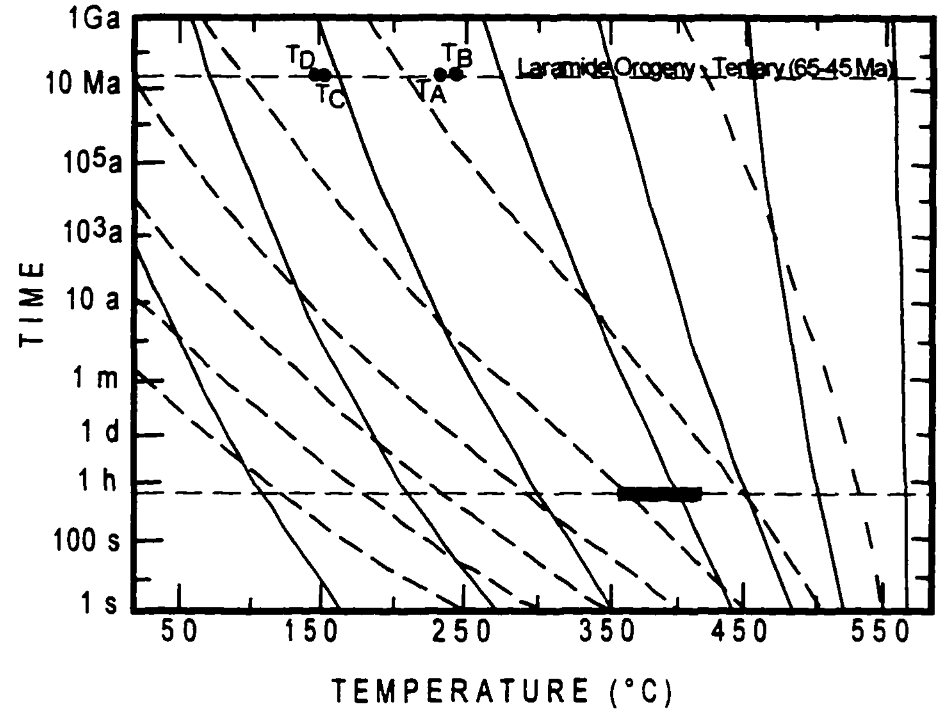

Figure. 2-13 Theoretical relaxation time versus temperature diagram for magnetite with Tertiary burial temperatures for Belden Formation locations in Colorado. Solid curves are from *Middleton and Schmidt* [1982] and are consistent with experimental evidence presented by *Kent* [1985] while dashed lines are from *Pullaiah et. al.* [1975]. Burial temperatures from Minturn (T_A), Hell's Gate-Sweetwater (T_C) and Miller Creek (T_D) are from *Nuccio et al.* [1989]; Trout Creek - Bassam Park (T_B) burial temperatures estimated from burial data from *Maughn*, [1989]. The shaded box indicates the maximum laboratory unblocking temperature range for Component 2 from these locations.

temperatures and the blocking temperature-relaxation time curves for magnetite from *Pullaiah et al.* [1975] for single domain magnetite and experimental evidence presented by *Smith and Verosub* [1994]. A component with similar directions and interpreted as a TVRM has also been reported in the older Leadville Formation [*Horton et al.*, 1984].

The reason that the results from the different areas seem to agree with the different relaxation time curves is not apparent. This could be due to a difference in the size of the magnetite that carries component 2 in the different areas, although there is no evidence for this based on the rock magnetic results (e.g., hysteresis properties, Lowrie-Fuller tests, low temperature demagnetization). If the magnetite is of the same size, the maximum unblocking temperatures should be higher in the areas that were heated to higher burial temperatures. Whereas thermal demagnetization results for some specimens from South Park indicate that component 2 may extend up to 425°C, at all other areas the maximum unblocking temperature is 400°C.

If component 2 is a TVRM, the rock magnetic characteristics should reflect those of the original grains of magnetite. The intercept value of the best fit line for Type A samples (c = 0.56) is between that reported by *Parry* [1982] for SD+MD mixing and that of remagnetized carbonate as reported by *Jackson et al.* [1993]. One possible way to explain the lower intercept value compared to that for remagnetized carbonate [*Jackson et al,* 1993] is by having a mix of magnetite grains with a dominant fraction with shape anisotropy (c=0.5 as reported by *Stoner and Wohlfarth* [1948]) and a subordinate fraction with magnetocrystalline anisotropy (c=0.86 from *Joffee and Heuberger* [1974]). The hysteresis values (M_{rs}/M_s versus H_{cr}/H_c) for Type A samples are also close to values reported by *Channell and McCabe* [1994] for the unremagnetized Maiolica Limestone from Italy which carries only a primary magnetization. The rock magnetic results are thus consistent with a detrital origin for this magnetite. As previously noted, however, no obvious detrital magnetite was identified during petrographic/microprobe analysis.

Another possible remagnetization mechanism for component 2 is a thermochemical remanent magnetization (TCRM) or a CRM. Growth of new magnetite, perhaps by replacement of pyrite, might have been triggered by heating in the Tertiary, i.e., an extension of the same chemical remagnetization process which caused acquisition of the older component 3 CRM (see Chapter 1). The process could have been diagenesis of organic matter (see Chapter 1) or perhaps illitization of smectite [e.g., *Katz et. al.*, 1996]. Another possibility is the formation of magnetite by alteration of siderite, pyrite and iron-bearing clays which *Ellwood et. al.* [1986] suggest can cause acquisition of a magnetization in magnetite. Still, another possibility is that pyrite, which is abundant in the Belden Formation, was oxidized to magnetite solely by moderate burial temperatures (about 150-250°C) although previous studies [e.g., *Tkhoa*, 1985] have demonstrated that pyrite oxidation to magnetite in open air requires heating to 450-500°C.

Although a CRM or TCRM origin for component 2 is a possibility, the rock magnetic properties are distinct from other CRMs and are more consistent with a mixture of authigenic and detrital grains. The TVRM is thus interpreted to be carried by authigenic and detrital magnetite grains, all of which were reset subsequent to the Laramide heating. Although no obvious (i.e., Ti-rich) detrital grains were identified during microprobe analysis of selected Type A samples, this test is not considered to be conclusive. The presesence of Ti-poor detrital grains cannot be ruled out. Further, the grain-size (SD/PSD) of most of the magnetite carrying this magnetization would be below the resolution of the microprobe (~1 μm).

Component 3 is interpreted as a chemical remanent magnetization (CRM). The high unblocking temperature ranges for this component and the presence of authigenic magnetite rims around pyrite are consistent with this interpretation (see Chapter 1). The hysteresis values (M_{rs}/M_s and H_{cr}/H_c) are also consistent with this interpretation and show good correlation with data from other reported remagnetizaton in carbonate [e.g., *Jackson*, 1990; *Channell and McCabe*, 1994; *McCabe and Channell*, 1994]. The chemical magnetization process is interpreted to be a burial diagenetic process (see Chapter 1).

For chemically remagnetized carbonate, *Jackson* [1990] found that the linear trend of M_{rs}/M_s vs. H_{cr}/H_c on a log-log plot has a slope (m) of -0.6 and intercept (c) of 0.89. *Jackson* [1990] attributed the high value of c to indicate that the magnetization in remagnetized carbonate rocks was controlled by cubic magnetocrystalline anisotropy, which is more common in authigenic grains compared to detrital grains where the shape anisotropy effect dominates. The best fit line for Type B samples on a log-log plot has a similar slope but a lower intercept value (c = 0.68) compared to *Jackson's* [1990] trend for remagnetized carbonate. The lower intercept value could indicate that Type B samples are characterized by a mixture of grains carrying component 3 with magnetocrystalline anisotropy and component 2 with shape anisotropy (detrital?).

The site specific nature of the CRM is interpreted to be related to the presence or absence of magnetically finer, more coercive grains of magnetite. This CRM has been interpreted to have formed due to burial diagenetic processes co-genetic with organic maturation, which converted pre-existing pyrite to magnetite. As yet, the effects of various parameters, such as the amount of organic carbon present in the rocks and the quantity and size of pyrite grains present in the rocks has not been determined. It is speculated that the site specific nature of the CRM may be the result of some precursor chemical and physical inhomogeneity present in the rocks which controlled and affected this magnetite creating event.

CONCLUSIONS

The Belden Formation in Colorado contains two dominant components, an intermediate unblocking temperature interpreted as a TVRM and a high unblocking temperature component interpreted as a CRM. These components can be distinguished by their directional as well as rock magnetic properties. These properties indicate that most Belden Formation sites in Colorado acquired a Tertiary TVRM but only certain sites acquired and preserved an earlier CRM. Specimens with the CRM have hysteresis properties consistent with a rock magnetic fingerprint for chemical remagnetization. This component is carried by SD magnetite which was created by replacement of pyrite during burial diagenetic reactions. Hysteresis properties are consistent with those for magnetite dominated by cubic magnetocrystalline anisotropy, as would be expected in authigenically formed magnetite grains.

Rocks with only a TVRM are dominated by coarser grain magnetite than that which is interpreted to carry the CRM. The hysteresis properties indicate that the magnetite in these rocks could be dominated by shape anisotropy, as would be expected for detrital grains, although no obvious magnetite detrital grains were observed petrographically. The TVRM is interpreted to reside in a mixture of large authigenic and perhaps some detrital grains of magnetite.

REFERENCES CHAPTER 2

Channell J.E.T. and C. McCabe, Comparison of magnetic hysteresis parameters of unremagnetized and remagnetized limestone, *J. Geophys. Res.*, *99*, 4613-4623, 1994.

Cisowski, S. M., Interacting vs. non-interacting single domain behavior in natural and synthetic samples, *Phys. Earth Planet. Inter.*, *26*, 56-62, 1981.

Dunlop, D.J., Hysteresis properties of magnetite and their dependence on particle size: a test of pseudo-single-domain remanence models, *J. Geophys. Res.*, *91*, 9569-9584, 1986.

Dunlop, D.J. and K.S. Argyle, Separating multidomain and single-domain-like remanences in pseudo-single-domain magnetites (215-540 nm) by low temperature demagnetization, *J. Geophys. Res.*, *96*, 2007-2017, 1991.

Dunlop, D.J., Ö. Özdemir and P.W. Schmidt, Thermoviscous remagnetization of multidomain magnetite, IUGG XXI General Assembly, Boulder (Abstracts), B-136, 1995.

Ellwood, B.B., W. Balsam, B. Burkart, G.J. Long and M.L. Buhl, Anomalous magnetic properties in rocks containing the mineral siderite: Paleomagnetic implications, *J. Geophys. Res.*, *91*, 12,779-12,790, 1986.

Elmore, R.D. and C.R. McCabe, The occurrence and origin of remagnetization in the sedimentary rocks of North America, in, Contributions in Geomagnetism and Paleomagnetism, U.S. National Report 1987-1990, *Reviews in Geophysics, Supplement*, *29*, 377-383, 1991.

Fisher, R. A, Dispersion on a sphere, *Proc. R. Soc. London*, *A*, *217*, 295-305, 1953

Fruit, D, Testing the origin of a synfolding chemical remagnetization in the Belden Formation, Northwest Colorado, Ph.D. thesis, Univ. of Oklahoma, Norman, 1994.

Fruit, D., R.D. Elmore, and S. Halgedahl, Remagnetization of the folded Belden Formation, *J. Geophys. Res.*, *100*, 15,009-15,023, 1995.

Halgedahl, S.L. and R.D. Jarrard, Low-temperature behavior of single-domain through multidomain magnetite, *Earth Planet. Sci. Lett.*, *130*, 127-139, 1995.

Hart, M. and M. Fuller, Magnetization of a dolomite bed in the Monterey Formation: Implications for diagenesis, *Geophys. Res. Lett.*, *15*, 491-494, 1988.

Heider, F., D.J. Dunlop and H.C. Soffel, Low-temperature and alternating field demagnetization of saturation remanence and thermoremanence in magnetite grains

(0.037mm to 5mm), *J. Geophys. Res.*, *97*, 9371-9381, 1992.

Horton, R.A., J.W. Geissman and R.J. Tschauder, Paleomagnetism and rock magnetism of the Mississippian Leadville (carbonate) formation and implications for the age of sub-regional dolomitization, *Geophys. Res. Lett.*, *11*, 649-652, 1984.

Jackson, M., Diagenetic sources of stable remanence in remagnetized Paleozoic cratonic carbonate: a rock magnetic study, *J. Geophys. Res.*, *95*, 2753-2761, 1990.

Jackson, M., P. Rochette, G. Fillion, S. Banerjee and J. Marvin, Rock magnetism of remagnetized Paleozoic sedimentary carbonate: low temperature behavior and susceptibility characteristics, *J. Geophys. Res.*, 98, 6217-6226, 1993.

Joffe, I. and R. Heuberger, Hysteresis properties of distributions of cubic single-domain ferromagnetic particles, *Philos. Mag.*, *29*, 1051-1059, 1974.

Johnson, H.P., W. Lowrie, and D.V. Kent, Stability of ARM in fine and coarse magnetite and maghemite particles, *Geophys. J.R. Astron. Soc.*, *41*, 1-10, 1975.

Katz, B., R.D. Elmore, M. Cogoini and S. Ferry, Remagnetization and diagenesis of clays (abstract), *Eos Trans. AGU 77-46*, 159, 1996.

Kent, D.V., Thermoviscous remagnetization in some Appalachian limestone, *Geophys. Res. Lett.*, *12*, 805-808, 1985.

Kirschvink, J. L., The least square line and plane and analysis of paleomagnetic data, *Geophys. J. R. Astron. Soc.*, *45*, 699-718, 1980.

Lowrie, W., Identification of ferromagnetic minerals in a rock by coercivity and unblocking temperature properties, *Geophys. Res. Lett.*, *17*, 159-162, 1990.

Maughn, E.K, Hydrocarbon exploration plays in the Colorado Park Basin province, in, *Energy Frontiers in the Rockies*, edited by J.C. Lorenz and S.G. Lucas, Albuquerque Geological Society, 79-83, 1989.

McCabe C. and J.E.T. Channell, Late Paleozoic remagnetization in limestone of the Craven Basin (northern England) and the rock magnetic fingerprint of remagnetized sedimentary carbonate, *J. Geophys. Res.*, *99*, 4603-4612, 1994.

McElhinny, M. W., Statistical significance of the fold test in paleomagnetism, *Geophys. J. R. Astron. Soc.*, *8*, 338-340, 1964.

McClelland, E. , Experimental constraints on models of remanence in multidomain magnetite (abstract), *Eos Trans. AGU 77-46*, 160, 1996

McFadden, P. L. and D.L. Jones, The Fold test in paleomagnetism, *Geophys. J. R.*

Astron. Soc., *67*, 53-58, 1981.

Middleton, M.F. and P.W. Schmidt, Paleothermometry of the Sydney Basin, *J. Geophys. Res.*, *84*, 5351-5359, 1982.

Nuccio, V.F., S.Y. Johnson and C.J. Schenk, Paleogeothermal gradients and timing of oil generation in the Belden Formation, Eagle Basin, northwestern Colorado, *The Mountain Geologist*, 26, 31-41, 1989.

Özdemir, Ö., D.J. Dunlop and B.M. Moskowitz, The effect of oxidation on the Verwey transition in magnetite, *Geophys. Res. Lett.*, *16*, 1671-1674, 1993.

Parry, L.G., Shape related factors in the magnetization of immobilized magnetite particles, *Phys. Earth Planet. Inter.*, *22*, 144-154, 1980.

Parry, L.G., Magnetization of immobilized particle dispersions with two distinct particle sizes, *Phys. Earth Planet. Inter.*, *28*, 230-241, 1982.

Pullaiah, G., E. Irving, K.L. Buchan and D.J. Dunlop, Magnetization changes caused by burial and uplift, *Earth Planet. Sci. Lett.*, *28*, 133-143, 1975.

Roberts, A.P., Y. Cui and K.L. Verosub, Wasp-waisted hysteresis loops: mineral magnetic characteristics and discrimination of components in mixed magnetic systems, *J. Geophys. Res.*, *100*, 17,900-17,924, 1995.

Schmidt, P. W., Paleomagnetic cleaning strategies, *Phys. Earth Planet. Inter.*, *76*, 169-178, 1993.

Smith, R.T., and K.L. Verosub, Thermoviscous remanent magnetism of Columbia River Basalt blocks in the Cascade landslide, *Geophys. Res. Lett.*, *21*, 2661-2664, 1994.

Stoner, E.C. and E.P. Wohlfarth, A mechanism of magnetite hysteresis in heterogenous alloys, *Trans. R. Soc. London, A, 240.*, 599-642, 1948.

Suk, D. and S. L.Halgedahl, Hysteresis properties of magnetic spherules and whole rock specimens from some Paleozoic platform carbonate, *J. Geophys. Res.*, *101*, 25,053-25,075, 1996.

Tkhoa, N.T.K., On the stability relationships of the values of crystallization, ideal and thermoremanent magnetization of magnetite formed by alteration of pyrite, *Izvestiya-Earth Physics, 21*, 561-564, 1988.

Van der Voo, R., Paleomagnetism of North America: The craton, its margins and the Appalachian Belt, *Mem. Geol. Soc. Am.*, *172*, 447-470, 1989.

Zijderveld, J.D.A., A.C. Demagnetization of rocks: Analysis of results, in, *Methods in*

Paleomagnetism, edited by D.W. Collinson et al., Elsevier, New York, 254-286, 1967.

FINAL CONCLUSIONS

Samples from the lower Pennsylvanian Belden Formation in Central Colorado were paleomagnetically and geochemically evaluated to address the following issues (1) When were the magnetizations present in the rocks acquired? (2) What were the mechanisms that created these magnetizations? (3) Could the different magnetizations present in the Belden Formation be characterized using rock magnetic techniques?

A regional paleomagnetic and geochemical study of the Belden carbnonates was undertaken to test for a connection between a CRM residing in magnetite and maturation of organic matter. Thermal demagnetization of Belden carbonate samples show the presence of two components, in addition to a low unblocking temperature modern VRM. An intermediate temperature synfolding, Tertiary component, present at all locations, is interpreted to be a TVRM, acquired by the rocks during cooling from maximum burial and heating. A widespread, locally synfolding, CRM with high unblocking temperatures is present at selected locations within the basin.

Rock magnetic studies, including IRM analysis, hysteresis studies, and LTD/AF treatment suggest that the CRM is carried by magnetite. Based on petrographic analysis and results from previous studies [e.g. *Fruit et al.*, 1995], this CRM is interpreted to be carried by magnetite that has formed by replacing pyrite. Orogenic fluids are not considered a likely remagnetization mechanism for this CRM, as indicated by the results of contact vein tests,. The age of the CRM is found to vary across the basin, and its age correlates with the modeled timing of oil generation. This CRM is interpreted to be related to burial diagenesis. Although, further studies are needed to test this "burial diagenetic" model of CRM acquisition, it could apply to other pervasive CRM's in carbonate. Any CRMs acquired following the "burial diagenetic" model would be expected to show differences in age over different parts of the basin, though the mechanism for the CRM would be the same. This may necessitate the evaluation of magnetic components in such rocks in terms of their unblocking temperature range rather than just their directional properties.

The TVRM present in the Belden carbonate can be distinguished from the CRM by directional as well as rock magnetic properties. These properties indicate that most Belden Formation sites in Colorado acquired a Tertiary TVRM but only certain sites acquired and preserved an earlier CRM. Specimens with the CRM have hysteresis properties consistent with rock magnetic fingerprint for chemical remagnetization. This component is carried by SD magnetite which was created by replacement of pyrite during burial diagenetic reactions. Hysteresis properties are consistent with those for magnetite dominated by cubic magnetocrystalline anisotropy, as would be expected in authigenically formed magnetite grains.

Rocks with only a TVRM are dominated by coarser grain magnetite than that which is interpreted to carry the CRM. The hysteresis properties indicate that the magnetite in these rocks could be dominated by shape anisotropy, as would be expected for detrital grains, although no obvious detrital magnetite grains (e.g., Ti-rich) were observed petrographically. The TVRM is interpreted to reside in a mixture of large authigenic and perhaps some detrital grains of magnetite.

APPENDIX

APPENDIX 1

LISTING OF PROGRAM UNFOLD.C

```
/*****************************************************************************
                    INCREMENTAL FOLD TEST PROGRAM
Program written by Sanjay Banerjee, School of Geology and Geophysics, University of
Oklahoma, 1995-96. This program can accept directional information for paleomagnetic
vectors from the two limbs of a fold. Each individual vector can then be rotated in space by
user defined increments. Various statistical parameters related to McElhinny [1964] and
McFadden and Jones [1981] fold tests are calculated for each incremental rotation step.
*****************************************************************************/
#include <conio.h>
#include <dos.h>
#include <stdio.h>
#include <stdlib.h>
#include <string.h>
#include <math.h>
#include <iostream.h>


const double PI=3.14159265358979323846;
const double RAD=PI/180;
const double DEG=1/RAD;
float limb1[30][4],limb2[30][4];


//********* FUNCTION PROTOTYPE DECLARATIONS************

FILE *Graceful_open(char filename[], char mode[]);
void beeper(void);
void enter_array(float limb1[30][4], int *p, char limb[]);
void edit_array(float limb1[30][4], char limb[], int m);
void add_array (float limb1[30][4], int *p, char limb[]);
void delete_array(float limb1[30][4], int *p, char limb[]);
void print_array(int m, float A[60][4], char limb[]);
float antan2 (float x, float y);
float antan3 (float x, float y);
float rota_dec(float pdir, float plunge, float angle, float dec, float inc);
float rota_inc(float pdir, float plunge, float angle, float dec, float inc);

void main()
{
float bothdata[101][6],MACK[102][1];
float dip0,dip_percent,D3,I3,app_dip,max,sx,sy,sz,xx,
  xy,xz,rr;
int k,kk,percent,percent1,D,m=0,n=0,mm,dm,jj,zz,mmm,N,N1,N2,TT,pp,ee,kount,
  Kjj,kmm,p;
char inp1,inp3,name[15];
double incl,decl,Kparam,AA,AX,T,X2,Y2,Artan,PLUNGE,
   Xcosine,Ycosine,Zcosine,mac1,mac2,mac3,Mac,sb,
   level2,Alpha95;
{float combined[3000][3];
float unf_limb1[3000][3],unf_limb2[3000][3],
```

```
  limb1data[101][2],limb2data[101][2];
char limb_1[]="LIMB 1", limb_2[]="LIMB 2";
clrscr();
cout<<"\n\t#################################################################"<<"\n"
  <<"\t#        INCREMENTAL FOLD TEST         #"<<"\n"
  <<"\t################################################################"<<"\n\n"
  <<" 1. This program will perform plunge correction and unfolding followed "<<"\n"
  <<"\tby incremental fold test on user supplied directional data."<<"\n"
  <<" 2. The data for the two limbs of a fold have to be entered separately. The"<<"\n"
  <<"\tinput data for each vector consists of its inclination, declination"<<"\n"
  <<"\tand dip and strike of the bedding."<<"\n"
  <<" 3. The data can be entered either directly from the keyboard or from a file"<<"\n"
  <<"\tcreated previously by this program."<<"\n"
  <<" 4. Before entering or importing data, specify:"<<"\n"
  <<"\t[1] a filename, for the output data."<<"\n"
  <<"\t[2] percent amount for incremental unfolding (2-100)."<<"\n"
  <<" 5. K (McElhinny's parameter) and Mcfadden's parameter will be calculated"<<"\n"
  <<"\tfor each successive unfolding step and stored in the output file."<<"\n"
  <<" 6. The output file can be opened as a Text file (comma-delimited), using"<<"\n"
  <<"\tMicrosoft Excel, for further analyis."<<"\n"
  <<" NOTE: Maximum 20 data sets from each limb can be used in this program."<<"\n";
FILE *out_file, *inp_file, *dat_file;
dat_file=Graceful_open("unfold.dat","w");
printf("\n Give a file name for storing the output data: ");
scanf("%s",name);
out_file=Graceful_open(name,"w");
printf(" At what percent steps would you like to carry out unfolding (2-100)? ");
 do{
   scanf("%d", &percent);
   fflush(stdin);
   if(percent>=2 && percent<=100)
    break;
   else {
   beeper();
   printf("Percent should be between 2 and 100. Re-enter again: ");
   }
 }while(1);
 k=100/percent;
 percent1=k;
cout<<" Magnetic declination correction for this area: ";
float dec_corr;
cin>>dec_corr;
cout<<"\nChoose one of the following options:\n"
  <<"\tF - import Data from an existing File\n"
  <<"\tK - enter data from Keyboard"
  <<"\n\tEnter your Choice: ";
char choice;
do{
cin>>choice;
  if(choice=='f'||choice=='F'||choice=='K'||choice=='k')
  break;
  else{
  beeper();
  cout<<"\tEnter the proper choice, F or K: ";
  continue;
```

```
 }
}while(1);
/*-----------------Data Entry from the Keyboard-------------------*/
if(choice=='K'||choice=='k'){
cout<< "\tGive a filename for storing the input data: ";
char Inp_file_name[15];
cin>>Inp_file_name;
inp_file=Graceful_open(Inp_file_name,"w");
//***************Data entry for the first Limb*****************
enter_array(limb1,&m,limb_1);
do{clrscr();char inp2;
  print_array(m,limb1,limb_1);
  cout<<"\n\nDo you wish to edit(E), delete(D), add(A) or continue(C) ";
  do{
   cin>>inp2;
   if(inp2=='c'||inp2=='C'||inp2=='A'||inp2=='a'||inp2=='D'
          ||inp2=='d'||inp2=='E'||inp2=='e')
          break;
   else{
          beeper();
          cout<<"Enter the correct choice(E,D,A or C): ";
          }
  }while(1);
if(inp2=='E'||inp2=='e')
{edit_array(limb1,limb_1,m);
continue;}
if(inp2=='D'||inp2=='d') delete_array(limb1,&m,limb_1);
if(inp2=='a'|inp2=='A') add_array(limb1,&m,limb_1);
if(inp2=='C'|inp2=='c') break;
}while(1);
for(int m1=0;m1<=m;m1++){
fprintf(inp_file,"1,%.2f,%.2f,%.2f,%.2f\n",limb1[m1][0]*DEG,limb1[m1][1]*DEG,limb1[m1][2]*DEG,
limb1[m1][3]*DEG);
}
//*****************Data entry for the second limb*******************
enter_array(limb2,&n,limb_2);
do{clrscr(); char inp2;
  print_array(n,limb2,limb_2);
  cout<<"\n\nDo you wish to edit(E), delete(D), add(A) or continue(C): ";
  do{
   cin>>inp2;
   if(inp2=='c'||inp2=='C'||inp2=='A'||inp2=='a'||inp2=='D'
          ||inp2=='d'||inp2=='E'||inp2=='e')
          break;
   else{
          beeper();
          cout<<"Enter the correct choice(E,D,A or C): ";
          }
  }while(1);
if(inp2=='E'|inp2=='e') edit_array(limb2,limb_2,n);
if(inp2=='D'|inp2=='d') delete_array(limb2,&n,limb_2);
if(inp2=='a'|inp2=='A') add_array(limb2,&n,limb_2);
if(inp2=='C'|inp2=='c') break;
}while(1);
for(int n1=0;n1<=n;n1++){
```

```
fprintf(inp_file,"2,%.2f,%.2f,%.2f,%.2f\n",limb2[n1][0]*DEG,limb2[n1][1]*DEG,limb2[n1][2]*DEG,
limb2[n1][3]*DEG);
}
fprintf(inp_file,"3");
fclose(inp_file);
cout<<"\nThe input data has been stored in "<<Inp_file_name<<"\n";
}// end of "if choice==K" block
/*-----------------------Data Input from file-----------------------*/
if(choice=='F'||choice=='f'){
cout<< "\tName of existing input data file: ";
char Inp_file_name[15];
cin>>Inp_file_name;
inp_file=Graceful_open(Inp_file_name,"r");
int tag;
float data0,data1,data2,data3;

do{
 fscanf(inp_file,"%i,%f,%f,%f,%f\n",&tag,&data0,&data1,&data2,&data3);

 if (tag==1){
          limb1[m][0]=data0*RAD;
          limb1[m][1]=data1*RAD;
          limb1[m][2]=data2*RAD;
          limb1[m][3]=data3*RAD;
          m++;
          continue;
         }
 if (tag==2){
          limb2[n][0]=data0*RAD;
          limb2[n][1]=data1*RAD;
          limb2[n][2]=data2*RAD;
          limb2[n][3]=data3*RAD;
          n++;
          continue;
         }
if(tag==3) break;
else{
 cout<<"The specified input file is not properly structured for this program";
 cout<<"\nThe program is being terminated";
 exit(1);
 }
 }while(1);
m=m-1;n=n-1;
//***********Data modification for the first limb*****************
do{fflush(stdin); char inp2; clrscr();
 print_array(m,limb1,limb_1);
 cout<<"\n\nDo you wish to edit(E), delete(D), add(A) or continue(C): ";
 do{
  cin>>inp2;
  if(inp2=='c'||inp2=='C'||inp2=='A'||inp2=='a'||inp2=='D'
        ||inp2=='d'||inp2=='E'||inp2=='e')
        break;
  else{
        beeper();
        cout<<"Enter the correct choice(E,D,A or C): ";
```

```
        }
  }while(1);

if(inp2=='E'|inp2=='e') edit_array(limb1,limb_1,m);
if(inp2=='D'|inp2=='d') delete_array(limb1,&m,limb_1);
if(inp2=='a'|inp2=='A') add_array(limb1,&m,limb_1);
if(inp2=='C'|inp2=='c') break;
}while(1);
//**********Data modification for the second Limb***************
do{char inp2;clrscr();
 print_array(n,limb2,limb_2);
 cout<<"\n\nDo you wish to edit(E), delete(D), add(A) or continue(C) ";
 do{
  cin>>inp2;
  if(inp2=='c'||inp2=='C'||inp2=='A'||inp2=='a'||inp2=='D'
        ||inp2=='d'||inp2=='E'||inp2=='e')
        break;
  else{
        beeper();
        cout<<"\nEnter the correct choice(E,D,A or C): ";
        }
 }while(1);

if(inp2=='E'|inp2=='e') edit_array(limb2,limb_2,n);
if(inp2=='D'|inp2=='d') delete_array(limb2,&n,limb_2);
if(inp2=='a'|inp2=='A') add_array(limb2,&n,limb_2);
if(inp2=='C'|inp2=='c') break;
}while(1);
}//*******END OF IF CHOICE==k BLOCK****************************

//*******************Plunge value*****************************
double dmax1=limb1[0][1]*DEG;
for(int PP1=1;PP1<=m;PP1++){
 if (dmax1<limb1[PP1][1]*DEG)
        dmax1=limb1[PP1][1]*DEG;
 else
        continue;
}
double dmax2=limb2[0][1]*DEG;
for(int PP2=1;PP2<=n;PP2++){
 if (dmax2<limb2[PP2][1]*DEG)
        dmax2=limb2[PP2][1]*DEG;
 else
        continue;
}
cout<<"\nHow much is the plunge of this Fold (0-90): ";
do{
 fflush(stdin);
 cin>>PLUNGE;
 if (PLUNGE<=dmax1 && PLUNGE<=dmax2)
  break;
 else
 {beeper();
 cout<<"Plunge should be less than or equal to the dip of each limb."
   <<"\nRe-enter a correct value for Plunge: ";
```

```
 }
}while(1);
PLUNGE=PLUNGE*RAD;
/*===========unfolding and sorting data (limb 1)===============*/
printf("\nCalculating.....");
delay(50);
for(jj=0;jj<m+1;jj++)
  { D=k+1;
        percent1=k;
        mm=jj;
        kount=jj;
        do {
                D--;
                dip_percent=0.01*percent*limb1[jj][1];
                app_dip=limb1[jj][1]-(dip_percent*D);

        D3=rota_dec((limb1[jj][0]+(dec_corr*RAD)),PLUNGE,app_dip,limb1[jj][2],limb1[jj][3]);

        I3=rota_inc((limb1[jj][0]+(dec_corr*RAD)),PLUNGE,app_dip,limb1[jj][2],limb1[jj][3]);
                        if(D3<(-90*RAD))
                                { D3=D3+360*RAD;}
                        if(D3>360*RAD)
                                { D3=D3-360*RAD;}
                unf_limb1[mm][0]=100-(percent*percent1);
                unf_limb1[mm][1]=D3;
                unf_limb1[mm][2]=I3;
                combined[kount][0]=100-(percent*percent1);
                combined[kount][1]=D3;
                combined[kount][2]=I3;
                printf("\nAt %3i percent unfolding D= %3.2f, I= %3.2f\n", (100-percent*percent1),
                        D3*DEG,I3*DEG);*/

                percent1=percent1-1;
                mm=mm+m+1;
          kount=kount+m+n+2;
        }while(percent1>=0);
  }
/*===========unfolding and sorting data(limb 2)===============*/
for(Kjj=m+1;Kjj<m+n+2;Kjj++)
  { D=k+1;
        percent1=k;
        mm=Kjj-(m+1);
        kount=Kjj;
        kmm=Kjj-(m+1);
        do {
                D--;
                dip_percent=0.01*percent*limb2[kmm][1];
                app_dip=limb2[kmm][1]-(dip_percent*D);

        D3=rota_dec((limb2[kmm][0]+(dec_corr*RAD)),PLUNGE,app_dip,limb2[kmm][2],limb2[kmm
                ][3]);

        I3=rota_inc((limb2[kmm][0]+(dec_corr*RAD)),PLUNGE,app_dip,limb2[kmm][2],limb2[kmm]
                [3]);
                        if(D3<(-90*RAD))
```

```
                    { D3=D3+360*RAD;}
                if(D3>360*RAD)
                    { D3=D3-360*RAD;}
            unf_limb2[mm][0]=100-(percent*percent1);
            unf_limb2[mm][1]=D3;
            unf_limb2[mm][2]=I3;
            combined[kount][0]=100-(percent*percent1);
            combined[kount][1]=D3;
            combined[kount][2]=I3;
            printf("\nAt %3i percent unfolding D= %3.2f, I= %3.2f\n", (100-percent*percent1),
                D3*DEG,I3*DEG);*/
            percent1=percent1-1;
            mm=mm+n+1;
            kount=kount+m+n+2;
        }while(percent1>=0);
  }
//************writing unfolding data to file UNFOLD.DAT********************
/*This file contains Percent,inlination and declination data that can be edited and used by a stereoplotting
software.*/
fprintf(dat_file,"Percent,Decl,Incl\n");
for(int KjJ=0;KjJ<=(m+n+2)*(k+1);KjJ++)
{
fprintf(dat_file,"%3.0f,%3.2f,%3.2f\n",combined[KjJ][0],combined[KjJ][1]*DEG,
        combined[KjJ][2]*DEG);
}
fclose(dat_file);
clrscr();
//************CALCULATING STATISTICS FOR COMBINED LIMBS***************
fprintf(out_file,"Combined Limbs
Data,N=%i\nPercent,K,Alpha95,Incl,Decl,R,X,Y,Z,Colat,Dp,Dm",m+n+2);
printf("\n\t\tpercent  K  Alpha95  Incl   Decl");
for(zz=0;zz<=k;zz++)
{       mmm=zz*(m+n+2);
        sx=0.0;
        sy=0.0;
        sz=0.0;
        for(ee=0;ee<=m+n+1;ee++)
        {       xx=cos(combined[mmm][1])*cos(combined[mmm][2]);
                xy=sin(combined[mmm][1])*cos(combined[mmm][2]);
                xz=sin(combined[mmm][2]);
                sx=sx+xx;
                sy=sy+xy;
                sz=sz+xz;
                mmm=mmm+1;
        }
        rr=(sx*sx)+(sy*sy);
        incl=antan3(sz,sqrt(rr))*DEG;
        Artan=(antan3(sy,sx));
         if(Artan<0)
         {Artan=Artan+2*PI;}
        decl=Artan*DEG;
        double R=sqrt(rr+(sz*sz));
        N=m+n+2;
        Kparam=(N-1)/(N-R);
        double Kn=N;    double Kr=R;
```

```
        AA=1-(((Kn-Kr)/Kr)*(pow((1/0.05),(1/(Kn-1)))-1));
        Alpha95=(antan3(sqrt(1-AA*AA),AA))*DEG;
        double p=antan2(2,tan(incl*RAD));
        double Dm=((Alpha95*RAD)*(sin(p)/cos(incl*RAD)))*DEG;
        double Dp=(2.0*(Alpha95*RAD)*(1/(1+3*cos(incl*RAD)*cos(incl*RAD))))*DEG;
        Xcosine=(sx/R);
        Ycosine=(sy/R);
        Zcosine=(sz/R);
        fprintf(out_file,"\n%3.2f,%3.3f,%3.3f,%3.3f,%3.3f,%3.3f,%3.4f,%3.4f,%3.4f,%3.4f,%3.4f,%3.4
f",
        combined[mmm-1][0],Kparam,Alpha95,incl,decl,R,Xcosine,Ycosine,Zcosine,p*DEG,Dp,Dm);
        bothdata[zz][0]=combined[mmm-1][0];
        bothdata[zz][1]=Kparam;
        bothdata[zz][2]=Alpha95;
        bothdata[zz][3]=incl*RAD;
        bothdata[zz][4]=decl*RAD;
        bothdata[zz][5]=R;
        printf("\n\t\t%-3.1f %3.3f %3.3f  %3.3f  %3.3f",
        combined[mmm-1][0],Kparam,Alpha95,incl,decl);
}

//****************CALCULATING STATISTICS FOR LIMB 1**************************
fprintf(out_file,"\nLimb1 Data,n=%i\nPercent,K,Alpha95,Incl,Decl,R,X,Y,Z",m+1);
printf("\n\t\tpercent K  Alpha95 Incl  Decl");
for(zz=0;zz<=k;zz++)
{       mmm=zz*(m+1);
        sx=0.0;
        sy=0.0;
        sz=0.0;
        for(ee=0;ee<=m;ee++)
        {       xx=cos(unf_limb1[mmm][1])*cos(unf_limb1[mmm][2]);
                xy=sin(unf_limb1[mmm][1])*cos(unf_limb1[mmm][2]);
                xz=sin(unf_limb1[mmm][2]);
                sx=sx+xx;
                sy=sy+xy;
                sz=sz+xz;
                mmm=mmm+1;
        }
        rr=(sx*sx)+(sy*sy);
        incl=antan3(sz,sqrt(rr))*DEG;

        Artan=antan3(sy,sx);
         if(Artan<0)
         {Artan=Artan+2*PI;}
        decl=Artan*DEG;
        double R=sqrt(rr+(sz*sz));
        N1=m+1;
        Kparam=(N1-1)/(N1-R); double kN1=N1; double KR=R;
        AA=1-(((kN1-KR)/KR)*(pow((1/0.05),(1/(kN1-1)))-1));
        Alpha95=(antan3(sqrt(1-AA*AA),AA))*DEG;
        Xcosine=(sx/R);
        Ycosine=(sy/R);
        Zcosine=(sz/R);

        fprintf(out_file,"\n%3.2f,%3.3f,%3.3f,%3.3f,%3.3f,%3.3f,%3.4f,%3.4f,%3.4f",
```

```
            unf_limb1[mmm-1][0],Kparam,Alpha95,incl,decl,R,Xcosine,Ycosine,Zcosine);
        limb1data[zz][0]=unf_limb1[mmm-1][0];
        limb1data[zz][1]=R;
        printf("\n\t\t%3.1f %3.3f %3.3f  %3.3f  %3.3f",
        unf_limb1[mmm-1][0],Kparam,Alpha95,incl,decl);
}
//*************** CALCULATING STATISTICS FOR LIMB 2*************************
fprintf(out_file,"\nLimb2 Data,n=%i\nPercent,K,Alpha95,Incl,Decl,R,Xcosine,Ycosine,Zcosine",n+1);
printf("\n\t\tpercent K  Alpha95  Incl   Decl");
for(zz=0;zz<=k;zz++)
{       mmm=zz*(n+1);
        sx=0.0;
        sy=0.0;
        sz=0.0;
        for(ee=0;ee<=n;ee++)
        {       xx=cos(unf_limb2[mmm][1])*cos(unf_limb2[mmm][2]);
                xy=sin(unf_limb2[mmm][1])*cos(unf_limb2[mmm][2]);
                xz=sin(unf_limb2[mmm][2]);
                sx=sx+xx;
                sy=sy+xy;
                sz=sz+xz;
                mmm=mmm+1;
        }
        rr=(sx*sx)+(sy*sy);
        incl=antan3(sz,sqrt(rr))*DEG;

        Artan=(antan3(sy,sx));
         if(Artan<0)
         {Artan=Artan+2*PI;}
        decl=Artan*DEG;
        double R=sqrt(rr+(sz*sz));
        N2=n+1;
        Kparam=(N2-1)/(N2-R);double KN2=N2; double kR=R;
        AA=1-(((KN2-kR)/kR)*(pow((1/0.05),(1/(KN2-1)))-1));
        //Alpha95=(acos(1-(((N2-R)/R)*(pow((1/0.05),(1/(N2-1)))-1))))*DEG;
         Alpha95=(antan3(sqrt(1-AA*AA),AA))*DEG;
        Xcosine=(sx/R);
        Ycosine=(sy/R);
        Zcosine=(sz/R);

        fprintf(out_file,"\n%3.2f,%3.3f,%3.3f,%3.3f,%3.3f,%3.3f,%3.4f,%3.4f,%3.4f",
                unf_limb2[mmm-1][0],Kparam,Alpha95,incl,decl,R,Xcosine,Ycosine,Zcosine);
        limb2data[zz][0]=unf_limb2[mmm-1][0];
        limb2data[zz][1]=R;
        printf("\n\t\t%-3.0f %-.3f %-.3f  %-.3f  %-.3f",
        unf_limb2[mmm-1][0],Kparam,Alpha95,incl,decl);
}

/*---------------------------- MCFADDEN'S TEST-------------------------*/
fprintf(out_file,"\nMcfadden Parameters\nPercent,McFadden,95ci\n");
for(zz=0;zz<=k;zz++){
        mac1=limb1data[zz][1]+limb2data[zz][1];
        mac2=(bothdata[zz][5])*(bothdata[zz][5]);
        mac3=2*(N-limb1data[zz][1]-limb2data[zz][1]);
        Mac=(mac1-mac2/mac1)/mac3;
```

```
		MACK[zz][0]=Mac;
		sb=m+n;
		level2=pow((1/0.05),(1/sb))-1; /* 95 % c.i.*/
		fprintf(out_file,"%i,%.5f,%.5f\n",zz*percent,Mac,level2);
}
fclose(out_file);
printf("\n\tThis data and Mcfadden values have been stored in the file %s\n",name);
}
max=bothdata[0][1];
TT=0;
for(pp=1;pp<=k+1;pp++)
 {	if(max<bothdata[pp][1])
		 {max=bothdata[pp][1];
		 TT=pp;}

		else
		 continue;
 }

float minMac = MACK[TT][0];

printf("\n\tStatistical parameters for position of best grouping\n\t--------------------------------------------
-");
printf("\n\tFor %i samples",m+n+2);
printf("\n\tMcElhinny Test\n\t---------------");
printf("\n\t\tBest grouping at %.0f percent unfolding", bothdata[TT][0]);
printf("\n\t\tK = %.3f",bothdata[TT][1]);
printf("\n\t\tAlpha-95 = %.3f",bothdata[TT][2]);
printf("\n\tMcFadden Test\n\t---------------\n\t\tAt %.0f percent unfolding",bothdata[TT][0]);
printf("\n\t\tF-value = %.3f ",minMac);
printf("\n\t\twith 95 percent confidence interval = %.3f",level2);
printf("\n\tInclination = %.3f",bothdata[TT][3]*DEG);
printf("\n\tDeclination = %.3f\n",bothdata[TT][4]*DEG);

}

// ***********LISTING OF THE FUNCTIONS************
//-------------------------------------------------------
FILE *Graceful_open(char filename[], char mode[]) {
FILE *FP;
FP=fopen(filename,mode);
 if (FP==NULL){
 beeper();
 cout<<"\n\tUnable to open File "<<filename
		<<"\n\tPROGRAM TERMINATED\n\n";
 exit(1);
 }
 return FP;
}
//-------------------------------------------------------
void beeper(void)
{
 sound(600);
 delay(100);
 sound(900);
```

```
 delay(100);
 nosound();
 return;
}
//-----------------------------------------------------------
void enter_array(float limb1[30][4], int *p, char limb[]) {
clrscr();
int dm,m=0;
float strike,dip,I2,D2;
char inp1;
for(dm=0;dm>=0;m++)
{  printf("\n %s, Data no. %i\n ------------------------\n",limb,m+1);
        printf(" Strike(between 0 and 360)= ");
        do{
                scanf("%f", &strike);
                if(strike>=0.0 && strike<=360.0)
                 break;
                else { beeper();
                   printf(" Strike should be between 0 and 360. Re-enter again: ");
                   }
          }while(1);
        limb1[m][0]=strike*RAD;
        printf(" Dip(between 0 and 90)= ");
                do{
                scanf("%f", &dip);
                if(dip>=0.0 && dip<=90.0)
                 break;
                else { beeper();
                   printf(" Dip should be between 0 and 90. Re-enter again: ");
                   }
          }while(1);

        limb1[m][1]=dip*RAD;
        printf(" Magnetization Directions\n Declination= ");
        do{
          scanf("%f", &D2);
          if(D2>=0.0 && D2<=360.0)
           break;
          else{
           beeper();
           cout<<" Re-enter a valid Declination value(0-360): ";
            }
        }while(1);
        limb1[m][2]=D2*RAD;
        printf(" Inclination= ");
        do{
          scanf("%f", &I2);
          if(I2>=-90.0 && I2<=90.0)
                break;
          else{
            beeper();
            cout<<" Re-enter a valid Inclination value(-90 to +90): ";
            }
        }while(1);
        limb1[m][3]=I2*RAD;
```

```
        fflush(stdin);
        if(m==29)
         {printf( "You have entered 30 data sets, the maximum possible\n");
         beeper();
         break;}
        else
         {printf("\n\n Would you like to enter another data set? (Return/N) ");
          scanf("%c", &inp1);}
          if((inp1=='n') | (inp1=='N'))
           break;
          else
           continue;
}
*p=m;
return;
}
//------------------------------------------------------------------------
void edit_array(float limb1[30][4], char limb[], int m) {
int kk;
float strike,dip,I2,D2;
char inp1;

do{ clrscr();
  printf("%s\n", limb);
  print_array(m,limb1,limb);
  printf("\nEnter the data set no. to be edited: ");
   do{
        scanf("%i",&kk);
        fflush(stdin);
        if(kk<=m+1)
         break;
        else
         printf(" Choice cannot be %i, re-enter correctly: ",kk);
         }while(1);
 printf("\n Data no. %i\n -----------\n",kk);
        printf(" Strike(between 0 and 360)= ");
        do{
                scanf("%f", &strike);
                if(strike>=0.0 && strike<=360.0)
                 break;
                else { beeper();
                   printf(" Strike should be between 0 and 360. Re-enter again: ");
                   }
         }while(1);
        printf(" Dip(between 0 and 90)= ");
                do{
                scanf("%f", &dip);
                if(dip>=0.0 && dip<=90.0)
                 break;
                else { beeper();
                   printf(" Dip should be between 0 and 90. Re-enter again: ");
                   }
         }while(1);
        printf(" Magnetization Directions\n Declination= ");
  do{
```

```
          scanf("%f", &D2);
          if(D2>=0.0 && D2<=360.0)
           break;
          else{
           beeper();
           cout<<" Re-enter a valid Declination value(0-360): ";
            }
         }while(1);

         printf(" Inclination= ");
         do{
          scanf("%f", &I2);
          if(I2>=-90.0 && I2<=90.0)
                 break;
          else{
            beeper();
            cout<<" Re-enter a valid Inclination value(-90 to +90): ";
            }
         }while(1);
         limb1[kk-1][0]=strike*RAD;
         limb1[kk-1][1]=dip*RAD;
         limb1[kk-1][2]=D2*RAD;
         limb1[kk-1][3]=I2*RAD;
}while(0);
return;
}
//------------------------------------------------------------------
void add_array (float limb1[30][4], int *p, char limb[])
{ int m;
 float strike,dip,D2,I2;
 m=*p;
 if(m==29)
 {printf("\nYou cannot add any more data sets.");
  return;}
 else
 { clrscr();
  fflush(stdin);
  m=m+1;
  cout<<limb<<"\n-----------\n";
  printf("\n Data no. %i\n ---------\n",m+1);
  printf(" Strike(between 0 and 360)= ");
         do{
           scanf("%f", &strike);
           if(strike>=0.0 && strike<=360.0)
                  break;
           else { beeper();
                  printf("\n Strike should be between 0 and 360. Re-enter again\n ");
                   }
           }while(1);
   printf(" Dip(between 0 and 90)= ");
         do{
           scanf("%f", &dip);
           if(dip>=0.0 && dip<=90.0)
                  break;
           else { beeper();
```

```
                  printf("\n Dip should be between 0 and 90. Re-enter again\n");
                  }
          }while(1);
         printf(" Magnetization Directions\n Declination= ");
         do{
          scanf("%f", &D2);
          if(D2>=0.0 && D2<=360.0)
           break;
          else{
           beeper();
           cout<<" Re-enter a valid Declination value(0-360): ";
           }
         }while(1);
         printf(" Inclination= ");
         do{
          scanf("%f", &I2);
          if(I2>=-90.0 && I2<=90.0)
                 break;
          else{
            beeper();
            cout<<" Re-enter a valid Inclination value(-90 to +90): ";
            }
          }while(1);
         limb1[m][0]=strike*RAD;
         limb1[m][1]=dip*RAD;
         limb1[m][2]=D2*RAD;
         limb1[m][3]=I2*RAD;
 }
 *p=m;
 return;
}
//---------------------------------------------------------------
void delete_array(float limb1[30][4], int *p, char limb[]) {
clrscr();
int kk,m,dm;
float strike,dip,I2,D2;
char inp1;
m=*p;
printf("%s\n", limb);
 do{
   clrscr();
   print_array(m,limb1,limb);
   fflush(stdin);
   printf("\n\nEnter the data set no. to be deleted ");
   do{
          scanf("%i",&kk);
          fflush(stdin);
          if(kk<=m+1)
           break;
          else
           {printf("\nChoice cannot be %i, re-enter correctly",kk);
           beeper();}
   }while(1);
   for(dm=kk;dm<=m;dm++){
          limb1[dm-1][0]=limb1[dm][0];
```

```
            limb1[dm-1][1]=limb1[dm][1];
            limb1[dm-1][2]=limb1[dm][2];
            limb1[dm-1][3]=limb1[dm][3];
   }
  }while(0);
  m=m-1;
*p=m;
return;
}
//-----------------------------------------------------------
void print_array(int m, float A[30][4], char limb[])
{
cout<<"\t "<<limb<<"\n\t---------\n";
int yy, mm=0;
printf("\tnumber\tstrike\tdip\tDec.\tInc.");

do{
yy=0;
printf("\n\t %i",mm+1);
do{
 printf("\t%.2f", A[mm][yy]*DEG);
  yy=yy+1;
  }while(yy<=3);
mm=mm+1;
}while(mm<m+1);
return;
}
//-----------------------------------------------------------
float antan2 (float x, float y){
float arctan;
 if (y==0 && x>0)
        {arctan=90*RAD;
        return arctan;}
 if (y==0 && x==0)
        {arctan=999*RAD;
        return arctan;}
 if (y==0 && x<0)
        {arctan=270*RAD;
        return arctan;}
 else
        {arctan=atan(x/y);
        if (y>0)
                {return arctan;}
        if (y<0 && x>0)
                {arctan=arctan-(180*RAD);
                return arctan;}
        if (y<0 && x<=0)
                {arctan=arctan+(180*RAD);
                return arctan;}}
}
//-----------------------------------------------------------
float antan3 (float x, float y){
float arctan;
 if (x==0 && y>0)
        {arctan=90*RAD;
```

```
        return arctan;}
 if (y==0 && x==0)
        {arctan=999*RAD;
        return arctan;}
 if (x==0 && y<0)
        {arctan=270*RAD;
        return arctan;}
 else
        {arctan=atan(x/y);
        if (x>0)
                {return arctan;}
        if (x<0 && y>0)
                {arctan=arctan-(180*RAD);
                return arctan;}
        if (x<0 && y<=0)
                {arctan=arctan+(180*RAD);
                return arctan;}}
}
//-----------------------------------------------------------------
float rota_dec(float pdir, float plunge, float angle, float dec, float inc)
{
double t,sa,tt,ca,a,in,decc,incc,sd,cd,invsd,invcd;
 if(angle==0.0)
  {decc=dec;
  return decc;}
 if(plunge==90*RAD)
  {decc=dec+angle;
  return decc;}
 else
  { t=(sin(inc)*sin(plunge))+(cos(inc)*cos(plunge)*cos(pdir-dec));
        tt=antan2(sqrt(1-t*t),t);
  sa=sin(dec-pdir)*cos(inc)/sin(tt);
  ca=(sin(inc)-sin(plunge)*cos(tt))/(cos(plunge)*sin(tt));
        a=antan2(sa,sqrt(1-sa*sa));
  if(ca<0)
        {a=(180*RAD)-a;}
  in=cos(tt)*sin(plunge)+sin(tt)*cos(plunge)*cos(a+angle);
        incc=antan2(in,sqrt(1-in*in));
  sd=sin(a+angle)*sin(tt)/cos(incc);
  cd=(cos(tt)-sin(plunge)*sin(incc))/(cos(plunge)*cos(incc));
        invsd=antan2(sd,sqrt(1-sd*sd));
        invcd=antan2(sqrt(1-cd*cd),cd);
  if(sd<0 && cd<0)
        {decc=pdir-invsd+(180*RAD);
        return decc;}
 if(sd<0 && cd>=0)
        {decc=pdir+invsd;
        return decc;}
  else
        {decc=pdir+invcd;
        return decc;}
}}
//-----------------------------------------------------------------
float rota_inc(float pdir, float plunge, float angle, float dec, float inc)
{
```

```
double t,sa,tt,ca,a,decc,incc,sd,cd,invsd,in;
 if (angle==0.0)
  {incc=inc;
   return incc;}
 if (plunge==90*RAD)
  {incc=inc;
   return incc;}
 else{
  t=(sin(inc)*sin(plunge))+(cos(inc)*cos(plunge)*cos(pdir-dec));
        tt=antan2(sqrt(1-t*t),t);
  sa=sin(dec-pdir)*cos(inc)/sin(tt);
  ca=(sin(inc)-sin(plunge)*cos(tt))/(cos(plunge)*sin(tt));
        a=antan2(sa,sqrt(1-sa*sa));
  if(ca<0)
        {a=(180*RAD)-a;}
  in=cos(tt)*sin(plunge)+sin(tt)*cos(plunge)*cos(a+angle);
        incc=antan2(in,sqrt(1-in*in));
        return incc;
}}
//---------------------------------------------------------------
void print_array1(float B[4000][3],int kkk)
{ int dy=0;
for(dy=0;dy<kkk;dy++){
fprintf(stdprn,"\n\t%.2f\t%.2f\t%.2f",B[dy][0],B[dy][1]*DEG,B[dy][2]*DEG);
}return;
}
void print_array2(float C[101][6],int kkk)
{ int dy=0;
for(dy=0;dy<kkk;dy++){
fprintf(stdprn,"\n\t%.2f\t%.2f\t%.2f\t%.2f\t%.2f",C[dy][0],C[dy][1],C[dy][2],C[dy][3]*DEG,C[dy][4]*D
EG);
}return;
}
```

APPENDIX 2

STRONTIUM ($^{87}Sr/^{86}Sr$) ISOTOPE RATIOS

LOCATION	SAMPLE	$^{87}Sr/^{86}Sr$	Uncertainity*
	NBS 987	0.710228	0.000009
FULFORD	FUL3	0.711259	0.000012
TROUT CREEK	TRC7	0.709349	0.000009
MILLER CREEK	MIL4	0.708999	0.000007
	NBS 987	0.710209	0.000008
DEEP CREEK	SL4	0.70918	0.000012
	SL6	0.709027	0.00001
	NL-2	0.708934	0.000013
	NL-1	0.708822	0.000012
EAST ELK CREEK	EEC17	0.708942	0.000014
	EEC5	0.708638	0.000013
RUEDI RESERVOIR	RR4-3	0.710489	0.000009
	RR5-6	0.710572	0.000008
SWEETWATER	sw11a-2	0.708828	0.00001
	nsw114-5	0.708808	0.000019

*2 X standard error of mean

APPENDIX 3

PETROGRAPHIC DESCRIPTION OF BELDEN CARBONATE SITES

LOCATION: CROSS MOUNTAIN

SITE: Y6

DUNHAM'S CLASSIFICATION: Crinoidal Packstone

ALLOCHEMS: Crinoid fragments, mollusk shells, brachiopod fragments.

CEMENT: Micrite/microspar

VEINS:.Thin (~100 µm) veins of twinned calcite spar.

OPAQUES: Very rare, very small (<1 µm) pyrite grains.

SITE: Y2/1

DUNHAM'S CLASSIFICATION: Fossiliferous Packstone

ALLOCHEMS: Foraminifer shells, echinoid/crinoid plates, brachiopod and mollusk fragments, rare incipient ooids.

CEMENT: Micrite

VEINS:. Thin (~100 µm) veins of twinned calcite spar.

OPAQUES: Very rare, very small (<1 µm) pyrite grains.

LOCATION: JUNIPER MOUNTAIN

SITE: JM1

DUNHAM'S CLASSIFICATION: Fossiliferous Packstone

ALLOCHEMS: Crinoid fragments, mollusk shells, brachiopod fragments.

CEMENT: Micrite

VEINS:. Very thin (<1 µm) veins of calcite.

OPAQUES: Very rare, very small (<1 µm) pyrite grains.

LOCATION: MILLER CREEK

SITE: MIL 1

DUNHAM'S CLASSIFICATION: Intraclastic Peloidal Packstone

ALLOCHEMS: Small (20-70 µm) mudstone intraclasts, peloids and few brachiopod fragments.

CEMENT: Micrite

VEINS: Thick (~400 µm) to thin (<1 µm) calcite veins; thick veins with coarse twinned, calcite spar.

OPAQUES: Abundant small rounded (<10 µm) iron-oxide grains occurring in patches; some iron-oxide grains with core of relict pyrite; rare small (~10 µm) unreplaced pyrite grains.

SITE: MIL 2

DUNHAM'S CLASSIFICATION: Mudstone

ALLOCHEMS: Few, small (~10 µm) subangular quartz grains.

CEMENT: Microspar

VEINS: None observed.

OPAQUES: Isolated, small (20-30 μm) pseudomorphs of iron-oxide after pyrite; rare, small (~10 μm) unreplaced pyrite grains.

SITE: MIL 3

DUNHAM'S CLASSIFICATION: Wackestone

ALLOCHEMS: Brachiopod shell fragments.

CEMENT: Micrite/microspar with dark (organic?) matter.

VEINS: Thin (20-30 μm) calcite veins with twinned calcite spar.

OPAQUES: Small (10-20 μm) framboidal pyrite grains; small (5-10 μm) isolated pyrite grains with replacement rims of iron-oxide.

SITE: MIL 4

DUNHAM'S CLASSIFICATION: Wackestone

ALLOCHEMS: Molluskan (replaced) and ostracod fragments.

CEMENT: Micrite

VEINS: Thin (10-30 μm) calcite veins.

OPAQUES: Small (<1-10 μm) iron-oxide pseudomorphs after pyrite; rare, very small (<1 μm) unaltered pyrite grains.

LOCATION: EAST ELK CREEK

SITE: EEC 1

DUNHAM'S CLASSIFICATION: Crinoidal Packstone

ALLOCHEMS: Crinoidal/echinoid and coral fragments.

CEMENT: Micrite with dark (organic?) matter.

VEINS: Calcite veins (4-300 μm); thick veins with coarse, twinned, sparry calcite.

OPAQUES: Small (1-10 μm) grains of iron-oxides, some with relict pyrite cores; most have a mottled surface pattern.

LOCATION: DEEP CREEK

SITE: DC1

DUNHAM'S CLASSIFICATION: Crinoidal Packstone

ALLOCHEMS: Large (~5 mm) crinoidal/echinoidal plates and fragments; trilobite, coral and brachiopod shell fragments, rare intraclasts.

CEMENT: Micrite with patches of gypsum.

VEINS: None observed.

OPAQUES: Small (1-10 μm) grains of iron-oxides, some with relict pyrite cores; most have a mottled surface pattern.

LOCATION: HELL'S GATE

SITE: HELL 1

DUNHAM'S CLASSIFICATION: Mudstone

ALLOCHEMS: None

CEMENT: Micrite

VEINS: Thin (20-30 μm) calcite veins.

OPAQUES: Pyrite grains (<1 to 40 μm) with corroded outlines and dark iron-oxide rims.

SITE: HELL 2

DUNHAM'S CLASSIFICATION: Fossiliferous Packstone/Wackestone

ALLOCHEMS: Echinoid plates, ostracod shell fragments, replaced gastropod shells, brachiopod fragments, foraminifer shells.

CEMENT: Micrite

VEINS: None observed.

OPAQUES: Rare, small (~1-10 μm) pyrite grains with corroded outlines.

SITE: HELL 3

DUNHAM'S CLASSIFICATION: Intraclastic Packstone

ALLOCHEMS: Mudstone intraclasts (10 μm to 1 cm).

CEMENT: Micrite

VEINS: Rare, thin (~ 10 μm) calcite veins.

OPAQUES: Abundant fresh pyrite grains (10-150 μm); smaller grains with dark iron-oxide replacement rims.

SITE: HELL 5

DUNHAM'S CLASSIFICATION: Molluskan Wackestone

ALLOCHEMS: Small replaced mollusk shell fragments.

CEMENT: Micrite

VEINS: Very rare, thin (~ 10 μm) calcite veins.

OPAQUES: Iron-oxide grains (100-150 μm) with relict pyrite cores; very small (<1-10 μm) pyrite grains, some with dark rim of iron-oxides.

LOCATION: CROOKED CREEK RESERVOIR

SITE: CCR 1

DUNHAM'S CLASSIFICATION: Oolitic Intraclastic Grainstone

ALLOCHEMS: Ooids (~300 μm diameter) with radial fabric and nucleii of intraclasts and replaced pelycypod shell fragments, large (~600 μm) intraclasts, subrounded to subangular quartz grains.

CEMENT: Sparry calcite to microspar.

VEINS: Very rare, thin (~20 μm) calcite veins.

OPAQUES: Pyrite grains (<1- 40 μm) with corroded margins and replacement rim of iron-oxide on some smaller grains.

LOCATION: FULFORD

SITE: FUL 1

DUNHAM'S CLASSIFICATION: Intraclast Peloidal Packstone.

ALLOCHEMS: Intraclasts (300-500μm), peloids, rare brachiopod fragments.

CEMENT: Micrite, with spar around some allochems.

VEINS: Multiple, thin (100-150μm) veins of calcite spar.

OPAQUES: Abundant pyrite grains (< 1μm to 20 μm); many pyrite grains with partial to almost complete iron-oxide replacement rims.

SITE: FUL2

DUNHAM'S CLASSIFICATION: Mudstone

ALLOCHEMS: None observed.

CEMENT:Micrite (with patches of microspar).

VEINS: Rare, very thin (<1μm) calcite veins.

OPAQUES: Very small (<1 μm) rounded to sub-rounded pyrite grains; some larger (about 20 μm) grains of iron-oxide pseudomorphed after pyrite.

SITE: FUL 3

DUNHAM'S CLASSIFICATION: Mudstone

ALLOCHEMS: Rare fossil (Ostracod ?) fragments.

CEMENT:Micrite

VEINS: Few thin (<40 μm) calcite veins.

OPAQUES: Pyrite grains, bimodally distributed: large (600-900 μm) fresh, unaltered pyrite grains mixed with very small (<1 μm) pyrite grains with corroded outlines and iron-oxide replacement rims.

SITE: FUL 5

DUNHAM'S CLASSIFICATION: Intraclastic Packstone

ALLOCHEMS: Large (600-1000 μm) mudstone intraclasts, rare ooids with intraclast nucleii, small (~1 μm) subangular quartz grains.

CEMENT: Micrite

VEINS: Very thin (~1 μm) calcite veins.

OPAQUES: Pyrite grains (~30 μm) fresh and mostly unaltered; some smaller grains with dark iron-oxide rims.

SITE: FUL 7

DUNHAM'S CLASSIFICATION: Intraclastic Wackestone

ALLOCHEMS: Intraclsts (1.5 cm to 10 μm), peloids, rare fossil fragments (mostly pelecypod shells).

CEMENT: Micrite, with patches of microspar to spar.

VEINS: Rare, very thin (<1 μm) calcite veins.

OPAQUES: Pyrite grains, small to medium size (15-100 μm), fresh and unaltered; some of the smaller grains have replacement rims of iron-oxide.

SITE: FUL 8

DUNHAM'S CLASSIFICATION: Intraclastic Packstone

ALLOCHEMS: Large (400-700 μm) intraclasts.

CEMENT: Micrite

VEINS: Very thick (2-10 mm) calcite veins.

OPAQUES: Small (1-10 μm) grains of iron-oxides, some with relict pyrite cores.

SITE: FUL 9

DUNHAM'S CLASSIFICATION: Mudstone

ALLOCHEMS: Very rare mollusk fragments, some sub-rounded, small (~40 μm) quartz grains.

CEMENT: Micrite

VEINS: Very rare, very thin (<1 μm) calcite veins.

OPAQUES: Pyrite grains, very small to medium size (<1 μm to 200 μm), relatively unaltered; thin iron-oxide replacement rims on some pyrite grains.

SITE: FUL A

DUNHAM'S CLASSIFICATION: Intraclastic Packstone

ALLOCHEMS: Very large (~1 cm) to small (~20 μm) intraclasts.

CEMENT: Micrite, with dark (organic?) matter.

VEINS: Thin (80-100 μm) calcite veins.

OPAQUES: Pyrite (< 1 to 40 μm) grains with corroded rims; some pyrite grains with iron-oxide replacement rims.

SITE: FUL B

DUNHAM'S CLASSIFICATION: Algal Boundstone

ALLOCHEMS: Intraclasts and quartz grains between alagal laminae.

CEMENT: Micrite

VEINS: none observed.

OPAQUES: Small (1-10 μm) grains of iron-oxides, some with relict pyrite cores.

SITE: FUL C

DUNHAM'S CLASSIFICATION: Algal Boundstone

ALLOCHEMS: Intraclasts and quartz grains between alagal laminae.

CEMENT: Micrite

VEINS: none observed.

OPAQUES: Small (1-10 μm) grains of iron-oxides, some with relict pyrite cores.

LOCATION: RUEDI RESERVOIR

SITE: RR1

DUNHAM'S CLASSIFICATION: Laminated Mudstone

ALLOCHEMS: Rare fossil fragments, silt-size quartz and chert grains.

CEMENT: Micrite, with dark (organic?) matter.

VEINS: Rare very thin (~1 μm) calcite veins.

OPAQUES: Small (<1 to 20 μm) pyrite grains with iron-oxide replacement rims; some pseudomorphs of iron-oxide after pyrite.

SITE: RR2

DUNHAM'S CLASSIFICATION: Wackestone

ALLOCHEMS: Mollusks, coral and echinoid fragments, peloids.

CEMENT: Micrite with microspar patches.

VEINS: Rare, very thin (~1 μm) calcite veins.

OPAQUES: Small (<1 to 20 μm) pyrite grains with partial to almost complete iron-oxide replacement rims.

SITE: RR4

DUNHAM'S CLASSIFICATION: Mudstone

ALLOCHEMS: None observed.

CEMENT: Micrite with dark (organic?) matter.

VEINS: Thin (~10 μm) calcite veins.

OPAQUES: Very small (<1 μm) pyrite grains with iron-oxide replacement rims; some pseudomorphs of iron-oxide after pyrite.

SITE: RR5

DUNHAM'S CLASSIFICATION: Mudstone

ALLOCHEMS: None observed.

CEMENT: Micrite

VEINS: None observed.

OPAQUES: Very small (<1 μm) pyrite grains with iron-oxide replacement rims; some pseudomorphs of iron-oxide after pyrite.

SITE: RR6

DUNHAM'S CLASSIFICATION: Intraclastic Packstone

ALLOCHEMS: Large (500-700 μm) intraclasts of grainstone, small (40-60 μm) intraclasts of mudstone, replaced pelecypod fragments.

CEMENT: Micrite

VEINS: Thin (20-50 μm) calcite veins.

OPAQUES: Abundant pseudomorphs of iron-oxide grains (<1 to 10 μm) after pyrite.

LOCATION: MINTURN

SITE: MIN 1

DUNHAM'S CLASSIFICATION: Silty Mudstone

ALLOCHEMS: Small (~10 μm) sub-rounded quartz grains as burrow fills.

CEMENT: Micrite

VEINS: Thin (~80 μm) veins of coarse, twinned, calcite spar.

OPAQUES: Pyrite grains (4-130 μm) with corroded edges and iron-oxide replacement rims; some pseudomorphs of iron-oxide after pyrite.

SITE: MIN 2

DUNHAM'S CLASSIFICATION: Intraclastic Grainstone

ALLOCHEMS: Mudstone intraclasts (20-600 μm), subangular quartz grains (10-30 μm).

CEMENT: Sparry calcite, with patches of evaporite (gypsum).

VEINS: Thin (~10 μm) calcite veins.

OPAQUES: Rare, very small (~1 μm) grains of pyrite, partly to almost completely replaced by iron-oxide.

SITE: MIN 3

DUNHAM'S CLASSIFICATION: Intraclastic Packstone

ALLOCHEMS: Mudstone intraclasts (30-600 μm), small, replaced gastropod shells;some crinoid fragments;small (~10 μm) angular quartz grains.

CEMENT: Micrite

VEINS: Multiple, thin (~10 μm) calcite veins.

OPAQUES: Iron-oxide grains (<1 to 30 μm) with irregular outlines; small (1-5 μm) pyrite grains.

SITE: MIN 5

DUNHAM'S CLASSIFICATION: Intraclastic Packstone

ALLOCHEMS: Intraclasts (30-400 μm) of dolomitic grainstone and mudstone, pelods, rare mollusk fragments.

CEMENT: Micrite

VEINS: Very rare, very thin (<1 μm) calcite veins.

OPAQUES: Pyrite (10-60 μm) with corroded outline; small (1-10 μm) grains of iron-oxides; some grains with relict pyrite cores.

SITE: MIN 6

DUNHAM'S CLASSIFICATION: Crystalline Limestone

ALLOCHEMS: Some possible replaced mollusk fragments.

CEMENT: Coarse, sparry calcite with patches of microspar and evaporite.

VEINS: None observed.

OPAQUES: Small (1-10 μm) pyrite grains; small rounded grains of iron-oxides.

LOCATION: TURKEY CREEK

SITE: TC 1

DUNHAM'S CLASSIFICATION: Packstone

ALLOCHEMS: Intraclsts, crinoid fragments, peloids, angular quartz grains.

CEMENT: Micrite

VEINS: Thin (<1 μm) calcite veins.

OPAQUES: Pyrite (10-60 μm) with corroded outline; small (1-10 μm) grains of iron-oxides, some with relict pyrite cores.

LOCATION: KAUFMAN RIDGE

SITE: KAUF 1

DUNHAM'S CLASSIFICATION: Fossiliferous Intraclastic Packstone

ALLOCHEMS: Small (1-30 μm) replaced pelecypod shells and fragments, small (~100 μm) mudstone intraclasts.

CEMENT: Micrite

VEINS: Thin (10-30 μm) calcite veins.

OPAQUES: Pseudomorphs (10-250 μm) of iron-oxide after pyrite, some grains with relict pyrite in the core - all grains show a mottled surface pattern.

SITE: KAUF 2

DUNHAM'S CLASSIFICATION: Wackestone/Packstone

ALLOCHEMS: Replaced mollusk fragments; some small (50-70 μm) intraclasts of mudstone.

CEMENT: micrite

VEINS: None observed.

OPAQUES: Small iron-oxide pseudomorphs (1-10μm) after pyrite, some with relict pyrite cores.

LOCATION: TROUT CREEK

SITE: TRC 1

DUNHAM'S CLASSIFICATION: Intraclastic Packstone/Wackestone

ALLOCHEMS: Large (300-500 μm) intraclasts.

CEMENT: Micrite with dark (organic?) matter.

VEINS: Rare, thin (<1 μm) calcite veins.

OPAQUES: Very small to small (<1to 200 μm) framboidal pyrite: many pyrite grains partly to almost completely replaced by iron-oxide.

SITE: TRC 2

DUNHAM'S CLASSIFICATION: Fossiliferous Wackestone

ALLOCHEMS: Crinoid/echinoid fragments, brachiopod and ostracod shells, replaced mollusk (gastropod) shell fragments.

CEMENT: Micrite

VEINS: Calcite veins (300-600 μm thick) with microspar.

OPAQUES: Abundant large (~200 μm) pyrite grains with corroded outlines, with dark iron-oxide rims; pseudomorphs of iron-oxide after pyrite-some with relict pyrite cores.

SITE: TRC 3

DUNHAM'S CLASSIFICATION: Mudstone

ALLOCHEMS: None observed.

CEMENT: Microspar

VEINS: Rare thin (<1 μm) calcite veins.

OPAQUES: Large (~200 μm) pyrite grains, some with corroded outlines and dark iron-oxide rims;

pseudomorphs of iron-oxide after pyrite.

SITE: TRC 5

DUNHAM'S CLASSIFICATION: Mudstone

ALLOCHEMS: Some possible replaced pelecypod shells.

CEMENT: Micrite

VEINS: Thin (15-30 μm) calcite veins with microspar.

OPAQUES: Pyrite grains (~200 μm) with corroded outlines, with dark iron-oxide rims; very small (<1 μm) pseudomorphs of iron-oxide after pyrite-some with relict pyrite cores.

SITE: TRC 6

DUNHAM'S CLASSIFICATION: Packstone

ALLOCHEMS: Crinoid fragments, brachiopod and ostracod fragment, few intraclasts.

CEMENT: Micrite with dark (organic?) matter.

VEINS: Rare thin (<1 μm) calcite veins.

OPAQUES: Abuundant (100-150 μm) pseudomorphs of iron-oxide after pyrite-some with relict pyrite cores.

SITE: TRC 7

DUNHAM'S CLASSIFICATION: Mudstone

ALLOCHEMS: None observed.

CEMENT: Micrite

VEINS: Thin (~10 μm) calcite veins.

OPAQUES: Abuundant (100-150 μm) pseudomorphs of iron-oxide after pyrite-some with relict pyrite cores; some very small pyrite grains (~1 μm) with corroded outlines.

LOCATION: NEWETT

SITE: NWT 1

DUNHAM'S CLASSIFICATION: Fossiliferous Wackestone

ALLOCHEMS: Crinoid/echinoid fragments, replaced mollusk fragments.

CEMENT: Micrite

VEINS: Rare, very thin (<1 μm) calcite veins.

OPAQUES: Pseudomorphs (10-150 μm) of iron-oxide after pyrite, some grains with relict pyrite in the core - all grains show a mottled pattern on the surface.

SITE: NWT 2

DUNHAM'S CLASSIFICATION: Wackestone

ALLOCHEMS: Replaced mollusk shell fragments.

CEMENT: Micrite

VEINS: Thin (~10 μm) calcite veins.

OPAQUES: Scattered and clustered pseudomorphs (10-150 μm) of iron-oxide after pyrite, some grains with relict pyrite in the core - all grains show a mottled pattern on the surface.

LOCATION: BASSAM PARK

SITE: BAS 1

DUNHAM'S CLASSIFICATION: Echinoidal Wackestone

ALLOCHEMS: Large echinod fragments, ostracod shells.

CEMENT: Micrite

VEINS: Rare thin (<1 μm) calcite veins.

OPAQUES: Very small (<1 μm) pyrite grains; some partly to completely replaced by iron-oxide.

SITE: BAS 2

DUNHAM'S CLASSIFICATION: Wackestone/Packstone

ALLOCHEMS: Crinoids/echinoid plates and fragments, coral fragments, some possible pellets.

CEMENT: Micrite with dark (organic?) matter, with some patches of spar.

VEINS: Thin (5-10 μm) calcite veins.

OPAQUES: Very small (<1 μm) grains of pyrite; small to large (<2 to 250 μm) grains of iron-oxides pseudomorphed after pyrite - these grains show a mottled surface pattern.

SITE: BAS 3

DUNHAM'S CLASSIFICATION: Wackestone

ALLOCHEMS: Crinoid and coral fragments

CEMENT: Micrite with dark (organic?) matter.

VEINS: Thin (10-40 μm) veins of calcite spar.

OPAQUES: Very small (<1 μm) pyrite grains with corroded outlines; small (10-40 μm) pseudomorphs of iron-oxide after pyrite.

SITE: BAS 5

DUNHAM'S CLASSIFICATION: Mudstone

ALLOCHEMS: Rare echinoid fragments.

CEMENT: Micrite

VEINS: Thin (50-70 μm) veins of twinned calcite spar.

OPAQUES: Small (~1 μm) pyrite grains with iron-oxide replacement rims.

SITE: BP 3/1

DUNHAM'S CLASSIFICATION: Mudstone

ALLOCHEMS: Rare echinoid fragments.

CEMENT: Micrite

VEINS: Thin (20-30 μm) veins of twinned sparry calcite.

OPAQUES: Rare small (~1 μm) pyrite grains with iron-oxide replacement rims.

LOCATION:MONARCH PASS

SITE: MON 1

DUNHAM'S CLASSIFICATION: Mudstone

ALLOCHEMS: None observed.

CEMENT: Micrite/microspar

VEINS: Multiple, thin (40-60 µm) veins of coarse, twinned, sparry calcite.

OPAQUES: Pseudomorphs (<1 to 50 µm) of iron-oxide after pyrite; rare very small (<1 µm) grains of unreplaced pyrite.

SITE:MON 2

DUNHAM'S CLASSIFICATION: Intraclastic Peloidal Wackestone

ALLOCHEMS: Intraclasts (10-200 µm) of mudstone, pelods, small (~30 µm) angular quartz grains.

CEMENT: Micrite

VEINS: None observed.

OPAQUES: Pyrite grains(200-400 µm) with highly corroded outlines; small (10-40 µm) iron-oxide grains.

LOCATION:FOSSIL RIDGE

SITE: FOSSIL 1

DUNHAM'S CLASSIFICATION: Peloidal Fossiliferous Wackestone

ALLOCHEMS: Peloids, ostracod and mollusk fragments.

CEMENT: Micrite

VEINS: Rare, thin (~10 µm) calcite veins.

OPAQUES: Rare, small (10-30 µm) iron-oxide grains.

LOCATION:MOSCA

SITE: MOS 3

DUNHAM'S CLASSIFICATION: Intraclastic Packstone

ALLOCHEMS: Intraclasts (50 µm - 1 cm) of mudstone.

CEMENT: Micrite

VEINS: None observed.

OPAQUES: Rare, small (10-20 µm) iron-oxide grains with relict pyrite in the core.

LOCATION:DEADMAN GULCH

SITE: DEAD 2

DUNHAM'S CLASSIFICATION: Mudstone

ALLOCHEMS: None observed.

CEMENT: Micrite

VEINS: Few, thin (10-40 µm) to very thin (<1 µm) calcite veins.

OPAQUES: Very rare, very small (<1 µm) iron-oxide grains with relict pyrite in the core.

LOCATION:WALROD GULCH

SITE:WAL 1

DUNHAM'S CLASSIFICATION: Fossiliferous Intraclstic Packstone

ALLOCHEMS: Replaced mollusk fragments, mudstone intraclasts.

CEMENT: Micrite

VEINS: Thin (10-30 μm) calcite veins

OPAQUES: Rare, small (10-20 μm) iron-oxide grains with relict pyrite in the core.

LOCATION:CEMENT MOUNTAIN

SITE: CEMENT 1

DUNHAM'S CLASSIFICATION: Mudstone/Wackestone

ALLOCHEMS: Few (~400 μm) replaced mollusk fragments

CEMENT: Micrite

VEINS: Multiple, thin (~200 μm) veins of coarse, twinned, sparry calcite.

OPAQUES: Mostly very small (<1-10 μm), rounded to sub-rounded pyrite grains, some partially to almost completely replaced by iron-oxide.

SITE: CEMENT 3

DUNHAM'S CLASSIFICATION: Mudstone

ALLOCHEMS: Replaced mollusk fragments.

CEMENT: Micrite

VEINS: Thin (~200 μm) veins of coarse, twinned, sparry calcite.

OPAQUES: Very small (<1-10 μm), rounded to sub-rounded pyrite grains, some with partial to almost complete replacement rims of iron-oxides.

APPENDIX 4
TOC & ROCK EVAL PYROLYSIS DATA

SAMPLE NO.	SAMPLE DESCRIPTION	TOC & ROCK EVAL DATA					INTERPRETIVE RATIOS					NOTES	
		TOC	S1	S2	S3	TMAX*	HI	OI	S2/S3	PI	S1/TOC	Check	Pyrogram
1	TRC-1	0.25	0.08	0.11	1.16	433	44	464	0.09	0.42	32	c	n
2	TRC-7	0.18	0.04	0.04	1.10	594	22	611	0.04	0.50	22		n
3	RR-1	0.31	0.06	0.02	1.39	576	6	448	0.01	0.75	19		n
4	RR-2	0.10	0.01	0.02	1.23	505	20	1230	0.02	0.33	10		n
5	BAS-1	0.11	0.02	0.04	0.79	438	36	718	0.05	0.33	18		n
6	HELL-4	0.02	0.00	0.02	0.64	377	100	3200	0.03	0.00	0		n
7	FUL-5	0.64	0.08	0.02	0.99	498	3	155	0.02	0.80	13		n
8	FUL-3	0.89	0.04	0.01	0.61	472	1	69	0.02	0.80	4		n
9	BAS-3	0.16	0.03	0.04	0.96	423	25	600	0.04	0.43	19	c	n
10	EEC	0.02	0.03	0.06	0.78	405	300	3900	0.08	0.33	150		n
11	FUL-1	0.43	0.05	0.05	1.00	335	12	233	0.05	0.50	12		n
12	BAS-2	0.14	0.01	0.05	0.71	447	36	507	0.07	0.17	7	c	n
13	MIN-2	0.10	0.02	0.03	1.28	337	30	1280	0.02	0.40	20		n
14	TRC-5	0.04	0.00	0.02	0.77	341	50	1925	0.03	0.00	0		n
15	BAS-5	0.06	0.03	0.05	0.96	459	83	1600	0.05	0.38	50	c	n

*Tmax data not reliable due to low S2 values

Accuracy of TOC values: Below 0.1% - ∓ 20-30% of the TOC value
Above 1% - ∓ 2-3% of TOC value

TOC = weight percent organic carbon
S1, S2 = mg hydrocarbons/g rock
S3 = mg carbon dioxide/g rock
Tmax = °C

HI = S2*100/TOC
OI = S3*100/TOC
PI = S1/(S1+S2)
S1/TOC = S1*100/TOC

NOTES:
Check
c = sample analysis confirmed
Pyrogram
n = normal